AUS DEM LEHRSTUHL

FÜR PSYCHIATRIE UND PSYCHOTHERAPIE

PROF. DR. MED. HELMFRIED KLEIN

DER MEDIZINISCHEN FAKULTÄT

DER UNIVERSITÄT REGENSBURG

PROCESSING OF PAIN AND EMOTION IN THE HUMAN BRAIN

An fMRI Study

Inaugural – Dissertation

Zur Erlangung des Doktorgrades

der Medizin

der

Medizinischen Fakultät

der Universität Regensburg

vorgelegt von

Andreas Heckel

2010

AUS DEM LEHRSTUHL

FÜR PSYCHIATRIE UND PSYCHOTHERAPIE

PROF. DR. MED. HELMFRIED KLEIN

DER MEDIZINISCHEN FAKULTÄT

DER UNIVERSITÄT REGENSBURG

PROCESSING OF PAIN AND EMOTION IN THE HUMAN BRAIN

An fMRI Study

Inaugural – Dissertation

Zur Erlangung des Doktorgrades

der Medizin

der

Medizinischen Fakultät

der Universität Regensburg

vorgelegt von

Andreas Heckel

2010

Dekan: Prof. Dr. Bernhard Weber
1. Berichterstatter: Prof. Dr. Peter Eichhammer
2. Berichterstatter: Prof. Dr. Mark W. Greenlee

Tag der mündlichen Prüfung: 11.03.2010

Erklärung

gemäß § 6, Abs. 5 der Promotionsordnung der Medizinischen Fakultät und der
Naturwissenschaftlichen Fakultät III - Biologie und Vorklinische Medizin
(Medizinische Fächer) vom 12. Juni 2008

(1) Die Dissertation hat Prof. Dr. Peter Eichhammer (Universitätsklinik für Psychiatrie
und Psychotherapie) angeregt. Die Ausarbeitung haben Prof. Dr. Peter
Eichhammer, Dr. Christoph Rothmayr (Clinical Neuroscience Center for Emotions
and Social Cognition) und Dr. Katharina Rosengarth (Lehrstuhl für experimentelle
Psychologie) überwacht. Betreuer ist Prof. Dr. Peter Eichhammer.

(2) Ich erkläre hiermit, dass ich die vorliegende Arbeit ohne unzulässige Hilfe Dritter
und ohne Benutzung anderer als der angegebenen Hilfsmittel angefertigt habe. Die
aus anderen Quellen direkt oder indirekt übernommenen Daten und Konzepte sind
unter Angabe der Quelle gekennzeichnet. Insbesondere habe ich nicht die
entgeltliche Hilfe von Vermittlungs- bzw. Beratungsdiensten (Promotionsberater
oder andere Personen) in Anspruch genommen. Niemand hat von mir unmittelbar
oder mittelbar geldwerte Leistungen für Arbeit erhalten, die im Zusammenhang mit
dem Inhalt der vorgelegten Dissertation stehen. Die Arbeit wurde bisher weder im
In- noch im Ausland in gleicher oder ähnlicher Form einer anderen
Prüfungsbehörde vorgelegt.

Regensburg, den 4. März 2010

. . . .

Andreas Heckel

CONTENTS

0 ABSTRACT

INTRODUCTION

Chronic pain syndromes are characterized by a poor correlation between objective physical pathology and subjective pain perception. There is a high comorbidity rate between chronic pain syndromes and mood disorders. This observation suggests that pain and affect are represented in a common neural network. We tested this hypothesis on 15 healthy volunteers in a region of interest (ROI) approach using BOLD fMRI.

METHODS

Firstly, pain responsive regions were identified in a localizer experiment. Heat pain stimuli were equalized to a subjective pain rating of 8/10 (0: no pain; 10: unbearable pain) as determined by individual psychophysical assessments. Secondly, the response behavior of these ROIs was characterized in a separate fMRI experiment. A paradigm of emotional induction (matching of aversive faces and neutral forms) was combined with heat pain to yield a 2 x 2 factorial design with factor 'pain' (pain *vs.* no pain) and factor 'affect' (Faces *vs.* Forms) reflecting a physical stressor and a non-painful emotional stressor, respectively. A moderately painful heat stimulus was chosen here (rating: 5/10) in order to prevent saturation of the hemodynamic response to pain. Heat stimuli were applied through a contact thermode (Medoc Inc., Israel). BOLD fMRI data were acquired using a 1.5 Tesla MR scanner (Siemens Sonata, Erlangen).

RESULTS

Pain related activation clusters were found in the midline thalamus and bilateral insula/SII cortices comprising the 'pain neuromatrix' for the sample at hand. These independently mapped ROIs were activated by both factors in similar relative proportions. The main effect of factor 'affect' was statistically significant in the right insular ROI. The amygdala was activated by intense pain (rating: 8/10). In all ROIs including the bilateral amygdala, we found a saturation of the hemodynamic response in trials, where aversive faces and painful stimuli were presented simultaneously.

CONCLUSION

Our findings suggest a common neural network for pain and emotion processing supporting the idea of pain as a homeostatic emotion. Neural correlates of pain and emotion aggregate subadditively (less than additively), possibly reflecting a mechanism of overload protection. Furthermore, our findings suggest a dual representation of threatening stimuli in terms of their affective and somatic significance in the amygdala and insular cortex, respectively. In this conceptual framework, chronic pain syndromes and affective disorders may reflect extremes of either somatic or affective augmentation of stress along an insula–amygdala axis, respectively. Further investigations on patients are warranted.

ZUSAMMENFASSUNG

EINFÜHRUNG

Chronische Schmerzsyndrome zeichnen sich durch eine mangelnde Korrelation zwischen objektiven pathologischen Befunden und subjektivem Schmerzempfinden aus. Es gibt eine hohe Komorbidität zwischen diesen Syndromen und affektiven Störungen. Diese Beobachtung legt nahe, dass Schmerz und Affekt in einem gemeinsamen Netzwerk im Gehirn repräsentiert werden. Wir testeten diese Hypothese an 15 gesunden Probanden in einem „Region of Interest" (ROI) Ansatz unter Einsatz der funktionellen Kernspintomographie (BOLD fMRI).

METHODEN

In einem ersten Schritt wurden schmerzresponsive Regionen im Gehirn identifiziert. Zuvor wurden die Intensitäten der schmerzhaften Hitzestimuli durch ein psychometrisches Verfahren festgelegt. Dabei wurde die Reizintensität für jeden Probanden so gewählt, dass sie einer subjektiven Schmerzempfindung von 8 auf einer Skala von 0 (kein Schmerz) bis 10 (unerträglicher Schmerz) entspricht. Das Antwortverhalten dieser ROIs wurde in einem separaten fMRI Experiment charakterisiert. Dabei wurde ein etabliertes Paradigma zur emotionalen Induktion (Matching aversiver Gesichter und neutraler Formen) mit einem Hitzereiz kombiniert, so dass sich ein 2 x 2 faktorielles Design mit Faktor „Schmerz" (Schmerz *vs.* kein Schmerz) und Faktor „Affekt" (Gesichter *vs.* Formen) ergab. Hierbei repräsentiert der Faktor „Schmerz" einen physischen Stressor und der Faktor „Affekt" einen nichtschmerzhaften, emotionalen Stressor. Als Schmerzreiz wurde hier ein moderater Hitzereiz gewählt (entsprechend einer subjektiven Schmerzbewertung von 5 aus 10), um einer Sättigung der neuronalen Antwort vorzubeugen. Hitzereize wurden über eine Kontaktthermode appliziert (Medoc Inc., Israel). BOLD fMRI Daten wurden mit einem 1.5 Tesla MR Tomographen erhoben (Siemens Sonata, Erlangen).

ERGEBNISSE

Schmerzbezogene Aktivierungscluster wurden im Bereich des mittelliniennahen Thalamus und des bilateralen Insula/SII Kortex identifiziert. Sie bilden die „Schmerzneuromatrix" für die vorliegende Stichprobe. Diese separat identifizierten ROIs wurden sowohl durch den emotionalen als auch durch den physischen Stressor in vergleichbaren Proportionen

aktiviert. Der Haupteffekt des Faktors Affekt erreichte statistische Signifikanz im rechtshemisphärischen insulären ROI. Die bilaterale Amygdala zeigte eine robuste Aktivierung durch intensiven Hitzeschmerz (subjektive Bewertung: 8 aus 10). In allen untersuchten ROIs stellten wir eine Sättigung der hämodynamischen Antwort bei gleichzeitiger Darbietung von Schmerzreizen und aversiven Gesichtern fest.

SCHLUSSFOLGERUNG

Unsere Ergebnisse legen ein gemeinsames Netzwerk für die Prozessierung von Schmerz und Affekt im Gehirn nahe und bestätigen damit die Auffassung von Schmerz als einer homöostatischen Emotion. Neuronale Korrelate von Schmerz und negativem Affekt aggregieren im gesunden Gehirn unteradditiv. Möglicherweise wird dadurch eine Überlastung limbischer Netze durch kombinierte Stressoren verhindert. Außerdem sprechen unsere Ergebnisse für eine duale Repräsentation bedrohlicher Stimuli hinsichtlich ihrer affektiven und somatischen Relevanz in der Amygdala beziehungsweise im insulärem Kortex. In dieser Konzeption spiegeln affektive Störungen und chronische Schmerzsyndrome eine vorwiegend affektive beziehungsweise somatische Augmentierung von Stress entlang einer Insula-Amygdala Achse wieder. Weitere Untersuchungen an Patienten sind gerechtfertigt, um diese These zu stützen.

1 Psychometric Profiling of Pain Perception

1.1 Introduction

Pain is a highly subjective sensation that displays considerable interindividual variability (Mogil, 1999). Preexisting neuroimaging studies agree that neural correlates of noxious stimulation correlate with the intensity of subjective pain sensation (Schneider and others, 2001;Gracely and others, 2002;Bornhovd and others, 2002). Moreover, perceived pain intensity is coded throughout the pain neuromatrix, i.e. is not confined to the somatosensory cortex of the 'lateral pain system' (Coghill and others, 1999). Due to its widespread distribution, pain intensity information is an integral component of the multidimensional representation of pain at the neural level. It is therefore advisable to incorporate pain intensity information in neuroimaging paradigms that aim to define the pain neuromatrix reliably. Specifically, the interindividual variability of the pain related neural response can be reduced by employing stimuli that evoke the same pain intensity in all subjects. This approach optimizes the signal to noise ratio in group level analyses but requires psychometrical procedures to be conducted prior to the imaging experiment.

We therefore devised a psychometric thresholding procedure to equalize perceived pain intensity in the sample by recording stimulus response functions (SRF) for each participant. SRFs describe the relationship between physical stimulus intensity and perceived pain intensity. Heat stimuli above the individual pain threshold are presented in a pseudo-randomized sequence and are rated on a visual analogue scale (0: no Pain; 10: unbearable pain). The temperature corresponding to a given pain intensity (0-10) can be determined from a fitted curve.

Stimulus response functions (SRF) provide a rationale for choosing the most appropriate pain intensity level for a given experimental purpose. In the present dissertation we use BOLD fMRI in order to a) functionally define the pain neuromatrix as region of interest and b) assess the interaction between pain related and emotionally related neural responses within this definition. In the former case, the pain related response should be as strong as possible without causing subject movement to permit a statistically reliable region of interest definition. In the latter case, we opted to use medium pain intensity with the reasoning more intense stimulation might lead to a saturation in the pain related response and therefore obscure a potential impact of the emotional factor. Secondly, we assume the SRF curves to be more sigmoid in shape and steepest near the center of the

visual analogue scale or VAS range. Hence, a small perturbation in stimulus intensity has a large impact on perceived pain intensity. We speculate that an emotional perturbation may have an analogous effect on the pain related BOLD response thus increasing chances to detect such interactions.

Despite its benefits in terms of statistical power, psychometric procedures are not routinely applied in most imaging studies. Instead, the same temperatures are employed for all subjects and a rating scheme is incorporated into the fMRI paradigm. This approach is disadvantageous in that the pain related response is compromised by i) cognitive/evaluative effects introduced by the rating task and ii) the poor correlation between stimulus intensity and perceived pain intensity (Clark and Bindra, 1956). In the present study we addressed these issues by conducting a psychometric profiling procedure prior to the fMRI experiment. This allowed us to homogenize the intersubject variability of pain perception thus improving the statistical power to detect changes in the pain related BOLD response. In the following, we describe the procedure and demonstrate that it yields reliable stimulus response functions at the subject level and group level.

1.2 Materials and Methods

The procedure involves two steps. Firstly, individual pain thresholds and tolerance thresholds were determined. Following this, these thresholds are referred to as thermal pain onset (TPO) and thermal pain tolerance (TPT), respectively. Subsequently, six equidistant temperatures (including the TPO and TPT) were sampled from the interval between both thresholds and presented in a balanced, blocked design. Participants rate perceived pain intensity on an analogue scale ranging from 0 (no pain) to 10 (unbearable pain). Temperatures corresponding to a rating of 5 and 8 out of 10 were interpolated from a fitted curve.

1.2.1 Subjects

15 healthy subjects (7 male, 12 right-hander, mean age: 24 years, SD: 3.4 years) participated in the investigation. They gave written informed consent to a protocol approved by the local Ethics Committee of the Medical Faculty and received payment (20 €) as allowance. Subjects with clinical history of central nervous system or CNS disease, peripheral neuropathies, limb trauma, psychiatric and internal diseases were excluded from the study. No participant reported drug intake except for oral contraceptives. Participants were advised to avoid consummation of alcohol, nicotine or caffeine on the day of the

experiment. Measurements were carried out between 9:00 AM and 2:00 PM. All subjects also participated in the fMRI experiment scheduled later on the same day. There was a four hour gap between both sessions to allow any local erythema to subside.

1.2.2 Apparatus

Thermal stimuli were delivered by the Thermosensory Analyzer II (TSA II, Medoc Inc., Israel) through a 30x30mm^2 contact thermode attached to the volar surface of subject's left wrist. The system is used in fMRI configuration: an fMRI compatible thermode connected to a filter element was employed rather than the standard variant. Results of pain profiling can therefore be applied to the fMRI experiment without bias caused by thermode exchange. Stimulus parameters (baseline temperature, ramping speed, target temperature, stimulus duration) and stimulus sequence are defined and controlled using the TSA II software (v. 3.20). This program runs on an IBM compatible Laptop (MS Windows XP) connected to the TSA II via the 9 pin serial port. An USB keyboard was also attached to the laptop. Pressing the space bar forces the system to return to the baseline temperature immediately. During the psychometric thresholding procedure, participants rate painful sensation on a computerized visual analogue scale by moving a slider with the computer mouse. This scale is embedded in a self-developed computer program (see below) that guides the subject through the entire acquisition process (see **Fig. 1-1**). This software runs on a second IBM compatible laptop under MS Windows XP. Once a rating is entered into the computer (via mouse click) a 150 ms square wave pulse is sent from the laptop's parallel port (pin 2) to the TSA's TTL input port. The TSA software subsequently receives a signal from the TSA to initiate the next trial in the predefined trial sequence. VAS ratings were saved to a log file from which an individual psychometric profile was created using customized MATLAB scripts.

The VAS rating software was written in C++. Microsoft Visual C++ 2008 Express Edition was employed as integrated development environment (available at http://www.microsoft.com/germany/express/product, as of 3/1/2010). Computer graphics were rendered in OpenGL at a resolution of 1024 x 768 pixels and a vertical refresh rate of 60 Hz. The OpenGL header file (gl.h, v.1.1, Silicon Graphics, Inc.) and corresponding library functions are included in the Microsoft Software Development Kit for Windows Server 2003, which is freely available at http://www.microsoft.com/downloads (as of 3/1/2010). Mouse interaction was programmed using standard MS Windows XP APIs included in the Microsoft Foundation Class Libraries (v. 7.0). The parallel port was

interfaced employing the TVicPort library (http://www.entechtaiwan.com/dev/port, as of 3/1/2010).

1.2.3 Pain Thresholding Procedure

The subjects were comfortably seated in a dimly illuminated room that was kept comfortably warm (23 °C). The thermode was attached to the subject's left wrist. Thermal pain onset (TPO) and thermal pain tolerance (TPT) were determined by an ascending Method of Limits with a rise time of .8 °C per second starting from a baseline temperature of 32°C. Prior to each measurement, the respective task instruction was repeated.

For TPO measurements, the instruction was: "Press space bar when the thermal sensation becomes painful". Upon pressing the key, the thermode was rapidly cooled down (10 °C/s) to baseline temperature. The next temperature rise interval followed after a pause of 10 seconds. Three practice trials were run and discarded for later analysis. Four tests were performed and averaged. For TPT, measurements the task instruction was: "Press space bar when the thermal sensation becomes intolerably painful". Only one measurement was carried out. To safeguard the subject, the TSA shuts down automatically when the thermode temperature reaches 53°C (hardware override). Values below 44 °C for TPT and below 39 °C for TPO suggest that the subject misunderstood the task instruction. These measurements were discarded and the corresponding trials were repeated.

1.2.4 Pain Profiling Procedure

1.2.4.1 Thermal stimuli

Heat pain stimuli were obtained by sampling six equidistant temperatures from the interval between TPO and TPT. It should be stressed that the administered temperatures differ across subjects according to individual pain and tolerance thresholds. To avoid confusion, thermal stimuli are hereafter referred to as thermal intensity levels ranging from 1 to 6 for each participant. Each intensity level is presented three times, yielding 18 trials in total. The stimulus sequence is shown in **Fig. 1-2**. Care was taken to control for sequence effects. For this purpose, the six intensity levels were classified as low, medium and high intensity stimuli. Each category thus comprises two stimuli. The sequence was designed so that each of the six intensity levels is preceded equally often by a weak, medium and strong stimulation. Sequence effects are thus distributed evenly across the three categories. The transition matrix is given in Table 1.2-1. The same sequence was used for all participants.

Table 1.2-1. Transition matrix of experimental conditions in the pain profiling paradigm.

			thermal intensity in trial *n*					
			low		medium		high	
			1	2	3	4	5	6
thermal intensity in trial *n-1*	low	1		X		X	X	
		2	X		X			X
	medium	3	X			X	X	
		4		X	X			X
	high	5	X			X		X
		6		X	X		X	

Thermal intensity levels (1 to 6) are categorized as weak, medium and high intensity stimuli. Conditions presented on consecutive trials (i.e. on trial *n-1* and trial *n*) are indicated (X).

1.2.4.2 Rating Scheme

Painful sensation was rated on a computerized visual analogue scale as shown in **Fig. 1-1** (middle picture). The scale ranges from 'no pain' (left end) to 'unbearable pain' (right end). The interval between both extrema is divided into eleven equidistant numerical steps (0-10). '1' denotes the pain threshold. The scale is color coded and begins with a green shade (0) that gradually changes into yellow at the pain threshold (1). Yellow smoothly blends into red at the right end of the scale (10). A verbal description is also provided: weak pain (1-3), medium pain (4-6) and intense pain (7-9). A slider can be moved smoothly along the scale with the computer mouse. Above the slider, the corresponding numerical value (rounded to the first decimal place) is shown. At the top of the screen the task description is displayed: "Move the slider according to the intensity of your pain sensation. Click at the signal tone." At the bottom of the screen, the participants are reminded that intolerable stimulation can be interrupted at any time by pressing the space bar.
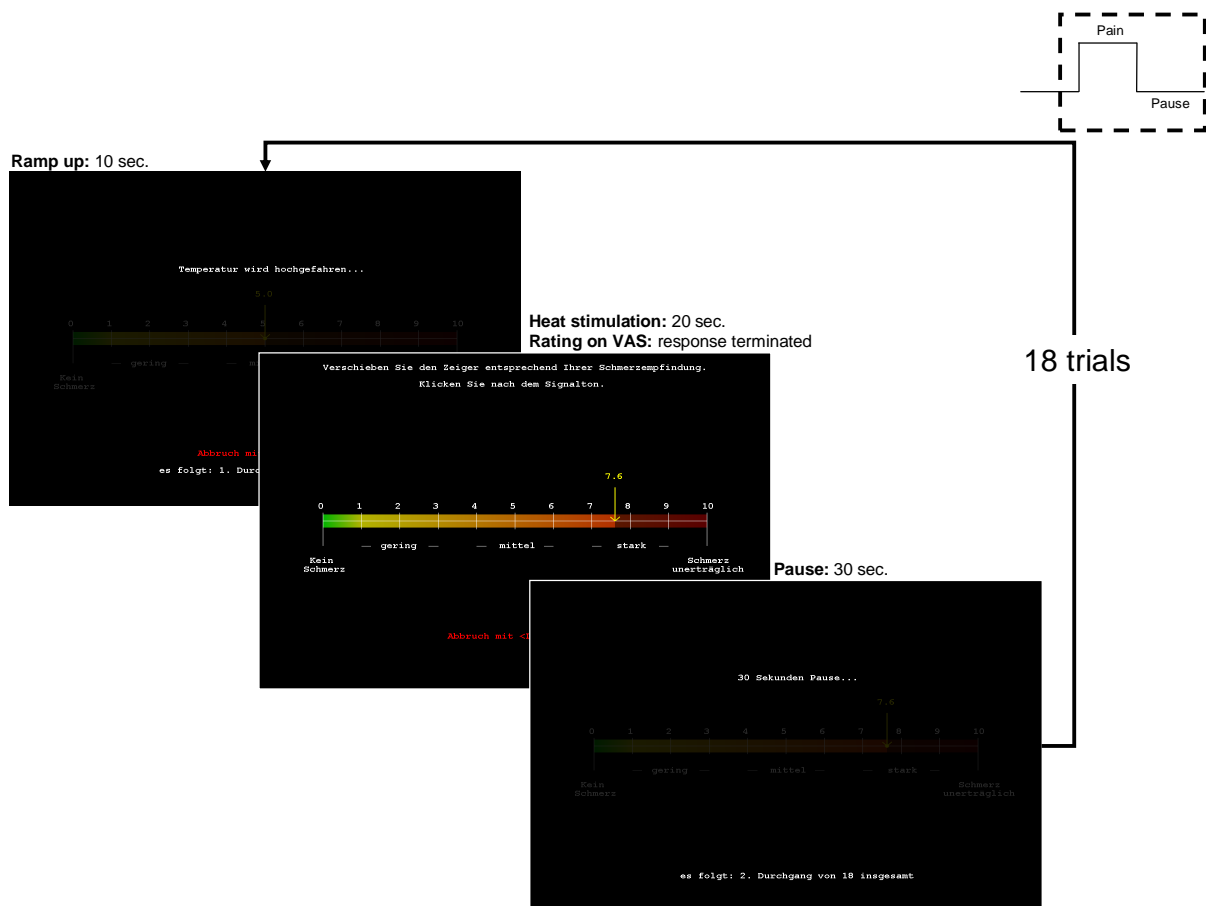
Fig. 1-1. Computer displays presented during the pain profiling paradigm. The upper screen announces the temperature rising interval. Ratings are performed on a visual analogue scale (VAS) via the computer mouse (middle screen). The lower screen is shown during the pause interval (with a countdown indicating the remaining time in seconds before the next trial ensues).

1.2.4.3 Procedure

Three test trials were conducted allowing the participant to adjust to the procedure. The participant initiates the paradigm by mouse click. 18 trials were carried out. A given trial consists of 20 seconds constant thermal stimulation followed by 30 seconds rest (**Fig. 1-2**). At the beginning of a trial, the temperature rises to the pre-defined destination at a ramping rate of 2 °C per second. When the target temperature is reached, the rating scale is presented to the participant who can move the slider along the scale with the computer mouse according to her pain sensation. After 20 seconds, the TSA software provides an auditory signal and thermal stimulation returns to baseline (32 °C) at a rate of 10 °C per second. The participant now enters the rating by pressing the left mouse button at the chosen slider position. No time constraints are imposed at this stage, i.e. the paradigm halts until a response is made. Rating is confirmed by a 50 millisecond signal tone. A pause of 30 seconds follows and the next trial ensues. The participant is guided through this sequence by the above mentioned computer program. Each step (ramp up interval, pain

rating, and pause) is accompanied by a corresponding computer screen as illustrated in **Fig. 1-1**. An on-screen message also informs about the number of trials that lie ahead. The subject can interrupt intolerable stimulation at any time by pressing the space bar. In this case, the subject is asked to commit a rating of 10. Pressing space bar does not cancel the experiment *per se*, i.e. the trial sequence continues. Hence, stimulus recording and interruption do not require any intervention by the experimenter.
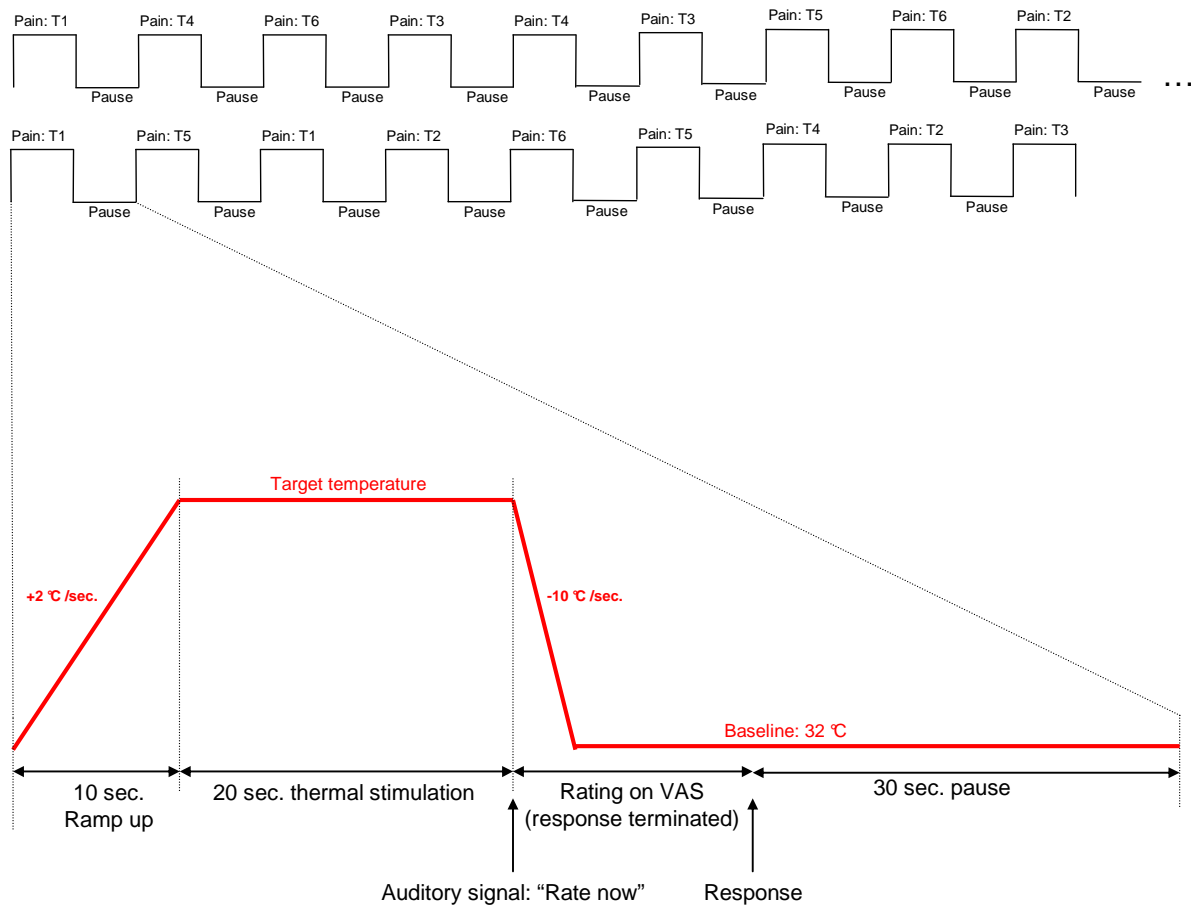
Fig. 1-2. Stimulus sequence and trial structure in the pain profiling paradigm. *Upper panel:* Thermal stimulation alternates with pauses. 18 pain / rest cycles were carried out. The sequence of thermal intensity levels (T1-T6) is indicated. *Lower panel:* Timecourse of thermal stimulation (red line) during a single trial relative to the four trial components (ramping, stimulation, rating and pausing).

1.2.5 Data analysis

Psychometric Profiles were created by employing MATLAB v. 7.5 (TheMathWorks, Natick, MA). At the subject level, per trial ratings were collapsed over the three stimulus repetitions and averaged. The resulting six mean values (one value per thermal intensity level) were accommodated by an interpolation curve using the MATLAB function

'INTERP1'. A piecewise cubic hermite interpolating polynomial (PCHIP) was chosen as interpolation method. PCHIP is more accurate than linear interpolation. As opposed to cubic spline interpolation, PCHIP respects monotonicity and has no overshoots. The method is thus well suited to accommodate psychometric functions. For each subject, the temperatures corresponding to a rating of 5 and 8 out of 10 were interpolated from the fitted curve. A paired samples t-test was carried out to assess, whether the two rating levels of interest (5/10 and 8/10) differ significantly at the group level.

A valid psychometric profile is assumed to increase monotonically with rising temperature. Monotonicity was assessed as follows: According to the null hypothesis (absence of monotonicity) the numerical difference between ratings of two adjacent intensity levels is equally often positive and negative. From the six employed intensity levels, five difference values were computed for each stimulus repetition, yielding 15 values per subject. These values are positively signed when ratings increase with increasing intensity. Under the null hypothesis, the number of positive differences follows a binomial distribution with parameters N=15 and p=.5.

Group level analysis is based on the individual interpolation curves. Distribution plots were created to provide a detailed illustration of these data. For this purpose we employed the MATLAB function 'distributionPlot.m' (programmed by Jonas Dorn, 2008). This function is freely available at the official MATLAB file exchange site (http://www.mathworks.com/matlabcentral/fileexchange, as of 3/1/2010). Distribution plots display the probability density functions (pdfs) of temperatures conditional on rating level, and vice versa. Densities are estimated using an Epanechnikov-kernel, whose default bandwidth was divided by 2.5 to avoid overblurring.

To provide a psychometric function at the group level, a fifth degree polynomial was modeled to group mean ratings (sampled at seven equidistant temperatures between 44°C and 50 °C) using the method of least squares. To assess the quality of this fit, a χ^2 goodness of fit measure was used (Bulmer, 1979).

Repeated measures ANOVAs were carried out to evaluate the impact of sequence and repetition effects, which are potential sources of systematic bias. Respectively, 'temperature' (6 levels) and 'antecedent intensity' (3 levels: low, medium, and high intensity), as well as 'temperature' (6 levels) and 'repetition' (3 levels: first, second, and third repetition) were declared as within-subject factors. Violations of the sphericity assumption were adjusted by the Greenhouse-Geisser correction.

Parametric statistical tests were carried out using SPSS (v. 15.0) software (SPSS Inc., Chicago, IL). A false positive rate of $p < .05$ was used as significance criterion. The distribution of pain ratings and temperatures were described by parametric (mean values, standard deviations) and non-parametric statistics (medians, interquartile range).

1.3 Results

Fig. 1-3 shows three examples of individual psychometric profiles. In the following, we refer to the profile depicted in panel *a*. As determined in the thresholding procedure, the participant experienced onset of thermal pain at 42.6 °C (thermal pain onset, TPO) and unbearable pain at 50.1 °C (thermal pain tolerance, TPT). From this interval, six equidistant temperatures (including both thresholds) were sampled and presented as stimuli in the pain profiling paradigm. Blue dots denote the participant's individual ratings at each of the six thermal intensity levels (at 43.7 °C, 44.1 °C, 45.6 °C, 47.12 °C, 48.6, and 50.1 °C). Rating variability is highest for medium intense temperatures. In this example, pain ratings span about 5 units at 47 °C. On the other hand, rating variability is relatively small when high or low temperatures were administered. At the TPO and TPT, ratings span only about 1 rating unit, respectively. Mean rating values (circles) are increasing monotonically with increasing temperature. The interpolating polynomial suggests a sigmoid relationship between temperature and pain rating. A sigmoid shape is typical for stimulus response functions that unfold between two fixed boundaries. Here, the upper and lower boundaries are represented by the TPO and TPT, respectively. In the medium temperature range, the relationship between temperature and rating is quasi-linear. The slope value of the interpolation curve is highest here, i.e. a given thermal change has a relatively high impact on subjective pain sensation. When ratings approach a boundary (TPO or TPT), they become increasingly less affected by thermal change. In other words, a relatively large change is necessary to elicit small alterations in subjective pain perception (ceiling and flooring effect). In this context panel *b* and *c* provide examples, where ceiling and flooring are prominent and comprise most of the psychometric function. In panel *b*, ratings are almost constant in the upper half of the temperature range, while in panel *c* the profile is flat in the lower half of the tested range.
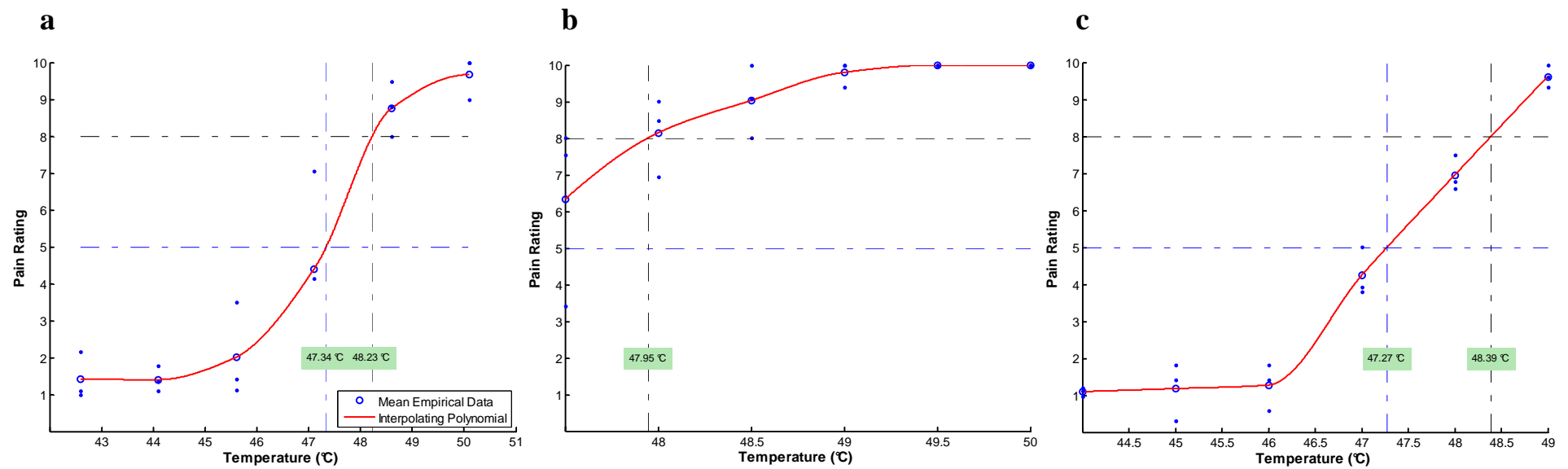
Fig. 1-3. Psychometric profiles from three participants (panel *a-c*). Pain ratings are plotted as a function of applied temperature. The temperature range is spanned by the subject specific pain and tolerance thresholds. Blue dots denote individual ratings at a given temperature. An interpolation curve (red line) is fitted to mean ratings (blue circles). Temperatures corresponding to a rating of 5 and 8 out of 10 are determined from the fitted curve. See text for details.

Monotonicity was assessed as described in the methods section. We subtracted single ratings of neighboring thermal intensities levels. Positive differences indicate that pain ratings increased with increasing temperature, which is the expected behavior of a valid profile of thermal pain. We counted at least 12 positive differences per subject. Based on this observation, the null hypothesis could be rejected for all participants at a false positive rate of below .05 using a binomially distributed test statistic [B(k≥12, N=15, p=.5)=.02]. We therefore assume that the psychometric profiles are consistently increasing in each subject. This result is in line with the examples shown in panels *a-c* (**Fig. 1-3**).
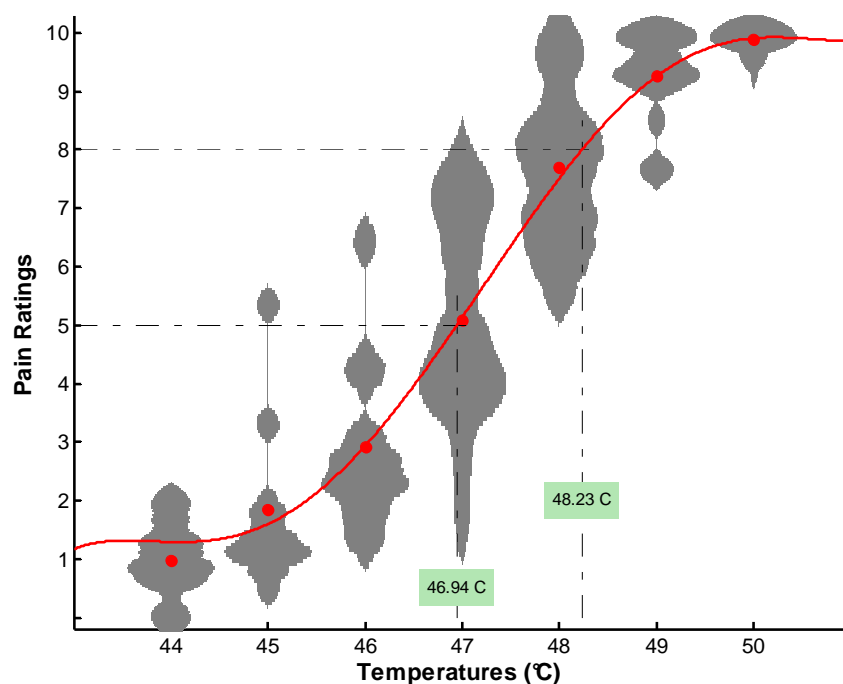
Fig. 1-4. Estimated psychometric profile at the group level. Grey patches represent probability density functions of pain ratings conditional on temperatures. Red discs denote average pain ratings at indicated temperatures. As determined from the fitted curve (red), a temperature of 46.9 °C and 48.2 °C was associated with a rating of 5 and 8, respectively.

Group analysis was based on the 15 individual psychometric functions, i.e. on the interpolation curves depicted in **Fig. 1-3**. Distribution plots were created to provide a detailed illustration of these data. **Fig. 1-4** illustrates the distributions of per subject pain ratings at seven equidistant temperatures between 44 °C and 50 °C. The investigated range conforms to the interval between the average thermal pain onset (mean TPO at 44.77 °C) and average thermal pain tolerance (mean TPT at 49.80 °C). Summary statistics are listed in Table 1.3-1. Medians and means are monotonically increasing as expected from the single subject analysis. For medium temperatures, intersubject variability is very prominent

and spans 5.5 rating units at 47 °C. On the other hand, distributions are rather narrow for high and low temperatures. They span 2 and .6 rating units at the left end (44 °C) and right end (50 °C) of the tested range, respectively. Concordantly, measures of statistical dispersion conjointly peak at 47 °C and continuously decrease towards 44 °C and 50°C (**Table 1.3-1**). At 47 °C, pain ratings are distributed symmetrically around the sample mean (red disc). For lower and higher temperatures, however, distributions appear skewed. This is a consequence of the closed rating scale: as temperatures approach the average TPO and TPT of the sample, ratings are increasingly approaching the fixed boundaries (at 0 and 10). In this context it should be noted that the non-parametric statistics in **Table 1.3-1** are less susceptible to bias introduced by skewed data than parametric statistics.

Table 1.3-1. Distribution of pain ratings at selected temperatures. Summary statistics.

Temperature (℃)	Pain ratings				
	N	Mean	Standard deviation	Median	Interquartile range
44	6	.98	.66	.95	.64
45	10	1.84	1.45	1.27	.82
46	12	2.93	1.43	2.48	1.26
47	13	5.08	1.73	4.39	2.74
48	15	7.69	1.31	7.90	1.61
49	15	9.25	.77	9.42	.78
50	15	9.89	.19	10.00	.20

Measures of central tendency (mean, median) and measures of dispersion (standard deviation, interquartile range) are provided. Note that not all listed temperatures (44 ℃ - 50 ℃) are found in every subject's data. N r efers to the sample size on which the statistics are based upon.

In order to obtain a representative psychometric function at the group level, a fifth degree polynomial (red curve in **Fig. 1-4**) was modeled to the sample means using the method of least squares. The fitted curve confirms the sigmoid relationship between temperature and pain rating as suggested on the subject level (in **Fig. 1-3**, panel *a*). To assess whether deviances from this fitted curve are statistically significant, a goodness of fit measure was derived as follows: The difference between an observed mean rating and the polynomial's prediction was divided by the observed standard error of that mean rating, and this quantity was squared yielding an approximate $\chi^2(df=1)$ (Bulmer, 1979;Morgan, 2000). This computation was performed for each of the seven mean ratings depicted as red discs in **Fig. 1-4**. The values were then summed yielding a single goodness of fit measure: $\chi^2(df=1)=2.07$. This corresponds to a p-value of .15 (n. sign.). Deviances from the sigmoid profile are thus compatible with chance. Of note, the slope value of the polynomial is highest at a rating value of 5.6. Here, small changes in thermal input have the highest impact on painful sensation.

To further explore the relationship between thermal intensity and painful sensation, the distributions of temperatures were plotted as a function of rating level (**Fig. 1-5**). Apparently, temperatures are i) distributed rather symmetrically around the sample means, and ii) the distributions are similar in shape across rating levels. Standard deviations and interquartile ranges amount to less than 1 °C (Table 1.3-2). To test the hypothesis that intersubject variability is constant across the rating scale, we performed Levene's Test for equality of variances. It revealed that the assumption of homoscedasticity was met $[F(9,114)=.47, p=.89]$.
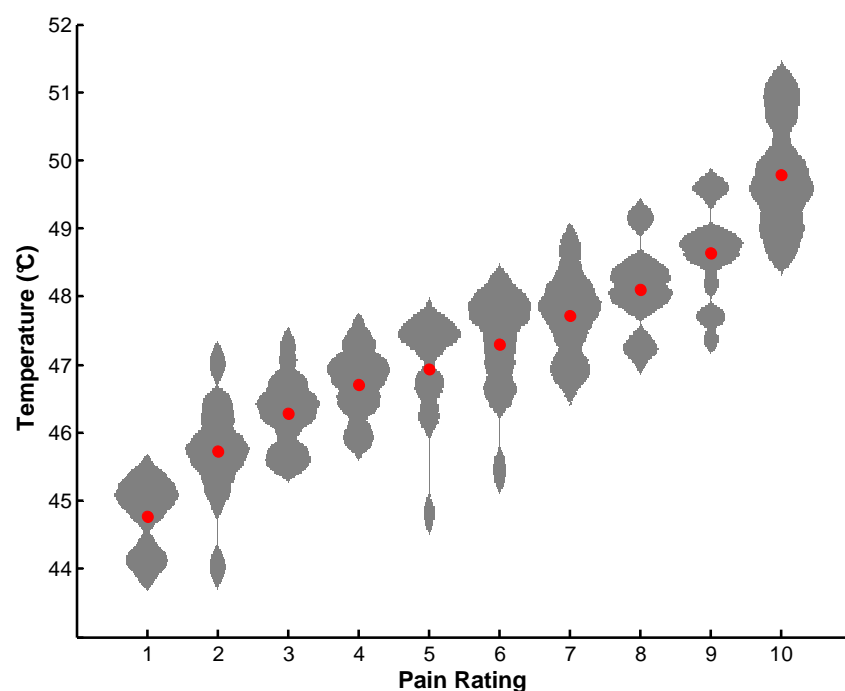
Fig. 1-5. Estimated distribution of temperatures at indicated pain levels. Grey patches represent probability density functions of temperature conditional on rated pain level. Red discs denote mean temperatures.

We can now estimate the accuracy with which differences in painful sensation can be resolved reliably. For this purpose we averaged the standard deviations listed in Table 1.3-2. Based on this quantity we computed the standard error of the mean (s.e.m) assuming a sample size of N=15. Due to homoscedasticity we postulate that this s.e.m is representative for the temperature dispersion at all pain rating levels. The corresponding 95% confidence interval has a width of ±.36 °C. A change of .36 °C thus elicits a statistically significant change in pain sensation at the group level (p=.05, two-tailed). The magnitude of this thermal change in terms of rating units can be determined by using the psychometric function as transfer function. In the lower and upper third of the function, a

change of.56 and.52 rating units can be reliably resolved, respectively. In the middle portion, the resolution power drops to .85 rating units. From the determined resolving power, it follows that a rating of 5 (46.94 °C) is significantly different from a rating of 8 (48.13 °C). This is confirmed by a paired-samples T-test [$T(13)=8.38$, $p<.001$, two-tailed].

Table 1.3-2. Distribution of temperatures at selected pain intensities (0-10). Summary statistics.

Rating Level	Temperatures				
	N	Mean (°C)	Standard Deviation (°C)	Median (°C)	Interquartile Range (°C)
0	1	43.98	N/A	43.98	N/A
1	6	44.77	.53	44.93	.76
2	12	45.72	.75	45.75	.65
3	12	46.29	.52	46.34	.74
4	12	46.71	.49	46.82	.54
5	14	46.94	.78	47.27	.82
6	14	47.30	.75	47.54	.96
7	15	47.72	.59	47.66	.78
8	15	48.11	.59	48.08	.53
9	15	48.63	.68	48.67	.56
10	9	49.80	.78	49.73	.98

Measures of central tendency (mean, median) and measures of dispersion (standard deviation, interquartile range) are provided. Please note that not all listed rating levels (0-10) can be found in each individual dataset. N refers to the sample size on which the statistics are based upon.

We next investigated two sources of systematic bias that may have affected pain ratings, namely i) the effect of stimulus sequence and ii) repetition effects (each temperature is applied three times). The effect of stimulus sequence on group mean rating is illustrated in **Fig. 1-6** (panel *b*). Note that the employed temperatures were grouped into three intensity categories (low, medium and high). Accordingly, pain ratings depend on the antecedent thermal intensity. When a medium or high intensity stimulus was administered in the previous trial, painful sensation is weaker compared to stimulation with low thermal intensity. The effect is small, however. A repeated measures ANOVA with factor 'temperature' (6) and factor 'previous intensity' (low, medium, high) was carried out. In line with panel *b*, the main effect of factor 'previous intensity' is not reliable [$F(2,28)=1.87$, $p=.18$, G.G. corrected]. The 6 x 3 interaction between both factors is unreliable, as well [$F(10,140)=1.56$, $p=.175$, G.G. corrected]. In **Fig. 1-6** (panel *a*), the effect of stimulus repetition on group mean rating is shown. Apparently, pain rating does not change systematically on subsequent repetitions. We again performed a 6 x 3 repeated measures ANOVA with factor 'temperature' (6 intensity levels) and factor 'repetition' (3 levels: first, second, and third repetition). The main effect of factor 'repetition' is non-

significant [$F_{(2,28)}=.173$, $p=.825$, G.G. corrected]. The 6 x 3 interaction between both factors is also unreliable [$F_{(10,140)}=2.12$, $p=.07$, G.G. corrected].

a

b
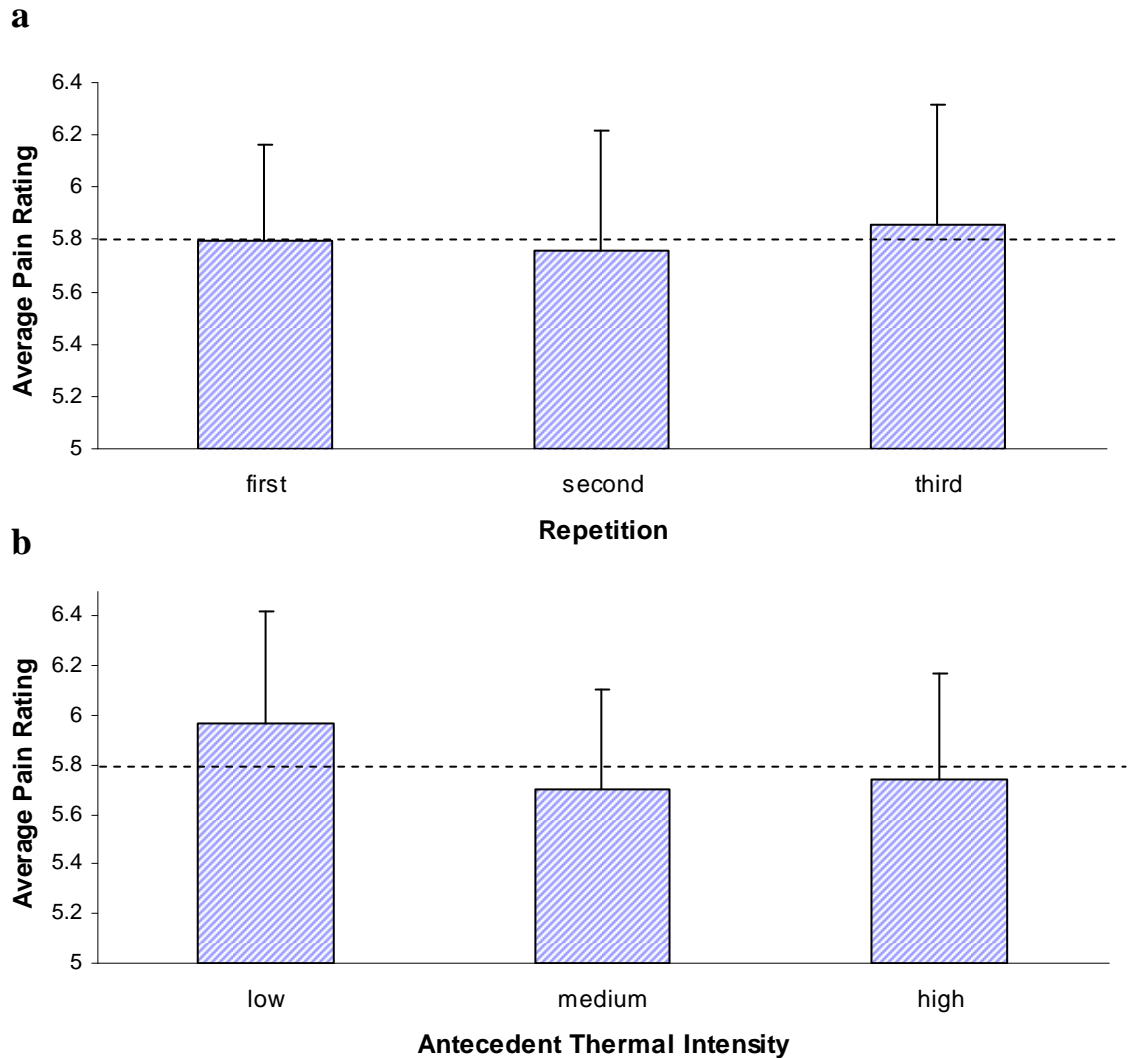
Fig. 1-6. Repetition and sequence effects on group level pain ratings. *Panel a:* Pain rating as a function of repetition. *Panel b:* Pain rating as a function of antecedent thermal intensity, which is grouped into three categories (low: levels 1-2; medium: levels 3-4; high: levels 5-6). Ratings were averaged across the six thermal intensity levels (at each repetition or antecedent intensity category). The global mean rating of the sample (5.8) is shown in both diagrams (dotted line). Error bars denote the standard error of the mean.

1.4 Discussion

In the present study we have introduced a methodology to probe thermal pain perception in the suprathreshold range. Acquired stimulus response functions (SRF) are consistently increasing at the subject level. At the group level, differences in pain perception below 1 rating unit can be resolved reliably. The profiling paradigm is robust against bias introduced by repetition and sequence effects. Data acquisition has been completely automated thus minimizing disruptive interactions between participant and instructor.

Objective assessment of pain is a challenge due to its subjective and multidimensional character. Melzack proposed three separate dimensions of painful experience: sensory, affective and evaluative. This conception led to a number of verbal scales of which Melzack's McGill questionnaire (Melzack, 1975) and the Brief Pain Inventory (Cleeland and Ryan, 1994) are most widely used for evaluating chronic pain. These are, however, not suitable for experimentally induced pain. For this purpose, reflex measures have been devised. Nociceptive reflexes are widely used in human and animal research. A common protocol in humans includes electrical stimulation of the sural nerve in the retromalleolar space and subsequent recording of the impulse from the surface of the ipsilateral biceps femoris. Stimulus intensity is increased until impulses can be reliably detected by electromyography (Willer, 1977). This thresholding technique is objective in that it is based on the observation of an involuntary, physiologic response. It is, however, less suited to obtain responses to graded stimuli.

Our design is based on rating scales, which focus on pain intensity, i.e. the 'salient dimension of pain', as Melzack put it. These unidimensional scales function well for the assessment of acute pain. There are three variants: the four point verbal rating scale (VRS) categorizes pain as none, mild, moderate, and severe. It is a very coarse screening instrument, but easy to understand (Keele, 1948). The visual analogue scale (VAS) comes as 10 cm line labeled with 'no pain' at one end and 'the pain is as much as I can bear' at the other (Bond and Pilowsky, 1966). Subjects mark their pain sensation on this line, which is thus expressed as the distance between the 'no pain' end and the mark relative to the total length of the line. The VAS is appealing in that pain intensity is described in a continuous way. In theory, infinitely small differences can be resolved with the VAS. However, the approach requires some abstract geometrical understanding since the scale is devoid of any further verbal or numerical descriptions. Moreover, the golden section at 6.2 centimeters interferes with rating accuracy (Noble and others, 2005). The third type of

unidimensional scale is 11 point numerical rating scale or NRS: Subjects describe their pain sensation on a scale of 0-10. The NRS is more fine-grained than the VRS but again demands abstraction capabilities from its user. The VAS and NRS agree well and are equally sensitive in assessing acute pain (Breivik, Bjornsson, and Skovlund, 2000). In a report published by the European Association for Palliative Care (EAPC), the expert working group in 2001 recommended the use of a standard 0–10 NRS and a 100-mm horizontal VAS while pointing to the poorer compliance associated with the VAS (Caraceni and others, 2002).

We merged the three unidimensional schemes into a single rating scale with the purpose to facilitate the self assessment of pain. We augmented a classical VAS with numerical and verbal descriptors by superimposing a NRS and a VRS. A numerical 0 thereby corresponds to the VAS label 'no pain', whereas a numerical 10 corresponds to 'as much pain as I can bear'. The remaining numerals are distributed evenly across the VAS. The VRS label 'no pain' coincides with the homonymous VAS label. The mapping between the remaining verbal categories and the NRS / VAS is much less clear. We adapted the suggestion depicted in Breivik et al. (Breivik, Bjornsson, and Skovlund, 2000). According to individual preference, subjects can freely choose a coding scheme (verbal, numeric, and geometric) or a combination of schemes.

Three constraints were imposed on the pain profiling paradigm: a) it should be composed of many conditions (intensity levels) to ensure an accurate sampling of psychometric profiles. Conditions should be repeated often, but the paradigm should also be short so as to preserve compliance, avoid skin irritation and habituation or sensitization effects. b) Results should be portable to the fMRI experiment. c) Sources of bias must be controlled.

a) We measured TPO and TPT for each subject to derive individually tailored sampling windows rather than using fixed temperatures for all subjects. In this way, optimal sampling is ensured with as few intensity levels as possible. We employed six levels, each being repeated three times. This sufficed to obtain credible psychometric profiles (see below). Moreover, the paradigm has a good resolving power at the group level. At a sample size of 15 subjects, differences in pain sensation below .85 rating units can be resolved reliably using a significance criterion of $p \leq .05$.

b) To ensure portability of results, the TSA II was used in fMRI configuration to avoid bias introduced by thermode exchange. The duration of painful stimulation

(20 s) and the applied ramping rate (2 °C/s) are identical for both the fMRI experiment and the profiling procedure.

c) We have shown that pain ratings do not change significantly on subsequent stimulus repetitions, ruling out repetition effects as a source of substantial bias. To control for sequence effects, we employed a balanced stimulus order. We nevertheless detected a small systematic effect: pain ratings were diminished when a moderately or highly intense stimulus was presented in the antecedent trial. This observation is compatible with habituation: the subjects adapt to the high intensity stimulus, which reduces pain sensation in the subsequent trial. However, this source of bias is also not significant.

Psychometric profiling resulted in convincing stimulus response functions (SRFs). Ratings consistently increased with increasing temperature in each participant. Interpolation curves have a sigmoid shape, which is a hallmark of psychometric functions with fixed boundaries. However, deviances from this canonical shape also occur on the subject level. For example, the function in panel *b* (**Fig. 1-3**) appears hyperbolic. This is the result of poorly defined thresholds in this participant: the TPO was chosen inappropriately high, i.e. only the upper portion of the psychometric function is visible. Conversely, the TPO in panel *c* was probably measured to low: The acquisition window is thus shifted towards lower temperatures and the stimulus response function is cut off in its linear portion, i.e. before saturation. At the group level, a fitted polynomial takes on a sigmoid shape. As confirmed by goodness of fit assessment, this shape is representative for the stimulus response function at the group level. Truncated profiles are assembled to a whole by pooling data across subjects. This finding underscores that abortive profiles as shown in panel *b* and *c* are the result of an improperly chosen sampling window but otherwise valid. We can therefore assume that the temperatures employed in the fMRI experiment elicit the same levels of painful sensation across participants and correspond to a subjective rating of 5/10 and 8/10. Hence, subjective pain perception is standardized in the sample as required by the fMRI experiment.

However, these results question the validity of the TPO and TPT pain thresholds that define the sampling window. In the thresholding step we adopted the method of ascending limits to measure TPO and TPT: starting from baseline, the stimulus intensity is increasing continuously until a threshold is reached; at that moment, subjects press a stop button to force a return to baseline. This is an established procedure widely used in the

literature. It nevertheless has some important drawbacks: i) measurement is obviously affected by reaction time artifacts; ii) employed stimuli are phasic and response terminated, which introduces two confounds, namely the gradient of temperature ascent and the time that passed since the beginning of the trial; iii) measurements are susceptible to expectation bias, since the stimuli are repeated several times in a row. The subjects are aware of that and can prepare their response accordingly; iv) measurements are prone to serial effects: it is the author's impression that participants feel committed to their response in the antecedent trial, even when this response is not plausible. This becomes very problematic as verbal intervention by the instructor may be required to prevent subjects from reproducing inappropriate responses in the upcoming trials; v) in this context, subtle social interactions are of concern. Subjects may subconsciously want to make a certain impression on the experimenter, whom they know is monitoring their responses. This again introduces unpredictable bias to the data, e.g. a bias to respond in a socially desirable way.

These sources of bias were carefully avoided in the pain profiling paradigm. Ad i) In line with deCharms and colleagues we employed constant stimuli of predetermined intensity (deCharms and others, 2005). These were administered for 20 seconds and rated afterwards (without time constraints). Thus, response time artifacts are absent. Ad ii) As stimulation intensity is constant, bias introduced by thermal gradient is absent. A trial always lasts 20 seconds, i.e. stimulus duration is equal across participants. Ad iii) Six stimulus intensities are presented in a pseudo-randomized order controlling for expectation bias. If intensity levels were, for example, arranged in an ascending order, subjects' expectations *per se* would encourage a linear, monotonic profile, which may actually not reflect pain perception. Ad iv) Since the same stimuli are not presented in a row, the serial effect as defined above is controlled. Ad v) Trial initiation, response recording and interruption of unbearable stimuli are controlled through a computer interface. Social interactions can thus be kept minimal. Intervention is only necessary in the case of malfunction. No malfunction was encountered during the entire acquisition process. The profiling paradigm can thus be run safely in a completely unattended mode.

The latter point is particularly noteworthy, since pain rating is known to be sensitive to context factors. Our profiling paradigm allows controlling the effect of the 'social factor' on pain sensation. Psychometric profiles can be acquired with and without the attendance of a supervisor, which allows the investigation of interactions between pain perception and the presence of a social context. This opens up interesting perspectives for psychiatric research. As to our knowledge social interaction pertaining to the data

acquisition process is an uncontrolled factor in many if not all studies investigating pain processing. This is particularly problematic for those studies that focus on drugs and diseases that relate to the social and emotional domains. For example, chronic pain syndromes are linked to disturbed processing of both sensory and social stimuli (Kosturek and others, 1998). Moreover, Oxytocin, a neuropeptide involved in the formation of social bonds, is known to have analgesic properties in animals (Petersson and others, 1996) and terminally ill cancer patients (Madrazo and others, 1987). Oxytocin was shown to modulate connectivity measures between the amygdala and midbrain region, where descending pain control systems are located (Kirsch and others, 2005). It has been suggested that Oxytocin is the mediator of the placebo response (Enck and Klosterhalfen, 2009) rather than having analgesic properties *per se*. Our paradigm allows assessing whether or not painful sensation altered by disease or pharmacological intervention requires the presence of a social context as a modulating or permissive factor.

Group level analysis showed a tremendous intersubject variability of pain ratings at medium temperatures (**Fig. 1-4**). At 47 °C, subjective pain ratings are dispersed across three verbal categories ('weak', 'medium' and 'severe'). A given temperature may thus elicit very different levels of pain sensation. Studies focusing on the subjective experience of pain rather than its physical component have to take this effect into account. Neuroimaging studies agree that activity in pain responsive brain regions correlates with the subjective perception of pain intensity (Schneider and others, 2001;Gracely and others, 2002;Bornhovd and others, 2002). In the present study we used psychometric profiling to find stimuli that equate pain perception across participants. If we used the same temperatures for all participants in fMRI instead, a substantial nuisance variable would be introduced to the hemodynamic response, i.e. a larger sample size would be required to reliably delineate pain responsive regions in the brain. When the BOLD response to pain is not equated across the sample, it is also more difficult to find a modulating influence of affective state on pain processing. Note in this context, that moderately painful stimuli (rating: 5/10) were applied for the latter purpose, since the stimulus response function is steepest at medium intensities and a saturation of the neural response is avoided. At moderate intensities, however, the intersubject variability of pain perception is particularly high, i.e. the usage of fixed temperatures would be particularly detrimental in terms of signal to noise ratio of the pain related hemodynamic response.

At high and low thermal intensities, however, intersubject variability is much smaller. This may relate to the biological purpose of pain, namely to avoid tissue damage.

Tissue composition - and thus tissue vulnerability - at the volar surface of the wrist presumably is similar across the sample. In this sense, the temperatures at TPO and TPT are warning cues that elicit relatively uniform responses, whereas temperatures in the center of this 'warning window' may be less well defined biologically thus allowing for more variability between subjects. A different picture arises when plotting temperature as a function of perceived pain intensity. From this perspective, intersubject variability is preserved across the rating scale. This suggests that thermal intensities conditional on subjective sensation are less bound to biological constraints. We estimated that a .36 °C change suffices to elicit significantly different pain sensations at the group level. This value corresponds to not more than .85 rating units. On the basis of these data, detailed power analysis can be conducted to plan further experiments, i.e. required sample sizes can be easily computed according to a particular research question.

In psychiatric research, pain thresholds have been studied in various diseases, e.g. schizophrenia, depression and anxiety disorders (Lautenbacher and Krieg, 1994). These studies aim to reduce the complexity of a disease to a biomarker (pain threshold) that is amenable to measurement and has a clear connection to a physiologically distinct system. Generally, these studies yielded conflicting results. In depression, for example, both an increase (Marazziti and others, 1998;Kundermann and others, 2008;Adler and Gattaz, 1993) and a decrease (Ward and others, 1982;Otto, Dougher, and Yeo, 1989;Moroz and others, 1990) of pain thresholds have been found. Most studies focus on pain thresholds as determined by the ascending method of limits. As outlined above this methodology is susceptible to many forms of bias that may contribute to the ambiguity and low statistical reliability of existing reports. Moreover, the general approach to map pain processing to one single threshold, could be misleading. The distinctive features of pain perception in patients may be hidden in the suprathreshold range, i.e. between pain onset and the tolerance threshold. To comprehensively assess pain processing at the behavioral level, the acquisition of entire stimulus response functions (SRF) is necessary, therefore.

Characterizing pain perception with stimulus response functions as opposed to single thresholds will certainly increase chances to detect a reliable impact of illness or pharmacological intervention on pain processing. We have shown that psychometric profiling can be reliably conducted within a 15 minutes paradigm that is robust against habituation and carry over effects and has a high resolving power for medium sized samples. It should be noted in this context, that pain is a warning signal that subserves homeostasis (Craig, 2003). One may postulate that the width of the warning window (the

interval between pain onset and pain tolerance) and the course of the SRF therein depends on the activity of homeostatic effector mechanisms that are strained during chronic stress. A stimulus response function can be shifted, flattened, steepened, and distorted by pathological condition. In contrast, single thresholds can only be reduced or increased. The more elaborate account may thus allow uncovering maladaptive mechanisms of pain control and homeostasis. Hence, psychometric profiling as conducted in the present dissertation may offer a new conceptual perspective.

2 Pain Processing and Emotion Processing in the Human Brain

2.1 Introduction

The International Association for the Study of Pain (IASP) defines pain as: "An unpleasant sensory and emotional experience associated with actual or potential tissue damage, or described in terms of such damage." This definition highlights the emotional and subjective nature of pain, which implies a top-down modulation of nociceptive inputs. On the contrary, another common conception of pain, which originated in the 17th century and is owed to Rene Descartes, posits a one way pain pathway from the periphery to the brain. Here, pain is passively received rather than actively modulated suggesting a 1:1 psychophysical mapping of noxious intensity to perceived pain intensity. This account, however, contradicts the everyday experience that pain is dependent on context, e.g. we do not easily notice a finger cut when being distracted by more salient events. Moreover, chronic pain syndromes are characterized by intense pain that is disproportionate to input. The phenomenon of phantom limb pain in people with total spinal section (Melzack and Loeser, 1978) suggests that pain can be elicited and maintained without any nociceptive inputs to the brain. These observations indicate that the brain itself can generate the pain experience independent from peripheral sensory inputs.

Pain is actively generated by central nervous processes rather than passively received from the periphery. Melzack proposed that pain is a multidimensional experience that includes sensory-discriminative, motivational-affective and evaluative-cognitive dimensions (Melzack, 1975). As a complex conscious experience, pain emerges as a neurosignature pattern maintained by processing loops between thalamus and cortex and cortex and limbic system. The pain neuromatrix is thus comprised of multiple interacting regions. Modern imaging techniques confirm, that pain is not processed by a single region in the brain but in a distributed network, the structural equivalent of the neuromatrix theory (**Fig. 2-1**). The insula, secondary somatosensory cortex (SII), the anterior cingulate (ACC) and the thalamus are most consistently reported as pain responsive anatomical structures across studies (Apkarian and others, 2005;May, 2007;Peyron, Laurent, and Garcia-Larrea, 2000;Tracey, 2008). Experimental accounts from fMRI/PET and EEG/MEG studies of the last two decades can be summarized in a general model of pain perception in the human brain (Chen, 2008): 1) sensory transmission takes place at the brainstem area acting in

descending regulation and the thalamic relay nuclei. The somatosensory cortices (SI, SII) are involved in sensory discrimination of spatial/temporal features of pain. 2) Affect transaction takes place at the insular cortex (IC) and amygdala, which trigger autonomous effector mechanisms via projections to the hypothalamus. They are also involved in descending pain control via projections to the midbrain periaqueductal grey (PAG). 3) Anterior cingulate (ACC), prefrontal cortex (PFC), posterior parietal cortex (PPC), and supplemental motor area (SMA) are involved in cognitive attention, response selection, and action planning.
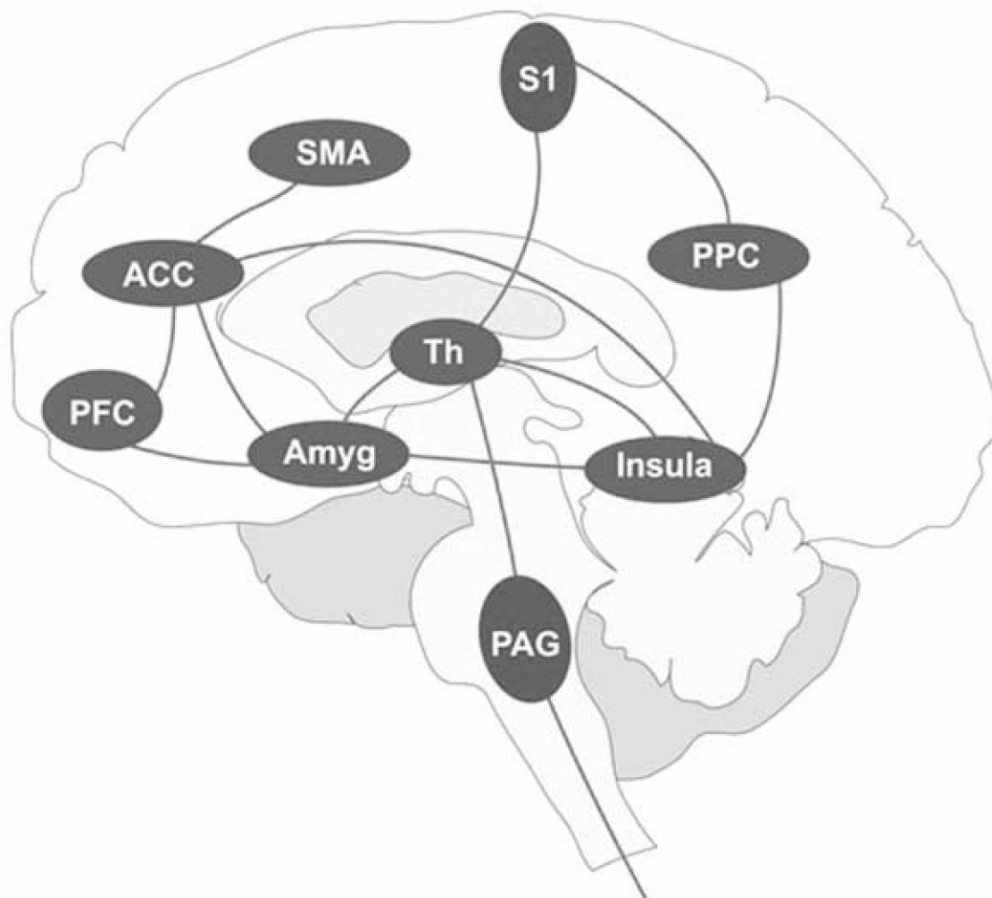
Fig. 2-1. Illustration of the pain neuromatrix according to May (2007). The sensory perceptual system is composed of brainstem (periaqueductal grey, PAG), thalamus (Th), primary and secondary somatosensory cortices (SI, SII). It is involved in ascending transmission, localization and descending regulation of pain. The affective motivational system is composed of amygdala, insular cortex, anterior cingulate (ACC) and hypothalamus. It is involved in affective reaction, autonomous activation and homeostasis regulation. The cognitive-evaluation system is composed of the posterior parietal cortex (PPC), ACC, supplemental motor area (SMA), and prefrontal cortex (PFC). It is involved in spatial/bodily attention, action planning and execution.

Neuroimaging studies mainly focus on the cognitive modulation of the painful percept. Much less is known about the interaction between pain and emotion. There are, however, numerous observations that suggest a link between sensory and affective

domains. Clinically, patients with affective disorders can suffer increased clinical pain. About 50% of patients with depressive disorders report facial pain, headache, and musculoskeletal symptoms (Knorring, 1975). Lower back pain is more than 2 times as likely in patients with symptoms of anxiety and depression compared to controls (Croft and others, 1995). A longitudinal cohort study has shown that depressive symptoms predict future episodes of musculoskeletal pain (Leino and Magni, 1993). On the other hand, subjects with chronic pain (defined as pain for most days for at least a month) are 3 times as likely to meet depression criteria as those without chronic pain (Magni and others, 1993). The association between depression and pain correlates with severity of either condition. Specifically, as the severity of pain increases, depressive symptoms and depression diagnoses become more prevalent (Moldin and others, 1993). Conversely, as depression and anxiety symptoms increase in severity, somatic complaints are reported more often (Von and others, 1988).

Affective disorders are characterized by an altered perception of sensory inputs suggesting that a disturbed affective state may impact on the processing of pain. For example, increased thermal pain thresholds were reported in depressive patients (Lautenbacher and others, 1994). In adjustment disorder, depression scores correlate with thermal pain thresholds (Bär and others, 2006). It has been shown that pain thresholds in patients with major depression or adjustment disorder depend on modality. Specifically, patients are more sensitive to ischemic pain as an exampled for 'deep somatic pain', whereas pain thresholds are increased for phasic stimuli applied on the skin surface (Bär and others, 2005). This led to the idea that visceral, endogenous pain is perceived as particularly distressing in these disorders. Concordantly, Kudoh et al. have shown an increase in pain scores in depressed patients after surgery, which correlates with the degree of depressive symptoms (Kudoh, Katagai, and Takazawa, 2002). This finding has been linked to a persistent increase in plasma cortisol postoperatively in depressed patients (Kudoh, Ishihara, and Matsuki, 2000).

Dysregulation of the hypothalamic-pituitary-adrenal axis (HPA) has been proposed as a common denominator for both major depression and chronic pain syndromes. Emotional distress causes an increased release of 'stress hormone' corticotrophin releasing factor (CRF) in the hypothalamus via afferents from the amygdala resulting in HPA hyperactivity in major depressive disorder (MDD) and other psychiatric illnesses (Robert, 2007). Increased plasma cortisol reduces neurogenesis, inflicts neuronal damage in the hippocampus and disrupts the negative glucocorticoid feedback on the HPA axis

(Blackburn-Munro and Blackburn-Munro, 2001;Nestler and others, 2002). Chronic pain is a persistent stressor, which augments HPA dysfunction by down-regulating glucocorticoid receptors in the brain and periphery, and promotes the generation of higher glucocorticoid levels due to diminished negative feedback control (Blackburn-Munro and Blackburn-Munro, 2001).

Pain is an unpleasant sensation, i.e. pain is emotionally salient *per se*. It follows that pain and emotion processing might overlap in the brain. Melzack proposes that pain has a motivational, affective and a sensory discriminatory component (Melzack, 2001). Anatomically, the Pain system can be subdivided into a lateral and medial component depending on whether spinal inputs are relayed via lateral thalamic or midline thalamic relays (Bowsher, 1957). The lateral system conveys sensory-discriminatory information about the painful agent to the somatosensory cortices. On the other hand, the medial pain system is widely connected to the limbic system including insula, amygdala, ACC and brainstem regions. Various studies emphasize a key role of these limbic regions in the processing of arousing and highly motivating stimuli such as fear and anxiety (Phillips and others, 2003). Increased activity in the amygdala and insular regions were reported in emotion related disorders, for example posttraumatic stress disorders, social anxiety disorder and phobias (Etkin and Wager, 2007). On the other hand the insular cortex is the most consistently found pain responsive brain region according to meta-analyses of imaging studies on experimentally induced pain (Apkarian and others, 2005;Peyron, Laurent, and Garcia-Larrea, 2000). Surgical section of the frontal cingulum fasciculus markedly decrease suffering from otherwise intractable pain (Foltz and White, 1968). After ablation of the amygdala and overlying cortex, cats show marked changes in affective behavior, including decreased responsiveness to noxious stimuli (Melzack, 1999). Lesions of the insula cortex have been implicated in a syndrome called 'asymbolia for pain', characterized by the absence of an adequate emotional response to painful stimuli while location and intensity aspects of noxious stimulation are preserved (Berthier, Starkstein, and Leiguarda, 1988).

Relief of depression during pharmacologic treatment is associated with a relief of pain symptoms suggesting a common mechanism for disturbed affective and disturbed somatic processing. More specifically, the degree of depression improvement has been reported to correlate with the amount of pain relief during treatment with doxepin, a tricyclic agent (Ward, Bloom, and Friedel, 1979). In a meta-analysis of placebo controlled studies, antidepressants were reported to be efficient in a variety of non malignant chronic

pain syndromes including arthritis, headache, facial and musculoskeletal pain (Onghena and Van, 1992). Moreover, their role in cancer pain management is established (Lussier, Huskey, and Portenoy, 2004). Animal studies indicate that tricyclic antidepressants have analgesic properties *per se*, which are particularly evident in models of subchronic inflammatory pain, but less prominent in acute noxious stimulation applied to the skin surface (Korzeniewska-Rybicka and Plaznik, 1998). Conceptually, the former type of pain is an example of endogenous, deep somatic pain that is emotionally salient due to its persistent and threatening character as opposed to phasic cutaneous simulation, which is more closely related to an exteroceptive sensory rather than an interoceptive affective sensation. The efficiency of antidepressants in endogenous, visceral pain and affective disorders suggest a common neurochemical basis for both conditions. The biochemical theory of depression posits an imbalance in monoaminergic neurotransmission. Serotonergic and noradrenergic neurons are prevalent in the output nuclei of descending pain modulation system in the rostral-ventromedial medulla and the dorsolateral pontine tegmentum; the system filters nociceptive information at the dorsal horn via descending projections. Depletion of these neurotransmitters in depression may compromise this filter such that innocuous signals from the body are amplified resulting in a painful percept (Stahl, 2002).

The amygdala is a key structure in attaching emotional significance to polymodal inputs. Interestingly, subdivisions of the amygdala are specialized for processing of nociceptive information that is conveyed in spinal, cortical and subcortical pathways (Neugebauer and others, 2004). Inflammatory pain can induce neuroplastic changes in the central amygdaloid nucleus (CeA) of the rat, which leads to a widespread decrease of mechanical pain thresholds (Neugebauer and Li, 2003). On the other hand, stereotactic stimulation of the CeA with glucocorticoids promotes the transcription of corticotrophin-releasing factor and increases anxiety related behavior in rats (Shepard, Barron, and Myers, 2000). Concomitantly, glucocorticoids produce visceral hypersensitivity to colorectal distension that correlates with anxiety scores (Greenwood-Van and others, 2001). Concordantly in humans, episodes of anxiety may exacerbate visceral pain in patients with irritable bowel. In a rodent model of arthritic pain, blockade of CRF receptors in the amygdala inhibited both anxiety-like behavior and nocifensive pain responses (Ji and others, 2007). The role of the amygdala for pain processing is further highlighted by the observation that microinjections of opioid agonists such as morphine into the amygdala have strong analgesic effects in rats (Helmstetter, Bellgowan, and Tershner, 1993).

Additionally, chronic pain in mice facilitates the development of anxiety-like behavior that is accompanied with changes in the opioidergic function in the amygdala (Narita and others, 2006).

Several imaging studies report limbic activation in response to pain underscoring its affective character and close relationship to emotion processing. Increased fear of pain predicts a higher activity in anterior cingulate cortex (Ochsner and others, 2006). A hypnotically induced negative affective state towards painful stimulation was reported to be associated with an activity increase in anterior insula and ACC (Rainville and others, 1997). Opioid analgetics have been shown to dampen the response to experimental pain in the lateral system in a dose dependent manner, whereas activity in the anterior insula and amygdala, which process the 'suffering' component of the pain experience, disappeared at the lowest dose confirming the clinical observation that low doses relief the affective but not the sensory component of pain (Oertel and others, 2008). In fibromyalgia patients insula and ACC, i.e. regions associated with the affective dimension of pain, become activated during epochs of rapidly increasing endogenous pain (Baliki and others, 2006). In chronic pain patients, depressive symptoms correlate with pain related activity in brain regions associated with affective processing such as amygdalae and insula, but not regions associated with the sensory dimension of pain, i.e. the somatosensory cortices (Giesecke and others, 2005). In healthy subjects it has been demonstrated that social exclusion ('social pain') activates regions implicated in the processing of somatic pain (Eisenberger, Lieberman, and Williams, 2003). Specifically, ACC activation correlated with self reported emotional distress arising from this unpleasant albeit non-physical experience. Additionally, the affective but not the sensory components of the pain neuromatrix have been suggested to mediate empathy for pain in others (Singer and others, 2004). Recently, Von Leupoldt and colleagues have shown that experimentally induced dyspnoe, which conforms to a strong anxiogenic stimulation, and heat pain engage a common limbic network in healthy subjects (von Leupoldt and others, 2009).

Human language implies that pain and emotionality are two different concepts. In the conventional view pain is categorized as an exteroceptive modality, i.e. related to external touch rather than to an internal feeling state. This view discounts the fact that physical pain is an unpleasant feeling *per se* and regularly evokes strong negative emotions in the sufferer. These emotions in turn drive adaptive behaviors that may be crucial for survival. Individuals who are unable to experience pain, die from infections injuries that remain undetected (Baxter and Olszewski, 1960). The above mentioned IASP definition of

pain emphasizes its function to preserve body integrity. Concordantly, clinicians appreciate pain as the fifth vital sign. It has been proposed that pain is an interoceptive rather than an exteroceptive sensation reflecting an adverse physiologic condition within the body that requires a behavioral response (Craig, 2002;Craig, 2003). Craig and colleagues suggest that the insular cortex maintains an encephalized representation of the physiological state of the body that receives inputs from sympathetic and parasympathetic afferents via a phylogenetical distinct thalamocortical relay (Craig and Blomqvist, 2002;Craig, 2003). Injury constitutes are threat to a balanced physiological state of the body; pain is therefore conceptually similar to respiratory distress, thirst, hunger, aversive taste and other sensations that announce or represent a threat to body homeostasis. A common limbic network including the insula and ACC might translate the physiologic relevance of these unpleasant signals into adaptive behavior that supports survival. Moreover, the conception of pain as a 'homeostatic emotion' (Craig, 2003) allows linking pain to perceptual signals that are of relevance for the survival of social animals like humans although they do not directly represent a physical threat. Language is abundant with examples that link social distress and emotionality to the experience of pain: The phrase "you hurt my feelings", for instance, suggests that a perturbation in the emotional domain in the context of social interactions can cause feelings that resemble pain and therefore may motivate adaptive social behavior. In this context it is interesting to note that patients with cortical lesions in the insular cortex not only show diminished emotional responses to painful stimuli, but also to aversive social signals like threatening gestures and verbal menaces (Berthier, Starkstein, and Leiguarda, 1988).

In conclusion, there is plenty of experimental evidence on various levels suggesting that pain and emotion related processing share a common neural substrate. According to the conception of pain as homeostatic emotion, the maintenance of a physiological body state is the common purpose of both sensations. We tested the hypothesis of a common neural network in a region of interest (ROI) approach using BOLD fMRI. In a first step we will define the pain neuromatrix in a separate localizer experiment (ROI localizer) by contrasting painful trials with non-painful trials. In a second step we will investigate how painful and emotional stimuli interact within this neuromatrix definition. For this purpose we adapted a paradigm that was repeatedly shown to elicit a strong and reliable amygdala activation (Pezawas and others, 2005;Meyer-Lindenberg and others, 2008;Hariri, Bookheimer, and Mazziotta, 2000;Hariri and others, 2002c;Hariri and others, 2002a;Hariri and others, 2002b). Angry and fearful facial expressions were used to induce a negative

affective state in the observer. It has been shown that a) these stimuli elicit an autonomous stress response and b) elicit a stronger amygdala response than nonsocial emotional stressors (Hariri and others, 2002c). In keeping with the experimental evidence outlined above, we expect the amygdala to respond to both aversive faces and physical pain. We further suggest that the conception of pain as 'homeostatic emotion' (Craig, 2003) allows linking pain to aversive social signals that do not directly represent a physical threat but are nevertheless survival relevant to social animals like humans. We therefore hypothesize, that the pain neuromatrix is responsive to aversive faces, i.e. a non physical but emotionally arousing stressor.

2.2 Materials and Methods

2.2.1 Subjects

cf. section 1.2.1.

2.2.2 Apparatus

Data acquisition was performed at the University of Regensburg on a 1.5 Tesla scanner (Siemens Sonata, Erlangen) equipped with an eight channel array head coil. Subjects lay supine in the MRI tube holding an MRI compatible response device in their right and a 'panic ball' in their left hand throughout the experiment. They were instructed to squeeze the panic ball when they wished to abort the acquisition procedure. Subjects were equipped with ear plugs and wore a headphone for protection against acoustic noise (100 dB). Thermal stimuli were delivered by the TSA II (Medoc Inc., Israel) that was operated outside the scanner room in fMRI configuration: the standard thermode was replaced by a 6 meter fMRI compatible variant, which was connected to the TSA II via a grounded filter element. The filter minimizes electromagnetic interference that would otherwise compromise image quality; it was inserted into a 2.5" diameter in-wall pipe collar. Filter grounding was verified with an ohmmeter. The 30x30 mm^2 contact thermode was attached to the participants left wrist (volar surface) and fastened with eudermic adhesive tape. The pre-defined thermal stimulus sequence was controlled by the TSA II software running on an IBM compatible Laptop under MS Windows XP. Visual stimuli were back-projected on a screen mounted at the rear end of the scanner and conveyed to the participant via a head coil mounted mirror. The visible stimulus screen subtended 20° of visual angle. Visual

stimuli were delivered at a resolution of 1024x768 pixels, a frame rate of 60 Hz, and a color depth of 24 bits per pixel. Stimulus presentation was controlled by Presentation software (v. 14.0, Neurobehavioral Systems Inc., Albany, CA) running under Windows XP on an IBM compatible Desktop PC. The parallel port (pin 2) of this PC was connected to the TSA TTL input port. Through this connection, Presentation software conveys a 150 ms trigger pulse that initiates the temperature ascent interval (10 seconds) that precedes every pain trial. The target temperature is then maintained until a return to baseline (ramp down interval, 10 seconds) is enforced by the next trigger pulse, which is sent 20 seconds later, i.e. at the end of that trial. Note that a constant temperature is maintained by the TSA software between any two pulses. Every TR (2.5 seconds), Presentation software receives a trigger pulse from the MRI scanner via pin 12 of the parallel port. This enables synchronization of visual and thermal stimulus presentation with fMRI data acquisition. Specifically, scanner pulses triggered the beginning of each trial and the beginning of each temperature ascent/descent interval. The participant's responses are submitted via an MRI compatible response device and recorded with millisecond precision by the presentation software. Thermal and visual stimulus sequences are recorded in separate logfiles generated by the TSA software and the Presentation software, respectively. These files were obtained from every participant and were carefully checked in order to verify that no triggers (MRI triggers and TSA triggers) had been missed.

2.2.3 Stimuli

Facial stimuli were drawn from the FEEST (Facial Expressions of Emotion: Stimuli and Tests) picture set (Young and others, 2002). FEEST stimuli are based on a subset of the Pictures Of Facial Affect (POFA) series (Ekman and Friesen, 1978): 10 models (4 males, 6 females) were selected based on how reliably their facial expressions can be identified. FEEST provides emotional continua ranging from neutral poses (0% intensity) over the prototype expressions of the POFA series (100% intensity) to the most extreme representation of each basic emotion (150 % intensity). These continua were generated from the original POFA images using image manipulation techniques. In our study, we hypothesize a modulation of pain responsive brain areas by a psychosocial stressor. Presumably, this stressor must be highly aversive so as to elicit activation in regions that are not specialized to process facial stimuli. We thus selected the angriest and most fearful expressions available (150% intensity). The hairlines of the FEEST stimuli are masked ensuring that participants base their responses in the face matching task (cf. section 2.2.4)

on facial features rather than on hairstyle or background details. **Fig. 2-2** shows the stimuli employed in the Matching Task paradigm.

Females
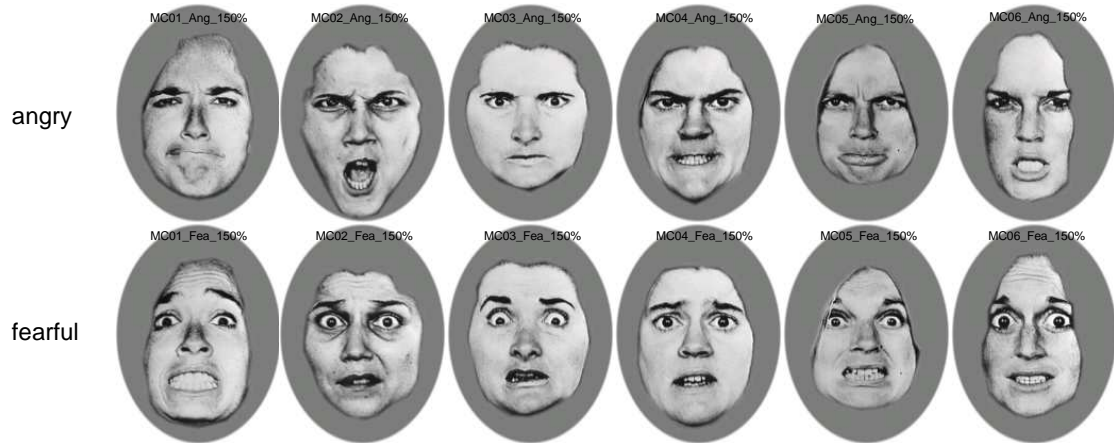
Males
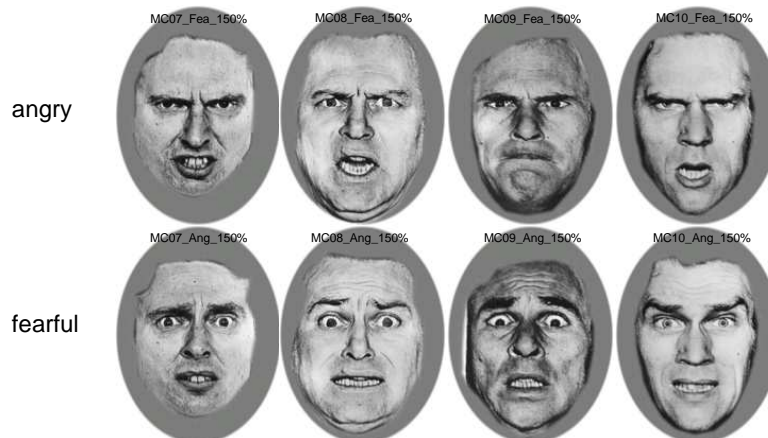
Forms

Fig. 2-2. Face and form stimuli employed in the Matching Task paradigm. Facial stimuli were drawn from the FEEST picture set (Young and others, 2002). The corresponding FEEST filenames are indicated (the file extension '.jpg' is omitted).

The FEEST images were adequately resized (scaling factor: .7) and cropped into an elliptical shape using customized MATLAB scripts. The ellipse's boundary smoothly blends with the background white in order to prevent retinal afterimages on stimulus change. Horizontal and vertical ellipses for the control task were produced by applying the

same cropping mask to an area of intermediate grey. The disk was generated by non-proportionally scaling an ellipse while preserving the area content. The pixel gray level was chosen to approximate the mean luminance level of the facial images (assuming a gamma value of 2.2 as measured with standardized scales). **Fig. 2-3** shows examples of two stimulus screens. These are comprised of either three geometric forms or three facial stimuli (here: angry males). The images are arranged in trios with their centers being aligned to the corners of an equally sided triangle. This ensures that stimuli are distributed evenly within the field of view subtending a visual angle of 20 degrees. The regular arrangement also helps equating visual search efforts across trials. In the preceding ramping intervals, a fixation cross is shown in the triangle center, i.e. in the center of the visual field.
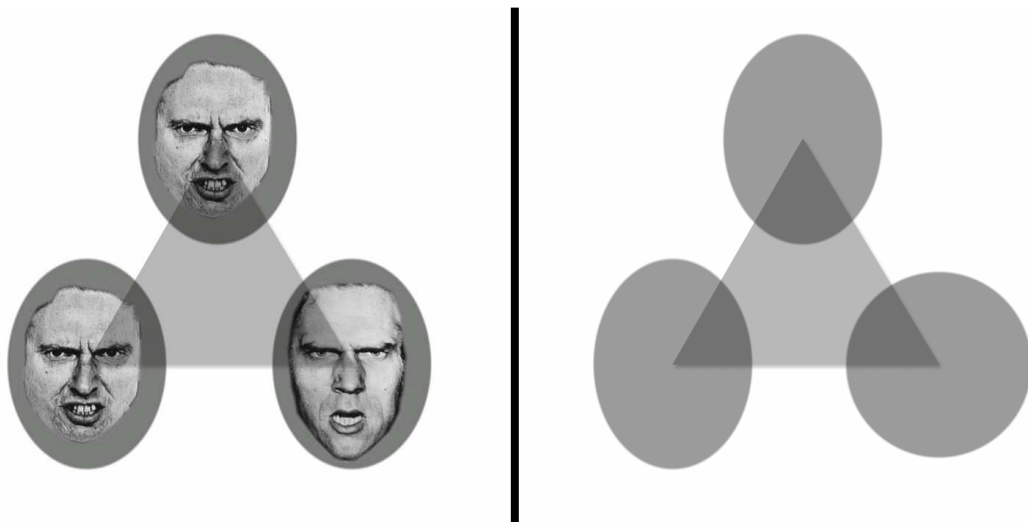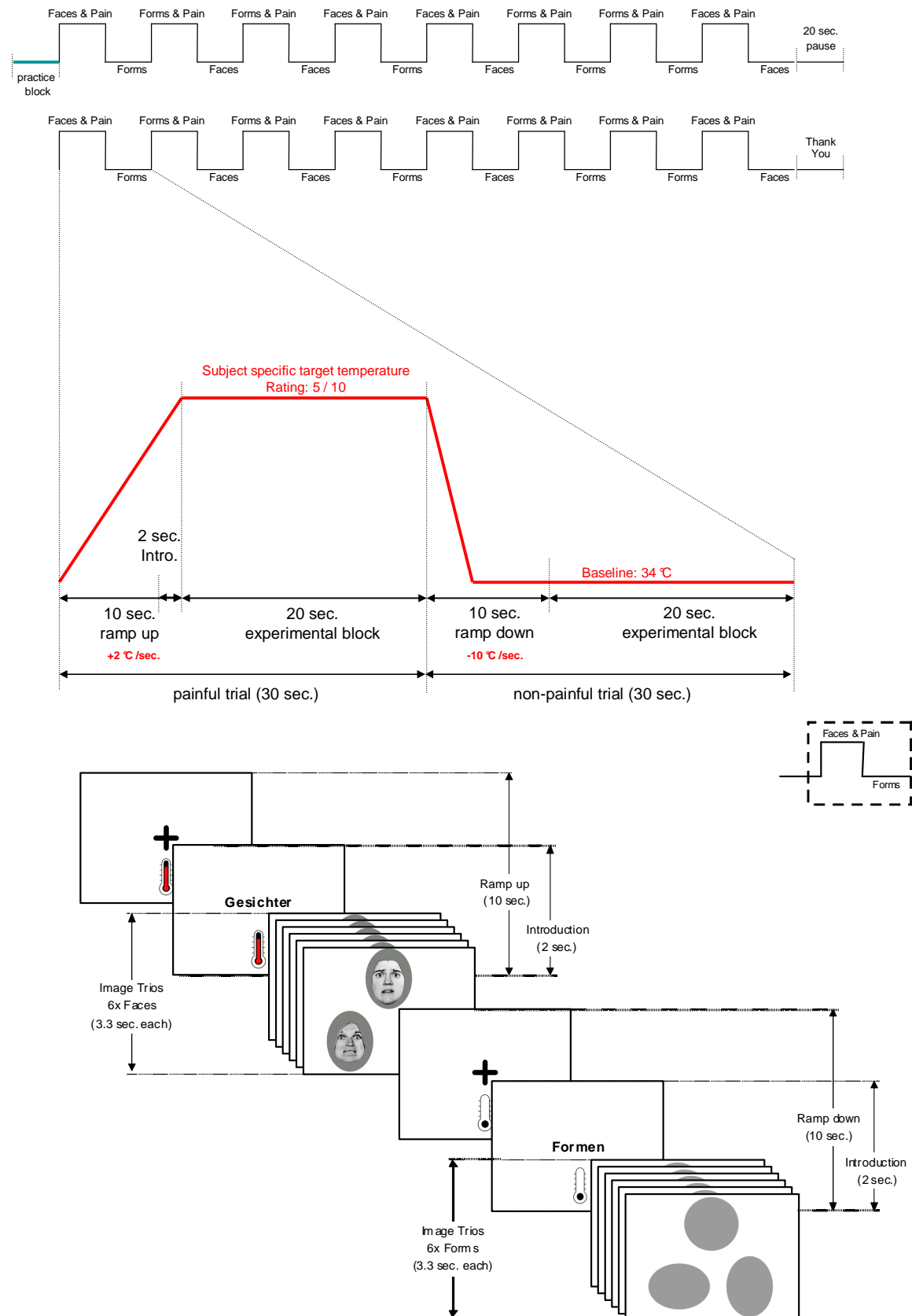

Fig. 2-3. Example of a stimulus screen in the face matching (left) and form matching task (right). In each image trio, one of the bottom images is identical with the top image (here: the right bottom image in both examples). The triangle illustrates the equidistant arrangement of images and is not displayed during the experiment.

2.2.4 Experimental Paradigm

2.2.4.1 Matching Task

We adapted an established paradigm of amygdala activation (Hariri, Bookheimer, and Mazziotta, 2000). In a blocked design, image trios of geometric forms (circles and ellipses) and faces of each gender (male / female) and emotional expression (angry / fearful) are combined with either innocuous warmth (34°C) or heat pain of medium intensity. The thermal stimulus corresponds to a subject-specific pain rating of 5 on a scale from 0 to 10,

where 0 and 10 indicate a non-painful and intolerably painful sensation, respectively. This conforms to a 2 x 2 full factorial design with factor 'pain' (pain *vs.* no pain) and factor 'emotion' (faces *vs.* forms). The top image of a trio is identical with one of the two bottom images. The incidental task was to find the identical image and press a corresponding button on the response device (left image: index finger; right image: middle finger). Response time and response accuracy were recorded. Good accuracy indicates that the subjects attended to the stimuli.

Faces & Pain   Forms & Pain   Forms & Pain   Faces & Pain   Faces & Pain   Forms & Pain   Forms & Pain   Faces & Pain

20 sec. pause

practice block

Forms   Faces   Faces   Forms   Faces   Forms   Forms   Faces

Faces & Pain   Forms & Pain   Forms & Pain   Faces & Pain   Faces & Pain   Forms & Pain   Forms & Pain   Faces & Pain

Thank You

Forms   Faces   Faces   Forms   Faces   Forms   Forms   Faces

Subject specific target temperature
Rating: 5 / 10

2 sec. Intro.

Baseline: 34 ℃

10 sec. ramp up   20 sec. experimental block   10 sec. ramp down   20 sec. experimental block

+2 ℃ /sec.   -10 ℃ /sec.

painful trial (30 sec.)   non-painful trial (30 sec.)

Faces & Pain

Forms

Ramp up (10 sec.)

Introduction (2 sec.)

Gesichter

Image Trios 6x Faces (3.3 sec. each)

Ramp down (10 sec.)

Introduction (2 sec.)

Formen

Image Trios 6x Forms (3.3 sec. each)

Fig. 2-4. Stimulus sequence and trial structure in the Matching Task paradigm. *Upper panel:* Temporal sequence of experimental blocks. Eight blocks per condition were presented (32 blocks total). *Middle panel:* Timecourse of thermal stimulation (red line) during two consecutive trials. The ramping intervals were not included in the SPM model. *Lower panel:* Visual stimulation during two consecutive trials.

The Matching paradigm is illustrated in **Fig. 2-4**. The paradigm is comprised of four experimental conditions conforming to a 2 x 2 full factorial design: form matching without pain ('Forms'), form matching with pain ('Forms & Pain'), face matching without pain ('Faces'), and face matching with pain ('Faces & Pain'). Following a short task description (5 seconds), a practice block ('Forms') is run. In total, 32 experimental blocks were presented (eight blocks per experimental condition). Painful stimulation is block-wise alternating with innocuous warmth (34 °C). After 16 blocks, there is a 20 second pause without stimulation except for a fixation cross. The paradigm closes with a screen displaying the phrase "Thank You!". In a given block, six stimulus screens of one category (faces or forms) are presented for 3.3 seconds each without interstimulus interval, yielding a block length of 20 seconds. In a face matching block, each sex (male/female), facial expression (angry/fearful) and target position (left/right) appear equally often (3x); image trios with male and female models are alternating. Each image (form or face) appears equally of often as target and distractor. Identical target-distractor pairings are distributed evenly across painful and non-painful conditions. A painful block is preceded by a ramp up interval (10 seconds): temperature rises linearly (at 2°C per second) until the target intensity is reached, which is held constant during the subsequent block. Similarly, a non-painful block is preceded by a ramp down interval, during which temperature linearly descents to baseline (34 °C) at a speed of 10°C per second. This interval again lasts 10 seconds to allow the BOLD signal to settle and the participants to recover from their painful experience. During these intervals the upcoming block is introduced: a temperature symbol indicates the type of thermal stimulation (heat pain or innocuous warmth); during the last 2 seconds a text label is shown announcing the stimulus category (faces or forms). The ramping intervals are not included in the SPM statistical model.

Four SPM contrasts were interesting to us, which correspond to the main effects and the interaction effect of a 2 x 2 full factorial design. Care was taken to optimize the block sequence in this regard. The transition matrix is shown in Table 2.2-1. A given block is preceded equally often by a block with forms and by a block with faces. First order sequence effects are thus balanced with respect to the interaction contrast and the 'Faces > Forms' contrast (that indicates the main effect of factor 'emotion'). As painful and non-painful blocks are alternating, sequence effects are not balanced with respect to the 'Pain > No Pain' contrast (that indicates the main effect of factor 'pain'). However, we opted for this design, since the alternation allows the subject to recover from the previous painful stimulation, which helps preserving compliance and limiting skin irritation (and,

consequently, habituation and sensitization effects). To optimize the frequency content of the sequence, each experimental condition appeared once within four consecutive blocks. This ensures that the conditions that we wish to contrast are not too far apart in time. At most 120 seconds pass between any two conditions; this is below the high pass filter cut off value (128 seconds). Experimental variance is thus preserved while low frequency noise is removed.

Table 2.2-1. Matching Task. Transition matrix of experimental conditions.

		Experimental condition in block *n*			
		Forms	Forms & Pain	Faces	Faces & Pain
Experimental condition in block *n-1*	Forms	-	4	-	4
	Forms & Pain	4	-	4	-
	Faces	-	4	-	4
	Faces & Pain	4	-	4	-

The table gives the number of experimental conditions that are presented in two consecutive blocks. A given condition is equally often preceded by a form matching and a face matching condition, namely four times. Sequence effects are thus partially balanced (see text).

2.2.4.2 Pain Neuromatrix Localizer (ROI Localizer)

The paradigm is illustrated in **Fig. 2-5**. In total, 20 blocks lasting 20 seconds each were presented. Painful stimulation corresponding to a subject-specific rating of 8 out of 10 is alternating with innocuous warmth (34 °C baseline temperature). In the center of the screen a fixation cross is shown throughout the experiment. The cross blinks twice during a block: after 5 and 15 seconds with a jitter of ±100 ms. Participants are instructed to press a button on the response device as soon as the cross blinks. This incidental task is to ensure constant vigilance during the experiment. Each block is preceded by a ramping interval of 10 seconds that is not included in the SPM analysis. Temperature rises at a rate of 2 °C per second, is held constant during the subsequent painful block and then falls back to baseline

(34 °C) at a rate of 10°C per second. The paradigm is concluded with a screen displaying the phrase: "Thank You!".
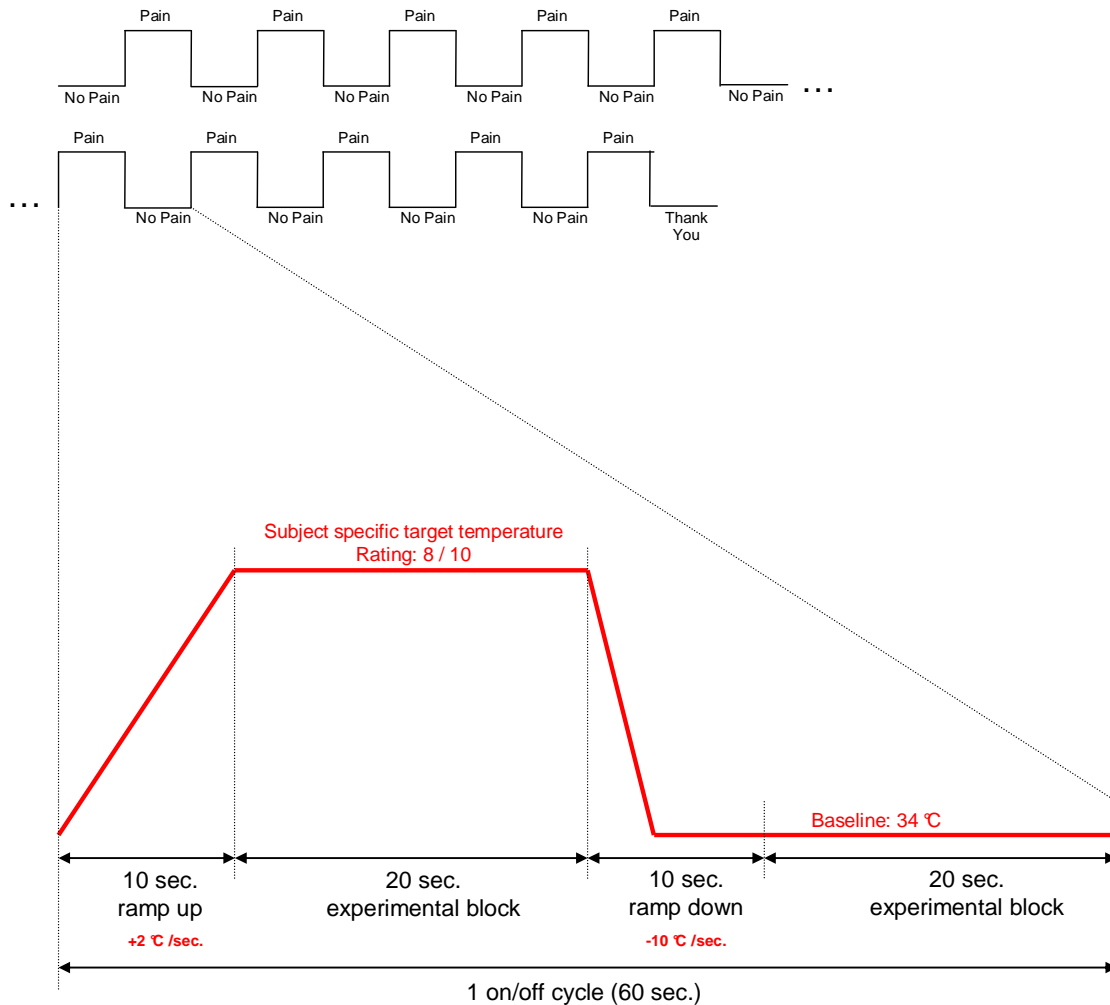
Fig. 2-5. Stimulus sequence and trial structure in the Localizer paradigm. *Upper panel:* Temporal sequence of experimental blocks. Painful stimulation ('Pain') is alternating with innocuous warmth ('No Pain'). *Lower panel:* Timecourse of thermal stimulation (red line) during two consecutive trials. Ramping intervals were not included in the SPM model.

2.2.5 Imaging Protocol

Prior to data acquisition, an automatic shimming procedure was applied to minimize magnetic field inhomogeneity. Locations of co-planar image planes were defined on a T1 weighted structural localizer scan. Slice orientation was parallel to the AC-PC plane. Functional data were acquired using the same imaging protocol for both experimental sessions (ROI Localizer and Matching Paradigm): a T2* weighted gradient echoplanar imaging (EPI) protocol (TR=2500 ms, TE=50 ms, 34 slices, FoV=192 mm, flip angle=90°, 3×3×3.3 mm voxel size, ROI Localizer: 249 scans, Matching Paradigm: 420 scans). Each

session started with two 'dummy' scans allowing for steady-state tissue magnetization. Slices were recorded in an interleaved order, i.e. acquisition of spatially adjacent slices was delayed by TR/2. This is to minimize artifacts caused by interactions between excited slices ('cross talk'). For each participant, a high resolution brain image was recorded in the same orientation as the functional images to enable accurate location of individual brain activity. For this purpose an MP-RAGE three dimensional T1 weighted, gradient echo sequence was used (TR=1880 ms, TE=3.42 ms, 176 slices, FoV=256 mm, flip angle=15°, 1×1×1 mm voxel size).

2.2.6 Procedure

FMRI sessions were scheduled between 4:30 PM and 8:00 PM. Prior to the experiment, the subjects completed several trials of a practice paradigm outside the scanner to get familiar with the task and response scheme. Instead of the FEEST stimuli, happy and neutral facial expressions from the NimStim picture set (Tottenham and others, 2009), which is available upon request at http://www.macbrain.org/ (as of 3/1/2010), were used to avoid carry over effects. No thermal stimulation was administered in the training paradigm, which was otherwise identical with the matching paradigm described above. Subjects were then positioned in the MR tube. After the automatic shimming procedure, the structural localizer scan was run and the subjects were re-positioned if necessary. The matching paradigm was run first (18 min), followed by the anatomical scan (4 min) and the localizer paradigm (10 min). The three sessions were announced via loudspeakers and succeeded without temporal gap. The participants stayed within the MR tube during the whole procedure, which they could abort at any time by squeezing the 'panic ball'.

2.2.7 FMRI data analysis

2.2.7.1 Preprocessing

Data analysis was conducted using the SPM 5 software package (Wellcome Department of Imaging Neuroscience, London) running under MATLAB 7.5 (TheMathWorks, Natick, MA). Prior to statistical analysis, anatomical and functional image files were converted from Digital Imaging and Communications in Medicine (DICOM) format into the Neuroimaging Informatics Technology Initiative (NIfTI) format which is more amenable to image processing operations and statistical data analysis.

Preprocessing of functional time series consists of fours steps, outlined in detail below: motion correction, coregistration with a structural brain scan, normalization to a common anatomical template and smoothing. This sequence serves four main goals:

i)   Optimization of signal to noise ratio (SNR) by means of motion correction and smoothing

ii)   Mapping of activation foci to structural anatomy by means of coregistration

iii)   Results reporting in a common stereotactic space by means of normalization

iv)   Facilitation of group level data analysis by means of normalization and smoothing.

2.2.7.1.1 Motion correction

Small involuntary head movements during image acquisition cannot be fully avoided, which poses a problem, since the acquisition window (field of view) is fixed. Consequently, the sampling location of a voxel changes depending on direction and magnitude of head movements. If left unchecked, these movements would constitute a substantial nuisance variable precluding statistical data analysis. The motion correction procedure reverses motion by translating and rotating each scan (source image) to be in alignment with a representative reference scan (reference image). Functional images were realigned to the first image of each session using a rigid body model (Friston and others, 1995). This model relies on a six parameter affine transformation that involves rotations around and translations along the x-,y-, and z axes. For a given scan, the algorithm finds the optimal solution by minimizing the voxel-by-voxel intensity difference between that scan and its reference using the method of least squares. Scans from the ROI localizer and matching paradigms were entered as separate sessions into the motion correction procedure. According to the SPM5 manual, the sessions are first realigned to each other by aligning the first scan of the first session to the first scan of the second session. Then the remaining scans within each session are aligned to the first scan of that session. In this way systematic differences between the sessions are accounted for. Motion correction is concluded with the creation of a mean functional image that is representative for the time series of both sessions. Note that motion also causes magnetic field inhomogeneities that influence signal to noise ratio and are not accounted for by the realignment algorithm. This issue was addressed by including the realignment parameters in the statistical model (see below).

2.2.7.1.2 Coregistration

Functional images are of low resolution and contrast and do not reveal structural details of the brain. Coregistration is needed to describe activation foci with respect to individual gyral anatomy. The procedure is conceptually similar to motion correction in that two neuroimages are aligned with each other. A twelve parameter affine transformation is applied to the high resolution structural scan (source image) to bring it into alignment with the functional mean image (reference image) that was created during motion correction. In contradistinction to motion correction, source and reference have different image characteristics. Cerebrospinal fluid, for example, appears dark in the T1 weighted structural scan but is bright in T2* weighted functional scans. Therefore, an intensity based similarity measure, as employed in the realignment step above, is not applicable here. Instead, the so called mutual information (Maes and others, 1997) is maximized to obtain optimal transformation parameters. Mutual information is a general measure describing the strength of statistical dependency between the two images irrespective of the modality they may have.

2.2.7.1.3 Normalization

Brain geometry naturally differs across subjects. To account for this variability each subject's structural scan is aligned ('normalized') to a template image that conforms to a common stereotactic space. This template is provided by the Montreal Neurological Institute and consists in the average of 152 brains of young and healthy subjects (Collins and others, 1994). The Talairach coordinate convention (Talairach and Tournoux, 1988) is imposed on this template-defined anatomical space. Specifically, the origin is set to the anterior commissure (AC). The line between the AC and the posterior commissure (PC) is assumed exactly horizontal, $x > 0$ is right of the midsagittal plane, $y > 0$ is anterior to the AC, and $z > 0$ is superior to AC–PC plane. Ideally, each x/y/z triple corresponds to the same anatomical location in all normalized brains. Note, however, that intersubject variability in gyral anatomy ranges from 9 to 18 mm after an affine stereotactic normalization (Thompson and others, 1996). Normalization allows for reporting activation foci within a common reference system and thus facilitates scientific communication and comparison of results across studies. For group level analysis, normalization to a common template is mandatory since otherwise anatomical variability inherent to the sample will largely preclude intersubject averaging of BOLD related activity (Ashburner and Friston, 1997). The found normalization parameters were then applied on the functional scans in

order to normalize them to the MNI template, as well. This is straightforward, since functional and anatomical scans have been coregistered in the previous step. Normalized functional images were resampled to 2 x 2 x 2 mm using trilinear interpolation to minimize partial volume effects. Each voxel thus encompasses a volume of 8 mm^3 (8 μl).

Normalization is similar to motion correction in that two neuroimages are aligned to each other. Specifically, the subject's structural scan (source) is aligned to the MNI template (reference). Source and reference are T1 weighted images, i.e. share the same image characteristics. Therefore, normalization uses an intensity based cost function. In contradistinction to motion correction, source and reference images belong to different subjects. The ensuing differences in brain geometry cannot be fully accommodated by a rigid body model. A more flexible approach is required: Firstly, a 12 parameter affine transformation of the source image is performed. Shape and size differences may thus be accommodated by zooming and shearing the brain in the three orthogonal image planes. Secondly, residual anatomical variability is accounted for by nonlinear transformations (Ashburner and Friston, 1999). These are described by combinations of three dimensional discrete cosine transforms (DCT). In the present study 7x9x7 DCT basis functions were used to describe warps along each coordinate axis. This nonlinear step in particular adds a lot of free parameters to the normalization model, which holds the risk of being overfitted. In other words: the minimization of the cost function may lead to distorted and implausible normalization results. To avoid overfitting a regularization of medium magnitude is incorporated in affine and nonlinear transformations (using the SPM5 default value: 1), i.e. parameter combinations that do not lie within the expected range were penalized to avoid implausible results (Ashburner and others, 1997;Ashburner and Friston, 1999). Additionally, the normalization result was verified by visual inspection. No misalignment or distortions were detected.

2.2.7.1.4 Smoothing

In the last preprocessing step, functional images a smoothed (convolved) with a Gaussian kernel (8 millimeters full width at half maximum), which is a way of averaging the signal of spatially adjacent voxels. According to the central limit theorem, smoothing will render the distribution of residuals more normal, which is a prerequisite for a valid General Linear Model estimation. Averaging will also reduce the noise component of the data and thus increase its signal to noise ratio (SNR) at the cost of spatial resolution. By the matched filter theorem, this tradeoff between sensitivity and spatial specifity is minimal when the width of the smoothing kernel matches the spatial extent of the anticipated signal. It has

been shown that a FWHM of 10 mm (full-width at half maximum) works best for subcortical regions and 6 mm is best for the cortex (Hopfinger and others, 2000). We chose 8 mm as a compromise. In the context of the group level analyses smoothing facilitates intersubject averaging of functional data. As mentioned above, normalization may leave a considerable amount of structural variability in the sample. Moreover, activation foci are not necessarily bound to the same anatomical structures in all participants and thus constitute an additional source of variability (Brett, Johnsrude, and Owen, 2002). This has to be taken into account by an adequately large smoothing kernel. Otherwise, functional homologous regions do not sufficiently overlap between subjects, precluding meaningful group level inference (White and others, 2001).

Smoothing ensures the applicability of the family-wise error, which is used in the present study to address the multiple comparisons problem. Adjacent voxels in the brain are functionally related and thus become activated conjointly. Bonferroni correction is overly conservative since the premise of independently distributed error terms does not hold. This spatial correlation of residuals ('intrinsic smoothness') can be described by a continuous Gaussian Random Field (GRF). However, a brain scan is composed of discrete units (voxels). If intrinsic smoothness does not sufficiently extend beyond one voxel, it cannot be approximated by a continuous field. To increase overall smoothness the image should be convolved with an adequately large Gaussian kernel. Otherwise the applicability of GRF theory and the family wise error, which is based thereon, is not granted (Worsley and others, 1996).

2.2.7.2 Statistical Analysis

2.2.7.2.1 Behavioral data analysis

For statistical analysis of response times (RTs), SPSS (v. 15.0) software was employed (SPSS Inc., Chicago, IL). Mean RTs were calculated for each condition and pooled across participants. With regards to the ROI localizer, RT differences between painful and non-painful conditions were assessed in a paired samples t-test. With regards to the matching task, RTs were analyzed in a 2 x 2 repeated measures ANOVA with factor 'pain' (pain vs. no pain) and factor 'emotion' (faces vs. forms). Violations of the sphericity assumption were adjusted by the Greenhouse-Geisser method. Response accuracy during the matching task was assessed under the assumption that incorrect responses are rare events that follow a Poisson distribution. 95% confidence intervals around the mean percentage of correct

responses in a given condition were obtained from a corresponding look up table (Schoenberg, 1983). Within-subject effects were evaluated in a Generalized Linear Model framework. This approach differs from the repeated measures ANOVA in that the response variable (number of incorrect responses) is linked to the linear model via a log function (instead of the identity) and assumed to follow a Poisson distribution (instead of a normal distribution). Statistical significance was determined by a two tailed p-value of less than .05.

2.2.7.2.2 FMRI Analysis

Functional data were statistically analyzed adopting a massive univariate approach. Basically, a model is phrased and tested at each voxel against the null hypothesis that any similarity between the observed signal and the model's prediction is due to chance. A statistic (Student's t-statistic) was calculated that reflects evidence against the null hypothesis. The probability of obtaining this statistic under the assumption of chance can be computed from the statistic's null distribution (t-distribution). If this p-value is smaller than a given significance criterion, the null hypothesis is rejected and the model's prediction is assumed to hold at the voxel considered. This conforms to classical inference based on parametric hypothesis testing. The approach is adopted for subject level (first level) and group level (second level) analyses.

In the region of interest (ROI) approach, the outlined strategy is applied to brain regions rather than individual voxels. The multiple comparisons problem is thus reduced from the number of voxels in the brain to the number of investigated regions, which dramatically increases statistically power. However, in contrast to exploratory, voxel-level analyses, the ROI approach requires a region-specific *a priori* hypothesis. In the present study we postulate an activation of the pain neuromatrix and the amygdala by both physical (thermal pain) and psychosocial stressors (facial expressions). Importantly, these regions of interest were defined independently from the experiment proper to rule out circular argument.

Model specification

A prediction model is specified in a so-called design matrix. Each row in this matrix refers to a functional scan; each column refers to an experimental condition. The columns contain binary index variables that indicate scans, during which condition-specific stimulation was delivered. The columns (predictor variables) are then convolved with the canonical hemodynamic response function (HRF). The HRF is the impulse response of the system,

i.e. it reflects the response to a single neural event. A blocked design can be viewed as a conglomeration of many such events. In this way, the predicted hemodynamic response time course is generated for each experimental condition.

Separate design matrices were formulated for ROI Localizer and Matching Task sessions (see **Fig. 2-6**). Experimental conditions were modeled as boxcars (20 seconds) convolved with the canonical hemodynamic response function. Each column (predictor variable) in the design matrix thus reflects the BOLD signal time course that is expected to be elicited in the respective experimental condition. The ramping phases (10 seconds each) were not explicitly modeled. The six realignment parameters were added to the model as covariates of no interest in order to reduce residual movement related variance that was not accounted for by the realignment procedure (cf. section 2.2.7.1.1). Another source of non-experimental variance is comprised of low frequency noise due to scanner drifts and aliased biorhythms, e.g. cardiac and respiratory cycles. Therefore, a high pass filter was incorporated into the design matrix to remove frequencies below 1/128 Hz. Note that this filter is not explicitly shown in SPM5 designs matrices (**Fig. 2-6**). To account for session specific signal gains, activity was ratio normalized to the whole brain global mean.
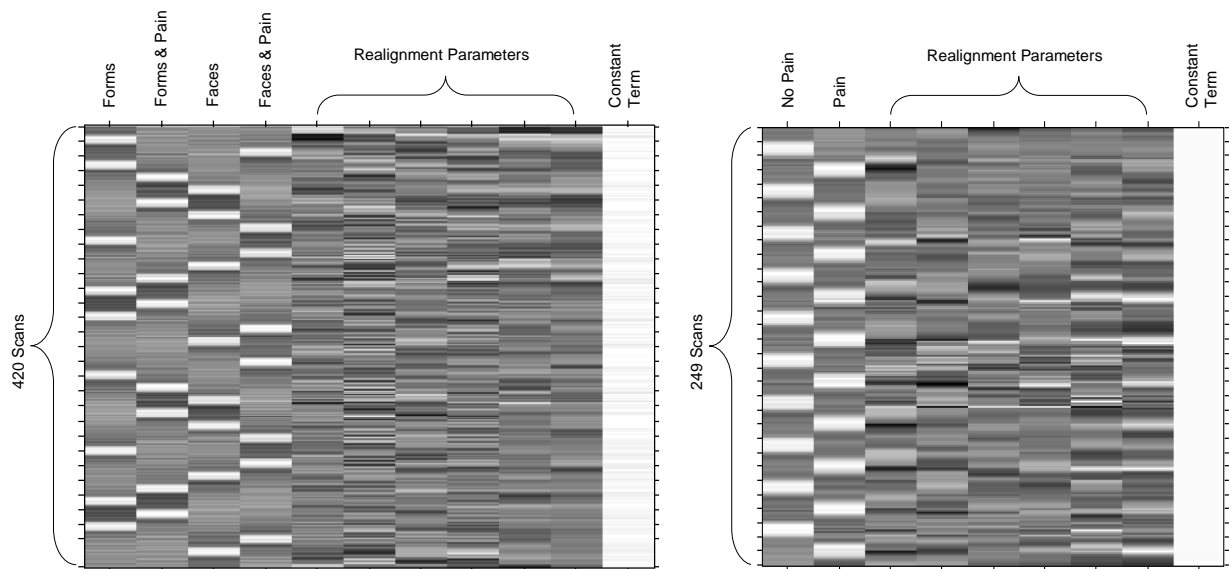
Fig. 2-6. SPM design matrices for a single subject. *Left:* Matching Task paradigm. *Right:* Localizer paradigm. In both paradigms, experimental conditions are modeled as boxcars convolved with the canonical hemodynamic response function resulting in predictors of BOLD signal time courses.

Model estimation

The model specified above is now estimated using a General Linear Model (GLM). Briefly, the GLM expresses the BOLD signal at each voxel as a linear combination of predictor variables as defined in the design matrix columns:

$$Y = X\beta + \varepsilon$$

Formula 1

Y is a column vector with the observed signal time course. X denotes the design matrix, whose columns are condition specific predictors of the signal time course. β is a column vector with scaling factors (fit coefficients, beta weights) assigned to each predictor in X; ε is a column vector with error terms.

An estimator for β is derived by minimizing the sum of squared differences ($\varepsilon^T\varepsilon$) between the model's prediction ($X\beta$) and the observed signal Y. The GLM assumes that the residuals ε are normally and independently distributed. Under this assumption the fit coefficients (beta weights) in β are maximum likelihood estimates and thus the best linear unbiased estimates. The estimation of β by the method of least squares is equivalent to the following computation, which is performed at every voxel:

$$\hat{\beta} = \left(X^T X \right)^{-1} X^T Y$$

Formula 2

The equation implies that the columns in the design matrix (predictor variables) are linearly independent, since $X^T X$ cannot be inverted otherwise. For overdetermined models the Moore Penrose pseudoinverse can be used, however. Nevertheless, correlations (collinearity) among predictor variables reduce estimation efficiency and should be avoided. Collinearity is minimized in our design, as there is a 10 seconds gap between subsequent blocks. The BOLD signal may settle during these intervals improving efficiency when estimating subtractions of conditions. Note that a constant term is by default added to the design matrix as a predictor variable of no interest to account for the session specific mean signal at each voxel. A beta weight, i.e. an element in β, may thus be interpreted as a voxel-wise measure of BOLD related response magnitude (effect size) in the respective experimental condition relative to the local mean signal.

After the beta weights have been estimated, a hypothesis is tested against the null hypothesis of no effect. Hypotheses are phrased as a linear combination of beta weights ($c^T\beta$) as indicated by a contrast vector. The contrast vector c = [1 -1], for instance, is equivalent to the hypothesis that condition 1 elicits a greater response than condition 2: β_1 > β_2 or β_1—β_2 > 0. Inference is based on the subtraction principle, i.e. brain areas that exhibit a positive (negative) contrast value are activated (deactivated) by the feature that distinguishes condition 1 from condition 2. Note that the contrast specific linear combination of betas ($c^T\beta$) is stored as a so-called contrast image in SPM. Group level analyses are based on these images. Next, a t-statistic that expresses evidence against the null hypothesis of no effect, is calculated at each voxel:

$$T = \frac{c^T \hat{\beta}}{\sqrt{\hat{\sigma}^2 c^T \left(X^T X\right)^{-1} c}}$$

Formula 3

Basically, the estimated effect is divided by its standard error to yield a statistic that follows a Student's t distribution. The nominator is a linear combination of beta weights ($c^T\beta$), which essentially reflects an estimator of effect size pertaining to the tested hypothesis. The denominator contains the estimated variability of the hypothesized effect (standard error). $X^T X$ describes the degree of overlap (collinearity) among predictor variables in the columns of X. In orthogonal designs, where overlap is by definition absent, the quantity $c^T \left(X^T X\right)^{-1} c$ is minimal, which leads to an optimal estimation efficiency. σ^2 denotes the standard deviation of the models' prediction from the observed response. Hence, the t-value is high, when the deviation from the observed response and collinearity among predictors are small and the estimated effect size is large. At each voxel the corresponding p-value is derived from a Student's t-distribution with n degree of freedoms, where n is the number of scans minus the rank of the design matrix. For each contrast of interest, voxel-wise statistics are stored as T-images that are commonly referred to as statistical parametric maps (SPMs).

Group level analysis

<u>Regions of Interest Definition</u>

We are interested in emotion and pain related brain activation sites that are consistently present in the population from which the sample was drawn. These activations, if present, permit the definition of functional regions of interest for later ROI analysis (see below). At the group level (secondary level) data were analyzed using a random effects model. This approach takes into account both within and between-subject variability of the measured signal. This is contrary to a fixed effects model that ignores between-subject variability and thus precludes statistical inference on the population level. As the ROI definitions in the present study are based on a random effects model, they are valid at the population level (healthy adult males and females).

The random effects analysis involves a two-stage 'summary statistics' procedure (Holmes and Friston, 1998). Firstly, the GLM is estimated for each subject (as described in the previous section). Next, contrast images are computed for each effect of interest. A contrast image is comprised of per voxel contrast values. Contrast values are linear combinations of beta weights as defined by the respective contrast vector ($c^T\beta$). Contrast images are forwarded to the group level, where per voxel contrast values are averaged across participants and divided by the standard error of the mean. The p-value of the ensuing statistic is obtained from a Student's t distribution with n degrees of freedom, where n is the number of subjects minus 1. The procedure is equivalent to a voxel-wise one sample t-test on contrast values.

Importantly, the summary statistic approach requires that the design matrix is identical for each subject. Otherwise, the sample mean of contrast values is not a maximum likelihood estimate for group level activity. This was a point of concern since the employed thermal stimuli differ in intensity across subjects. Consequently, at a constant ramping rate (2 °C per second) the respective target temperatures are reached at different time points calling for individualized design matrices. However, we found that the target temperatures were reached within the 10 seconds ramping interval (after 6.2 seconds on average) in both paradigms for all participants. The experimental conditions as modeled in **Fig. 2-6** were thus not affected by this effect.

For the Matching Task data, the summary statistics approach was implemented within a flexible factorial model. For each condition in the 2 x 2 factorial design, the corresponding beta weights were estimated and forwarded to the second level. Thus, four beta-images were entered per participant. The mapping between beta images and factors is

specified in the factor matrix (**Fig. 2-7**), where both main effects and the 2 x 2 interaction were entered as within-subjects factors. The subject factor was added as between-subjects factor. Main effects and interactions were modeled as non-independent factors in order to take correlations between factor levels into account.

The purpose of the ROI Localizer was to identify pain responsive regions, i.e. the pain neuromatrix. These were determined by a 'Pain > No Pain' contrast. Ensuing contrast values were statistically assessed using a one-tailed significance criterion, since we expect painful stimulation to increase rather than decrease brain activity. The statistical map was thresholded at a voxel-wise p value of .001 (one-tailed, uncorrected) and a cluster size of 165 voxels to yield a cluster-wise significance criterion of p=.05 (FWE corrected for multiple comparisons). This combination of per voxel p-threshold and cluster extent threshold yields an equivalent correction for multiple comparisons based on the assumption that true brain activation is not confined to a single voxel but extends to adjacent regions (Forman and others, 1995). Significant activation clusters were reported in MNI stereotactic space and anatomically labeled according to the Automated Anatomical Labeling (AAL) Atlas (Tzourio-Mazoyer and others, 2002). A corresponding SPM plugin is available at http://www.cyceron.fr/freeware/ (as of 3/1/2010). Cytoarchitectonic descriptions (Brodmann areas and subcortical nuclei) from the Talairach and Tournoux Atlas (Talairach and Tournoux, 1988) were also reported employing the MNI Space Utility (http://www.ihb.spb.ru/~pet_lab/MSU/MSUMain.html as of 3/1/2010).

Moreover, an emotion sensitive subregion of the amygdala volume was defined by contrasting face matching trials with form matching trials (Matching Task). Specifically, a 'Faces > Forms' contrast (collapsing over painful and non-painful conditions) was employed. A one-tailed significance criterion was used, because we do not expect aversive faces to decrease amygdala activity. SPM analysis was confined to the bilateral amygdala anatomical region using the Wake Forest University (WFU) Pick Atlas software (Maldjian and others, 2003), which is available at http://fmri.wfubmc.edu/cms/software (as of 3/1/2010). The amygdala region was defined according to the AAL atlas. The ensuing statistical map was thresholded at a voxel-wise p value of .05 (one-tailed, FWE corrected for multiple comparisons).
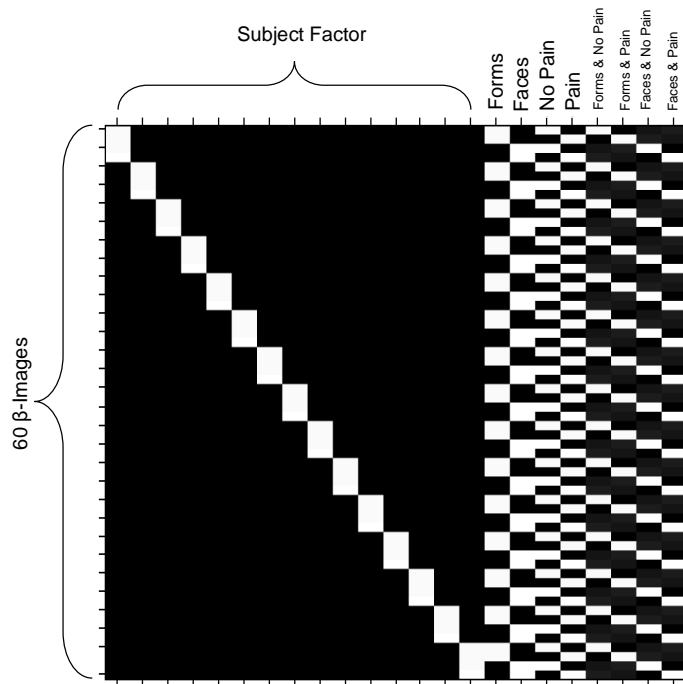
Fig. 2-7. Design matrix for group level data (Matching Paradigm). Four beta images were entered per subject. The first 15 columns model subjects effects. Columns 16-17 model the main effect of factor 'Emotion' (faces *vs.* forms); columns 18-19 model the main effect of factor 'Pain' (pain *vs.* no pain). The last four columns model the 2 x 2 interaction effect between both factors.

Region of Interest analysis

Characterization of pain responsive regions of interest

As outlined above, pain responsive regions were identified in a separate Localizer experiment. The modulation of regional activity by the two experimental factors in the Matching paradigm was studied as follows. Beta weights were extracted from each pre-defined region and averaged across voxels using Marsbar software v. 0.42 (Brett and others, 2002), which is available at http://marsbar.sourceforge.net (as of 3/1/2010). The resulting summary statistics were entered into a SPSS repeated measures ANVOA with factors 'ROI', 'Pain' ('No Pain' *vs.* 'Pain') and 'Emotion' ('Faces' *vs.* 'Forms'). Statistical significance was determined using a p-value of .05. Violations of the sphericity assumption were corrected with the Greenhouse Geisser method. ANOVA results were further investigated in one sample t-tests that were separately conducted for each region and contrast of interest. The emotion related response was defined as 'Faces > Forms' contrast collapsing over painful and non-painful conditions. A one-tailed significance criterion of p=.05 was adopted here, since we expected aversive facial stimuli to increase (and not decrease) brain activity in pain responsive ROIs. Likewise, the pain related response was

defined as 'Pain > No Pain' contrast collapsing over face and form matching conditions. Since a positive response to pain was expected, statistical significance was determined using a one-tailed p-value of .05. For statistical assessment of the 2 x 2 interaction effect ('Forms & No Pain' + 'Faces & Pain' > 'Forms & Pain' + 'Faces & No Pain'), however, a two tailed t-test was carried out, since we do not have an *a priori* hypothesis regarding the direction of this effect. In contradistinction to exploratory analyses, t-tests were performed on a single summary statistic per ROI rather than on individual voxels. The multiple comparisons problem is thus reduced from the number of voxels in the brain to the number of ROIs. Bonferroni correction was applied as indicated in the results section.

It should be noted that the summary statistic (mean contrast value) in a given contrast of interest can be interpreted as percent signal change relative to the whole brain global mean signal (Penny, 2004). This interpretation is valid because

i)   each time series was by default ratio normalized to a value of 100, i.e. each voxel in each scan was multiplied by 100/m, where m is the average value across all voxels and scans (SPM 'grand mean scaling');

ii)   a beta weight expresses activity relative to the local mean signal (see section 'Model estimation'); due to 'grand mean scaling', the local mean signal has an average value of 100;

iii) the constant term, i.e. the predictor for the local mean signal, and the condition-specific predictor variables (i.e. the columns in **Fig. 2-6**) are equally scaled.

Characterization of Amygdala response behavior

Amygdala response behavior towards painful heat and aversive faces was evaluated analogously. Furthermore, amygdala responses to medium and intense thermal pain administered in the ROI Localizer (pain rating: 8/10) and Matching Paradigm (pain rating: 5/10) were assessed i) within the anatomical amygdala volume as defined by the Marsbar AAL plugin (available at http://sourceforge.net/projects/marsbar/files as of 3/1/2010), and ii) within the emotion sensitive amygdala subregion. The latter was defined functionally by a 'Faces > Forms' contrast as described in the previous section. A repeated measures ANOVA with factor 'laterality' (left amygdala *vs.* right amygdala), 'ROI definition' (functional *vs.* anatomical) and 'pain intensity' ('5/10' *vs.* '8/10') was conducted. Statistical significance was determined using a p-value of .05. Violations of the sphericity assumption were corrected with the Greenhouse Geisser method. ANOVA results were further investigated in a separately conducted one sample t-tests. A one-tailed significance

criterion of p=.05 was used, because we expected painful stimulation to increase (and not decrease) amygdala activity.

Assessment of covariates

ROI activity may be influenced by two sources of intersubject variability: i) the subject specific temperatures that were employed to equalize pain perception in the sample, and ii) the response times related to the incidental task. For each contrast of interest, an ANCOVA design was formulated at the secondary level. Temperatures and response times (RT) were entered as covariates. The RT covariate was constituted of RT differences (in milliseconds) between experimental conditions as defined by the respective contrast vector. Both covariates were mean centered and normalized to their peak values. **Fig. 2-8** shows an example of an SPM ANCOVA design used to investigate covariate effects on pain related activity in the Localizer session. Covariate effects were statistically assessed in an F-test approach. A full model including the appropriate covariates in addition to the constant term was compared with a reduced model that only consists in the constant term. According to the null hypothesis, the full model does not explain more variance than the reduced model. ANCOVA designs were formulated to assess the covariate effect i) on the pain related response (both paradigms), ii) on the emotion related response (Matching Task), and iii) on the interaction effect (Matching Task). Note that for the 'Face > Forms' contrast (Matching Task) only the response time covariate was studied, since this contrast pools over painful and non-painful conditions. To investigate magnitude and direction of each covariate effect, separate t-tests were carried out. A two tailed significance criterion (p=.05) was applied since we do not have an *a priori* hypothesis regarding the direction of any covariate effect.
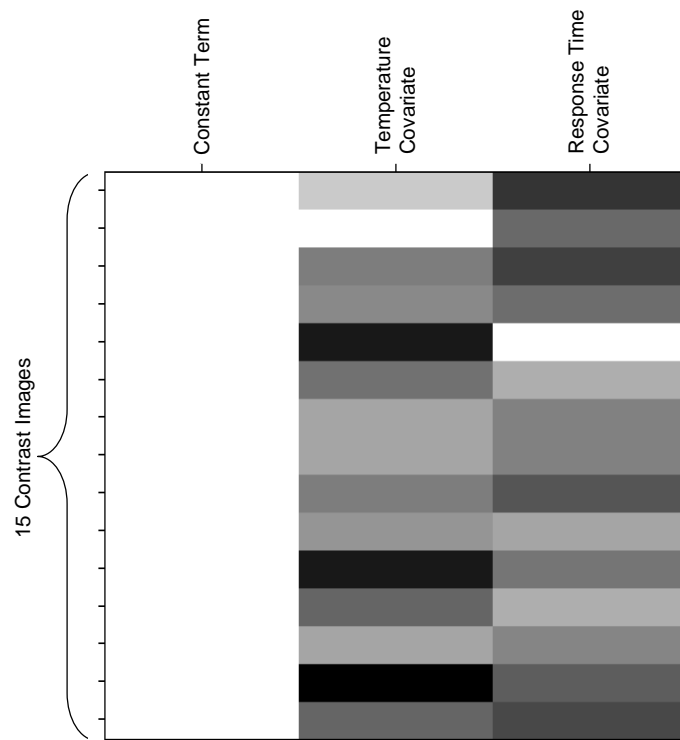
Fig. 2-8. SPM ANCOVA design for the assessment of covariate effects in the Localizer experiment. In the example given, the effect of response times (ms) and temperatures (°C) on pain related activity was studied. One contrast image ('Pain > No Pain') per subject was entered into this analysis.

2.3 Results

2.3.1 Behavioral Data

2.3.1.1 Localizer Paradigm

In one subject 50% of blink events were missed due to a disconnection in the response device wiring in the second half of the paradigm. Otherwise, the proportion of misses was below 10% in all participants. On average, one event was missed in each experimental condition. Mean response times in each condition were averaged across participants. **Fig. 2-9** shows the result. During painful stimulation subjects detected a blink event by 45.4 milliseconds faster than during stimulation with innocuous warmth. A paired samples t-test revealed that this difference is significant [T(14)=3.44, p=.004, two tailed].
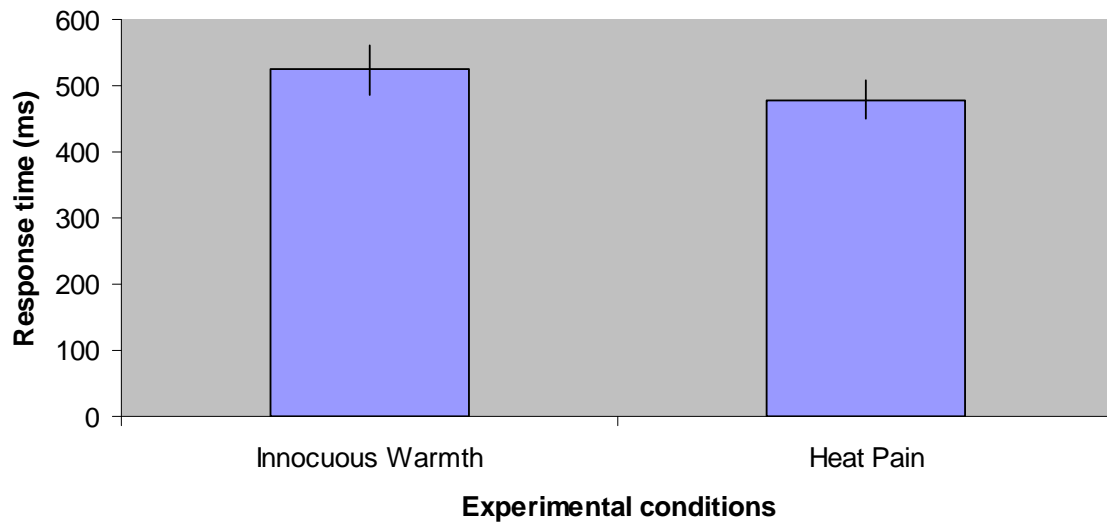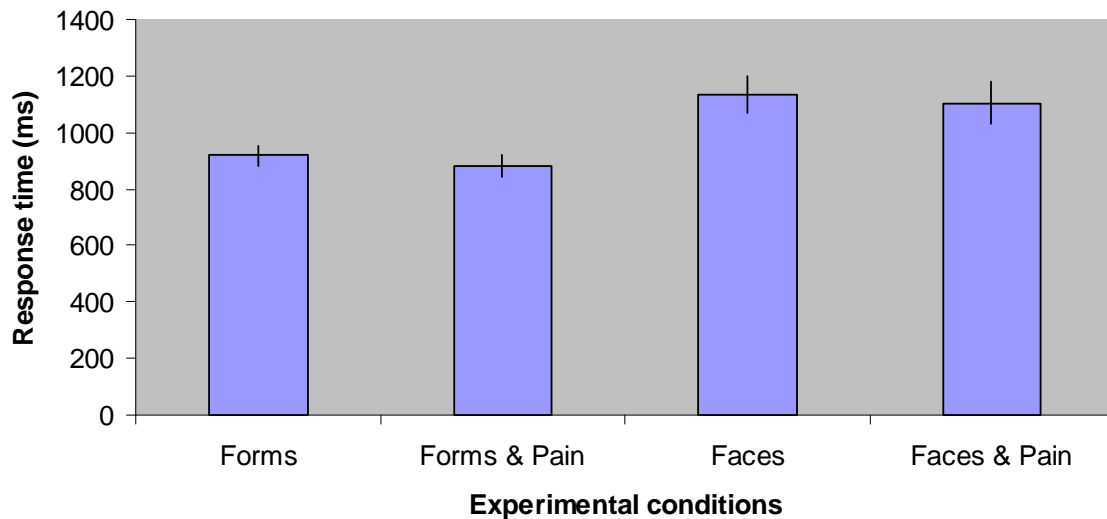
Fig. 2-9. Mean response time (in milliseconds) per condition in the localizer paradigm, averaged across participants. Error bars denote the standard error of the mean.
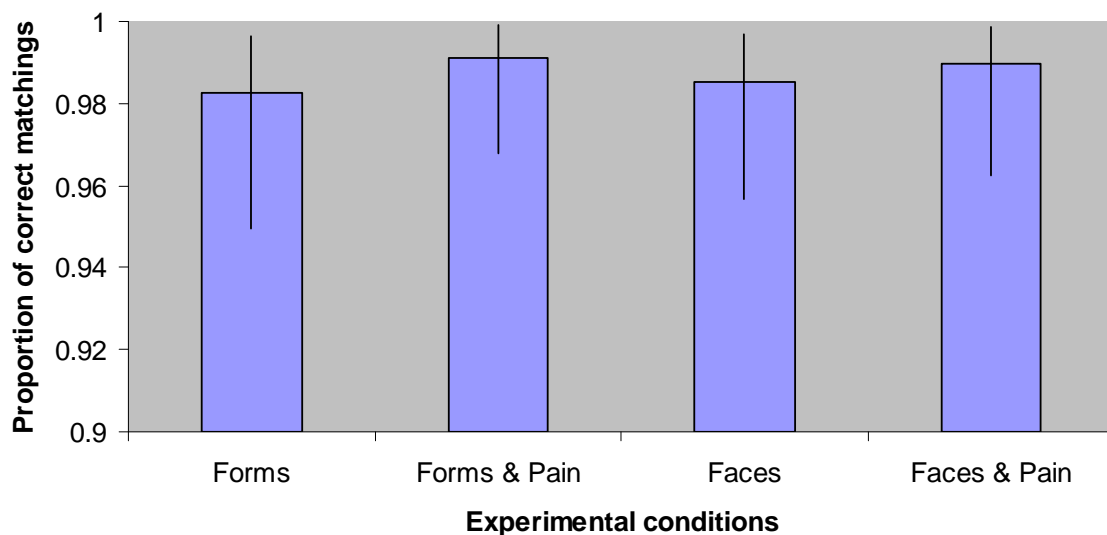

2.3.1.2 Matching Task

Due to incorrect mapping of response buttons in one subject, middle finger key presses (indicating a right target location) were not recorded resulting in 50% omissions. Otherwise, the proportion of misses was below 2.5% in all participants. All misses were distributed evenly across conditions. Mean response times in each experimental condition were averaged across participants. **Fig. 2-10** shows the result. Apparently, subjects needed more time to match faces compared to geometric forms. Responses were faster, when the matching task was combined with painful stimulation. The 2 x 2 repeated measures ANOVA revealed a significant effect of factor 'Pain' [$F(1,14)=8.65$, $p=.011$, G.G. corrected] and factor 'Emotion' [$F(1,14)=21.72$, $p<.001$, G.G. corrected]. The 2 x 2 interaction effect was not significant [$F(1,14)=.21$, $p=.66$, G.G. corrected]. As shown in **Fig. 2-11** response accuracy was higher when the matching task was combined with painful stimulation. Relative to the respective confidence intervals, however, this effect is negligible. The proportion of correct responses was almost 100% in all conditions. Evaluation of within-subject effects in a repeated measures Generalized Linear Model revealed a non-significant effect of factor 'Pain' (Wald $X^2(df=1)=.10$, $p=.75$). Factor 'Emotion' and the 2 x 2 interaction were also non-significant (Wald $X^2(df=1)<.001$, $p\approx1.0$ for both effects).

Fig. 2-10. Mean response time (in milliseconds) per condition in the Matching Task. Error bars denote the standard error of the mean.

Fig. 2-11. Proportion of correct responses per condition in the Matching Task. Error bars denote 95% confidence intervals (Schoenberg, 1983).

2.3.2 Functional Data

### 2.3.2.1 Definition of Pain Responsive Brain Regions

The first step was the definition of pain responsive regions of interest. These definitions were based on a second level random effects analysis of the functional data acquired in the localizer experiment. Neural correlates of painful sensation were identified by contrasting painful stimulation (corresponding to an individual pain rating of 8 out of 10) with innocuous warmth ('Pain > No Pain' contrast). The ensuing statistical map (**Fig. 2-12**)

reveals cortical regions that exhibit a pain related response. At the cluster level, four pain responsive regions could be reliably identified (P<.05, FWE corrected). These are located in the a) right Rolandic Operculum, b) bilateral thalamus, c) right insula, and d) left Rolandic Operculum. These anatomical labels were drawn from the Automatic Anatomical Labeling Atlas Atlas (Tzourio-Mazoyer and others, 2002). Specifically, from all possible AAL labels that overlap with a given activation cluster, the label with the greatest intersection area relative to the size of that cluster was chosen. These labels are used hereafter to refer to the four pain responsive regions of interest. Table 2.3-1 provides further details referring to the peak voxel value of each cluster. The largest cluster (388 voxels) mainly covers the right Rolandic Operculum (a). Here, the global maximum is located. The cluster extends dorsally into the right supramarginal gyrus (BA 40), where a secondary local maximum is found. Medially, the cluster extends into the right posterior insular region. According to the Talairach Atlas, the right insula constitutes 23 percent of the cluster volume. The thalamic cluster (b) is located bilaterally in the medial dorsal nuclei of the thalamus, predominantly on the left side, where a secondary maximum is present. The right focus extends ventrally to basal brain structures covering parts of the hypothalamus, the right mammillary body and a small medial portion of the right hippocampus. Note that the primary maximum was detected in the right pedunculus of the cranial midbrain, i.e. in the extra-nuclear region. The right insular cluster (c) is the second largest activation focus located anteriorly and medially to the Rolandic Operculum cluster (a). The primary maximum is located in the inferior frontal operculum, but the cluster mostly lies in the anterior insula (BA 13), where a secondary maximum is found. The cluster extends medially to cover an adjacent portion of the putamen. The fourth cluster (d) mainly covers the left Rolandic Operculum, where a secondary maximum is present. This focus is confluent with a medially and anteriorly located cluster in the left insular region (BA 13) that contains the primary activation maximum. Note that the largest cluster (right Rolandic Operculum) exhibits the highest peak voxel value, whereas peak value and cluster size are smallest in the left Rolandic ROI. The inverse contrast ('Pain < No Pain') does not reveal any voxels that meet the significance criterion (p=.05, corrected for multiple comparisons) at any level of inference.

Table 2.3-1. ROI Localizer. SPM Activation Clusters.

| Region of activation	Laterality	Brodmann's Area	MNI coordinates			Z-score	Cluster Size
			x	y	z		
Pain > No Pain							
Rolandic Operculum, Supramarginal Gyrus, Superior Temporal Gyrus	R	13/40/43	44	-20	20	4.59	388
Thalamus (**R**/L) [Medial Dorsal Nucleus], Hippocampus (R), Mammillary Body (R), Hypothalamus	R	N/A	6	-8	-10	4.26	174
Insula, **Inferior Frontal Operculum**, Putamen, Rolandic Operculum	R	13/22/44/45	44	14	4	4.25	317
Rolandic Operculum, **Insula**, Inferior Frontal Operculum, Heschl	L	6/13/43/44	-42	4	8	4.14	165
Pain < No Pain							
no significant voxels/clusters/map in whole brain search volume (p=.05, corrected)							

Pain > No Pain: The table shows clusters of 165 or more contiguous voxels whose global maxima exceed a t-statistic of 3.79 (P<.001 uncorrected), equivalent to a cluster-wise false positive rate of P<.05, FWE corrected for multiple comparisons. For each maximal activation focus per cluster, laterality, Brodmann's area, coordinates, Z-score, and number of contiguous voxels within a cluster are provided. The anatomical location of the maximal activation focus is printed in bold. Coordinates are defined in Montreal Neurologic Institute stereotactic space in millimeters.
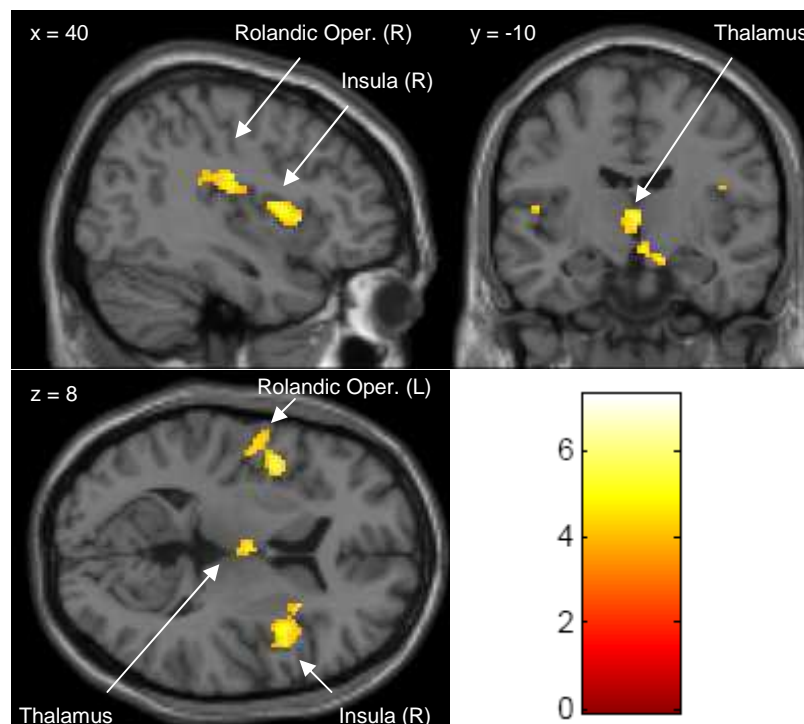
Fig. 2-12. SPM T-map showing clusters that exhibit significant activity during painful thermal stimulation ('Pain > No Pain'). Maps are thresholded at T = 3.79 (voxel-wise P=.001, uncorrected) and a cluster size of 165 voxels (1320 mm^3) to meet a cluster-wise significance level of P < .05 (FWE corrected). The colorimeter scale indicates per voxel T values. The SPM is overlaid on a canonical brain template and is displayed in neurological convention. Slice coordinates (in millimeters) refer to MNI stereotactic space. L: Left; R: Right.

At the region level, a measure of response magnitude is the mean activation in each cluster expressed as percent signal change relative to the whole brain global mean. This quantity was obtained by averaging the pain specific response (contrast values) across voxels in each ROI. According to **Fig. 2-13** the right Rolandic Operculum ROI exhibits the highest mean activity, followed by the right insular ROI, the thalamic ROI, and finally the

left Rolandic Operculum ROI. Note that the same ranking also applies to cluster size, i.e. a strong (weak) response in a given cluster is associated with a large (low) number of contiguous voxels contained therein. Per subject contrast values were then entered into a repeated measures ANOVA with factor 'ROI' (4 levels). The analysis revealed that the regions of interest do not differ significantly in their reactivity to painful stimulation $(F(3,42)=.611, p=.57, G.G. corrected)$.
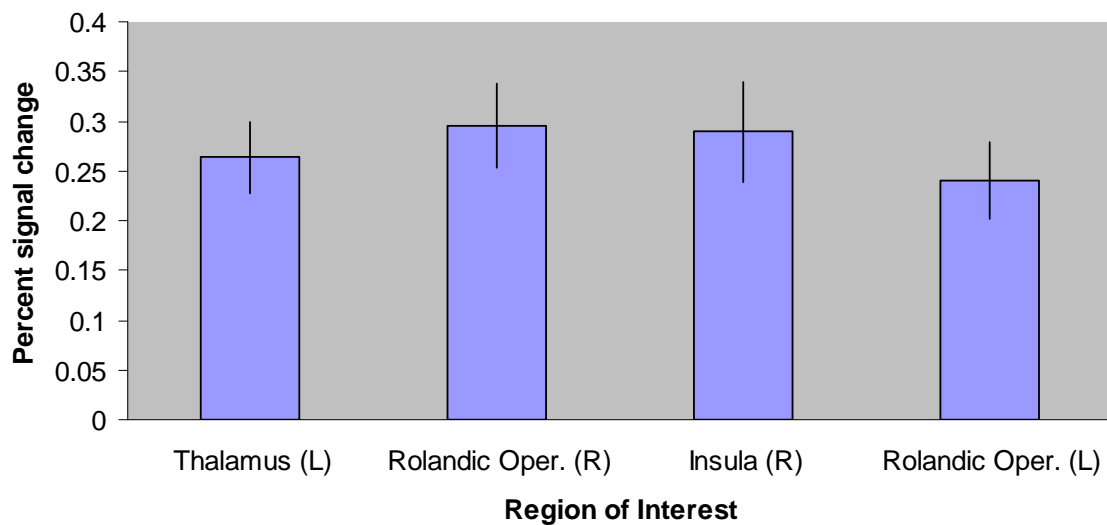
Fig. 2-13. Mean activation of pain responsive clusters in the localizer experiment. Activity refers to the 'Pain > No Pain' contrast and is expressed as percent signal change relative to the whole brain global mean. Error bars denote the standard error of the mean.

ROIs were further characterized by taking two sources of intersubject variability into account that may interact with the pain related cluster response: i) the subject specific temperatures that were employed to equalize pain perception in the sample, and ii) the mean RT difference between painful and non-painful blocks: RT(Pain) – RT(No Pain). The latter is of particular interest, as behavioral analysis revealed a significant decrease of detection times in the presence of painful stimulation. Individual RTs and temperatures were added as covariates to the random effects analysis. Statistical significance was conjointly evaluated in an F-test approach: a full model including the constant term and both covariates was tested against the reduced model that only consists in the constant term. It should be noted that both covariates were orthogonalized with respect to the constant term. Covariates thus do not affect the magnitude of the estimated group effect (Pain > No Pain) but its reliability. The results are listed in Table 2.3-2. The full model does not explain significantly more variance than the reduced model in any region of

interest, i.e. the pain related signal is unaffected by response time and temperature covariates.

Table 2.3-2. ROI Localizer. Covariate Assessment. Full model versus reduced model (F-test).

Region of Interest	Extra sum of squares	F value	P value	Percentage of active voxels
Thalamus	.05	1.35	.30	6.90
Rolandic Oper. (R)	.02	.33	.73	1.29
Insula (R)	.04	.48	.63	.63
Rolandic Oper. (L)	.02	.44	.66	.00

Models refer to the 'Pain > No Pain' contrast and were evaluated at the group level. The full model includes response time and temperature covariates in addition to the constant term. Magnitude of covariate effect (extra sum of squares), F values [F(2,12)] and uncorrected P values are provided for each pre-defined Region of Interest. The percentage of active voxels that exceed an F(2,12) value of 3.89 (corresponding to P=.05, uncorrected) is also given.

The effect of each covariate on the pain specific signal was then assessed in separate t-tests (two-tailed). The results are summarized in Table 2.3-3. The temperature covariate shows a small but consistently positive effect across ROIs, i.e. response to pain tends to increase with increasing temperature. This effect is not reliable, however (all two-tailed p values are above .44). Response times correlate negatively with ROI activity except for the right Opercular ROI, where correlation is close to zero. In other words: ROI activity in the sample tends to increase with increasing detection speed during painful stimulation. This finding is most prominent in the thalamic ROI [$T(12)=-1.62$, $p=.13$, two-tailed]. In concordance with the F-test above, covariate effects do not reach the significance criterion in any region of interest.

Table 2.3-3. ROI Localizer. Covariate Assessment (Pain > No Pain). Two-tailed t-tests.

Covariate	Region of Interest	Covariate effect	T value	P value
Temperature				
	Thalamus	.05	.74	.47
	Rolandic Oper. (R)	.06	.68	.51
	Insula (R)	.09	.79	.44
	Rolandic Oper. (L)	.04	.47	.65
Response Time				
	Thalamus	-.15	-1.62	.13
	Rolandic Oper. (R)	.03	.21	.84
	Insula (R)	-.11	-.79	.44
	Rolandic Oper. (L)	-.10	-.91	.38

Temperature and response time covariates were evaluated at the group level. Their interaction with pain related activity (defined as the 'Pain > No Pain' contrast) is indicated as covariate effect. Covariate effects (beta weights), T values and uncorrected P values are provided per pre-defined Region of Interest. The t-statistic has twelve degrees of freedom. P values refer to two-tailed t-tests.

2.3.2.2 Functional Characterization of Pain responsive Brain Regions

The *a priori* defined pain responsive cortical areas were used as regions of interest in the factorial analysis of the functional data acquired in the Matching Task experiment. Beta weights were extracted and entered into a 4 x 2 x 2 repeated measures ANOVA with factor 'ROI' (four ROIs), factor 'Pain' (Pain *vs.* No Pain) and factor 'Emotion' (Faces *vs.* Forms). The main effect of factor 'Pain' is equivalent to a SPM 'Pain > No Pain' contrast that collapses form matching and face matching conditions. Likewise, the main effect of factor 'Emotion' is equivalent to a SPM 'Faces > Forms' contrast collapsing painful and non-painful conditions. As expected, ROIs were activated significantly by factor 'Pain': $F(1,14)=29.14$, $p<.001$, G.G. corrected. Importantly, the effect of factor 'Emotion' also meets the significance criterion: $F(1,14)=6.01$, $p=.028$, G.G. corrected. To assess direction and magnitude of these main effects, separate t-tests were carried out (Table 2.3-4). As illustrated in **Fig. 2-14**, the emotion related response ('Faces > Forms') is positive throughout and most prominent in the right insular ROI [$T(14)=2.84$, $p=.007$, one-tailed], followed by the right Rolandic Operculum [$T(14)=2.19$, $p=.02$, one-tailed], the left Rolandic Operculum [$T(14)=1.54$, $p=.07$, one-tailed] and finally the thalamus [$T(14)=.33$, $p=.37$, one-tailed]. The same ranking applies to the pain specific ROI responses ('Pain > No Pain'). Note that the emotion related response in the right insular ROI survives Bonferroni correction for the number of regions (4) entered into the analysis ($p=.028$, corrected). On average, the activation by factor 'Emotion' amounts to 30.0 percent of the activation by factor 'Pain'.

Table 2.3-4. Matching Task. ROI reactivity to emotional and painful stimuli. T-tests (one-tailed).

Region of Interest	Signal change (%)	T value	P value	Percentage of active voxels
Faces > Forms				
Thalamus	.02	.33	.37	10.35
Rolandic Oper. (R)	.07	2.19	.02	30.93
Insula (R)	.13	2.84	.007	59.31
Rolandic Oper. (L)	.07	1.54	.07	6.06
Pain > No Pain				
Thalamus	.13	2.06	.03	36.78
Rolandic Oper. (R)	.33	5.46	< .001	84.28
Insula (R)	.33	4.71	< .001	99.05
Rolandic Oper. (L)	.20	5.13	< .001	96.97

For each main effect in the 2 x 2 factorial design, response magnitude (expressed as percent signal change relative to the whole brain global mean), T values and uncorrected P values are provided per region of interest. The T statistic has 14 degrees of freedom. P values refer to one-tailed t-tests. The percentage of active voxels that exceed a T value of 1.76 (corresponding to P=.05) is also given.
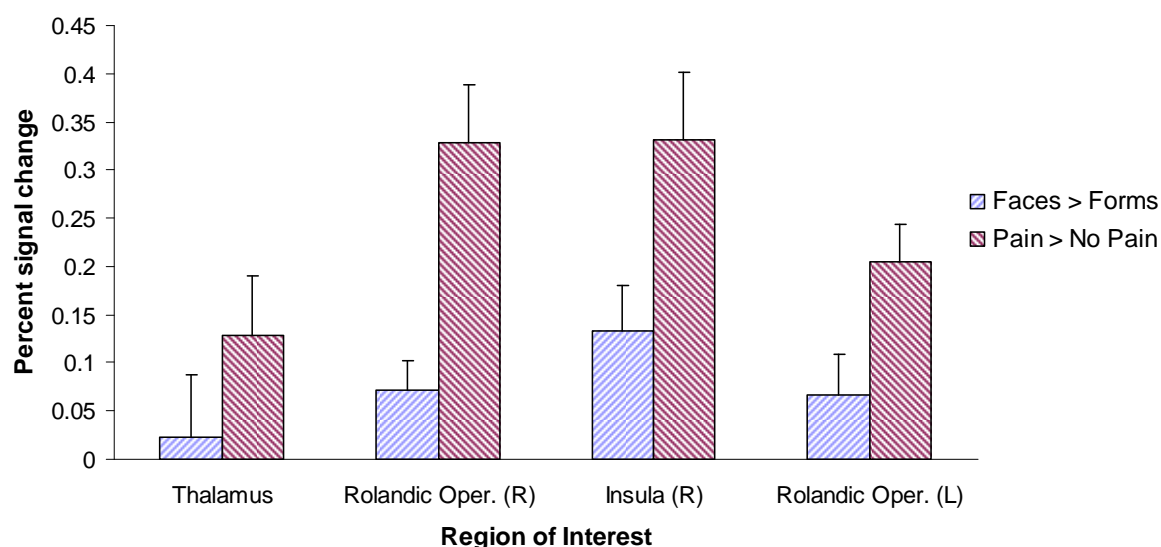
Fig. 2-14. Pain responsive regions are activated by emotional and painful stimuli in the matching paradigm. Pain and emotion related signals are defined as 'Pain > No Pain' and 'Faces > Forms' contrasts, respectively. Response magnitude is expressed as percent signal change relative to the whole brain global mean. Error bars denote the standard error of the mean.

Moreover, the ANOVA revealed a significant 'Pain x ROI' interaction effect [F(3,42)=5.33,p=.01, G.G. corrected]. As illustrated in **Fig. 2-14** the group response to painful stimulation in both right hemispheric ROIs is stronger than in the thalamic ROI and the left Rolandic ROI. A paired samples t-test confirmed that this difference is statistically significant: T(14)=3.68, p=.002, two-tailed. The 'Emotion x ROI' interaction effect is non-significant [F(3,42)=1.08, p=.35, G.G. corrected]. The same holds for the 'Emotion x Pain' interaction effect: F(1,14)=2.61, p=.13, G.G. corrected. However, two-tailed t-tests revealed that the 'Emotion x Pain' interaction effect is consistently negative in all ROIs (Table 2.3-5) and most reliable in the right insular and thalamic ROI [T(14)=-1.83, p=.09 and T(14)=-1.72, p=.11, respectively]. The three way interaction effect was unreliable [F(3,42)=1.56, p=.22, G.G. corrected].

**Table 2.3-5.** Matching Task. 2 x 2 interaction effect on ROI activity. T-tests (two-tailed).

Region of Interest	Signal change (%)	T value	P value	Percentage of active voxels
2 x 2 Interaction				
Thalamus	-.09	-1.72	.11	25.29
Rolandic Oper. (R)	-.02	-.41	.69	.77
Insula (R)	-.12	-1.83	.09	7.57
Rolandic Oper. (L)	-.05	-.93	.37	3.64

Effect size (expressed as percent signal change relative to the whole brain global mean), T values and uncorrected P values are provided per region of interest. The T statistic has 14 degrees of freedom. P values refer to two-tailed t-tests. The percentage of active voxels that exceed a T value of 2.14 (corresponding to P=.05, two-tailed) is also given.

To further explore ROI response behavior, beta weights were extracted from each ROI and plotted as a function of experimental condition (**Fig. 2-15**, panel *a*). The conditions were arranged along the x-axis in the direction of expected signal gain: Forms & No Pain -> Faces & No Pain -> Forms & Pain -> Faces & Pain. On average, BOLD related activity increases linearly across the first three conditions and saturates in the last (black line). Hence, the response amplitudes between 'Forms & No Pain', 'Forms & Pain' and 'Faces & No Pain' conditions are similar. This linear ascent is particularly evident in both right hemispheric ROIs and the thalamic ROI. In the right insular ROI, the greatest response amplitude is found between both non painful conditions, i.e. between 'Forms & No Pain' and 'Faces & No Pain'. This is striking given the fact that this region is actually pain responsive and was defined in an independent localizer experiment. The greatest response difference was actually expected to be found between non-painful and painful conditions instead of non-emotional and emotional conditions. Only in the right Rolandic Operculum, the response difference between face and form matching tasks is small and approximately equal in painful and non-painful contexts. In the 'Face & Pain' condition, the signal gain is small in the left Rolandic ROI or almost absent in both right hemispheric ROIs. In the thalamic ROI, the signal even decreases. On average, the signal tends to saturate in the 'Faces & Pain' condition (black line), where emotional and painful stimuli are combined. This ceiling effect is reflected in a negative 2 x 2 interaction effect, which is small but consistently present across ROIs as outlined above. To further illustrate this response behavior, beta weights were averaged across ROIs and displayed in an interaction plot: factor 'Emotion' has a high impact on the BOLD related activity in the context of innocuous warmth ('No pain'), whereas the emotion related effect ceases completely in the context of painful stimulation. This interaction between factors 'Pain' and 'Emotion' is, however, statistically not significant (Table 2.3-5).
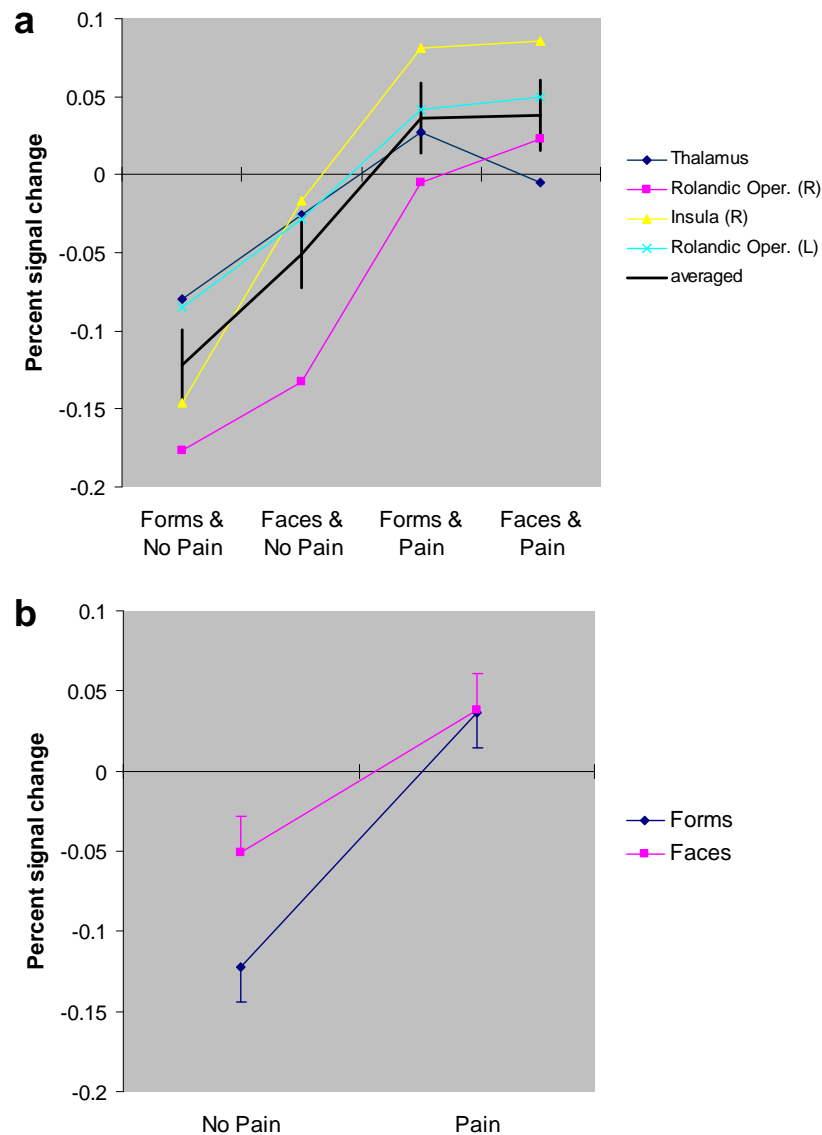
Fig. 2-15. Activity of pain responsive brain regions as a function of experimental condition in the Matching Task. *Panel a:* Activation profiles are provided in different colors per ROI. The mean activation profile (averaged across ROIs) is plotted in black. *Panel b:* Interaction plot. Mean activation (averaged across ROIs) in face matching (squares) and form matching (diamonds) tasks in the context of painful and non-painful stimulation. Error bars denote the standard error of the mean.

Covariate effects were assessed for each contrast of interest. In the 'Pain > No Pain' contrast, two sources of intersubject variability may affect the pain related signal: the subject specific temperatures that were employed to equalize pain perception in the sample, and the response time differences between painful and non-painful conditions. According to the behavioral analysis above, this RT difference was significant: $F(1,14)=8.65$, $p=.011$, G.G. corrected. In the 'Faces > Forms' contrast, the effect of RT differences between the face matching and form matching tasks was investigated. On the behavioral level, these RT differences were again highly significant: $F(1,14)=21.72$,

p<.001, G.G. corrected. The temperature covariate was not studied here, as the contrast collapses over painful and non-painful conditions. In the 2 x 2 interaction contrast ('Form & No Pain + Face & Pain > Form & Pain + Face & No Pain') the respective response time covariate and the temperature covariate were studied. Note that there was no reliable RT effect on the behavioral level, however: $F(1,14)=.21$, $p=.66$, G.G. corrected. Covariate effects were assessed in an F-test approach: A full model including the appropriate covariates in addition to the constant term was compared with a reduced model that only consists in the constant term. The results are given in Table 2.3-6. In summary, no significant amount of variance can be explained by covariates. However, the RT covariate in the 'Faces > Forms' contrast explains a relatively large amount of experimental variance, especially in the right insular ROI [$F(1,13)=3.73$, $p=.08$] and the thalamic ROI [$F(1,13)=2.30$, $p=.15$]. In the former ROI, 18.0 percent of voxels show a covariation effect between emotion related activation and response times.

Table 2.3-6. Matching Task. Covariate Assessment. Full model versus reduced model (F-test).

Region of Interest	Extra sum of squares	F value	P value	Percentage of active voxels
Faces > Forms				
Thalamus	.14	2.30	.15	10.35
Rolandic Oper. (R)	.03	1.76	.21	18.04
Insula (R)	.10	3.73	.08	10.41
Rolandic Oper. (L)	.05	1.85	.20	3.03
Pain > No Pain				
Thalamus	.02	.18	.84	.00
Rolandic Oper. (R)	.08	.73	.50	9.79
Insula (R)	.04	.23	.80	1.26
Rolandic Oper. (L)	.05	.99	.40	.00
2 x 2 Interaction				
Thalamus	.03	.39	.69	1.15
Rolandic Oper. (R)	.06	1.35	.30	.00
Insula (R)	.06	.39	.69	.00
Rolandic Oper. (L)	.03	.27	.77	.00

Models were evaluated at the group level. *Faces > Forms:* The full model includes the response time covariate plus the constant term [$F(1,13)$]. *Other contrasts:* The full model includes response time and temperature covariates plus the constant term [$F(2,12)$]. Magnitude of covariate effect (extra sum of squares), F values and uncorrected P values are provided for each pre-defined Region of Interest. The percentage of active voxels that exceed an uncorrected p-threshold of .05 (equivalent to a voxel-wise $F(1,13)=4.67$ and $F(2,12)=3.89$, respectively) is also listed.

Two-tailed t-tests were performed to assess size and direction of each covariate effect (Table 2.3-7). In the 'Faces > Forms' contrast, t-tests revealed a positive effect of RT on BOLD related activity in the right insular ROI [$T(13)=1.93$, $p=.08$] and the thalamic ROI [$T(13)=1.52$, $p=.15$]. Activity thus increases with increasing response times in the face matching task relative to the form matching task. A weaker effect in the opposite direction was found in both Rolandic Operculum ROIs: $T(13)=-1.36$, $p=.20$ (left Rolandic

ROI) and T(13)=-1.33, p=.20 (right Rolandic ROI). As to the pain specific response (defined as 'Pain > No Pain' contrast) the correlation between response times and ROI activity is less reliable and has an opposite profile. Activity in both Rolandic ROIs correlate with RT, i.e. activity decreases with pain related response acceleration: T(12)=1.19, p=.26 (right Rolandic ROI) and T(12)=1.40, p=.19 (left Rolandic ROI). RTs show some correlation with the interaction effect in the right Rolandic Operculum [T(12)=1.55, p=.15]. Note, however, that i) on the behavioral level, the interaction effect on response times was unreliable, and ii) on the functional level, the interaction effect in the right Rolandic ROI was very weak (see Table 2.3-5). Therefore, this finding should be interpreted cautiously. The temperature covariate shows a small and consistent positive effect in the contrasts considered, which is, however, rather unreliable (all p values are above .36). Importantly, and in concordance with the F-tests above, no covariate effect reached the significance criterion (p=.05, two-tailed) in any region of interest.

Table 2.3-7. Matching Task. Covariate Assessment. Separate t-tests (two-tailed).

Contrast	Covariate	Region of Interest	Covariate effect	T value	P value
Faces > Forms					
	Response Time	Thalamus	.26	1.52	.15
		Rolandic Oper. (R)	-.11	-1.33	.20
		Insula (R)	.22	1.93	.08
		Rolandic Oper. (L)	-.15	-1.36	.20
Pain > No Pain					
	Temperature	Thalamus	.01	.09	.93
		Rolandic Oper. (R)	.03	.36	.72
		Insula (R)	.04	.51	.62
		Rolandic Oper. (L)	.04	.77	.45
	Response Time	Thalamus	-.06	-.48	.64
		Rolandic Oper. (R)	.13	1.19	.26
		Insula (R)	.09	.63	.54
		Rolandic Oper. (L)	.10	1.40	.19
2 x 2 Interaction					
	Temperature	Thalamus	.05	.86	.41
		Rolandic Oper. (R)	.04	.94	.36
		Insula (R)	.05	.64	.53
		Rolandic Oper. (L)	.00	.00	1.00
	Response Time	Thalamus	.01	.05	.97
		Rolandic Oper. (R)	.12	1.55	.15
		Insula (R)	.11	.75	.47
		Rolandic Oper. (L)	.08	.71	.49

Covariates were evaluated at the group level. Their correlation with ROI activity in each contrast of interest is indicated as covariate effect. Covariate effects (beta weights), T values and uncorrected P values are provided per pre-defined Region of Interest. P values refer to two-tailed t-tests. *Faces > Forms:* The t-statistic has thirteen degrees of freedom. *Other contrasts:* The t-statistic has twelve degrees of freedom.

2.3.2.3 Functional Characterization of the Amygdala

The amygdala was defined as a structural region of interest using the WFU Pick Atlas. SPM analysis was thus confined to the bilateral amygdala anatomical region. The emotion related response was specified by a 'Faces > Forms' contrast collapsing painful and non-painful conditions. This contrast was employed to uncover emotion responsive subregions within both amygdalae. **Fig. 2-16** shows the ensuing SPM T-map overlaid on a canonical MNI template.
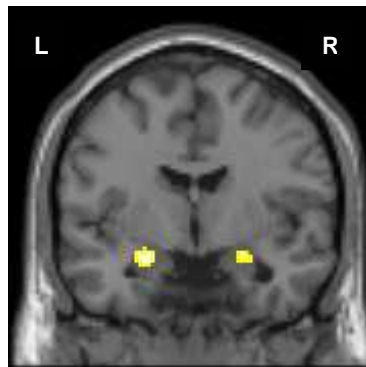
Fig. 2-16. Amygdala activation by factor 'Emotion' in the matching task ('Faces > Forms' contrast). The SPM T-map is thresholded at a voxel-wise p value of .05 (FWE small volume corrected) and is overlaid on a coronal slice of a structural MNI brain template (at MNI coordinate y=-4.3 mm). L: Left; R: Right.

Table 2.3-8 provides statistical details. The peak voxel value (Z=4.67) in the left hemispheric cluster is greater than in the right cluster. Moreover, the left cluster is larger. It comprises 46.4 percent of the left amygdala volume (816 mm^3) as defined by the Marsbar AAL plugin. The right cluster comprises 30.7 percent of the right hemispheric volume (608 mm^3). One further contrast yielded a significant activation focus, namely the negative 2 x 2 interaction contrast (Form & Pain + Face & No Pain > Face & Pain + Form & No Pain). This focus is comprised of only one voxel in the right amygdala surviving voxel level correction for multiple comparisons (p=.04, FWE corrected). Here, activation by emotional stimuli is attenuated during painful stimulation and vice versa. Note that other contrasts ('Faces < Forms', 'Pain <> No Pain' and the positive interaction contrast) did not reveal significant activation foci (p= .001, uncorrected) at any level of inference.

Table 2.3-8. Amygdala Characterization. SPM activation clusters in the Matching Task.

Region of activation	Laterality	MNI coordinates			Z-score	Cluster Size
		x	y	z		
Faces > Forms						
Amygdala (anatomical ROI)	L	-24	-4	-18	4.67	102
	R	26	-2	-18	4.07	76
2 x 2 Interaction < 0						
Amygdala (anatomical ROI)	L	*no significant voxels/clusters/map at p=.001, uncorrected*				
	R	28	-2	-24	3.21	1

The table shows clusters whose voxels exceed a t-statistic of 3.34 (P<.05 FWE corrected). The associated contrasts are indicated. For each maximal activation focus per cluster, laterality coordinates, Z-score, and number of contiguous voxels within a cluster are provided. Coordinates are defined in Montreal Neurologic Institute stereotactic space in millimeters.

Amygdala reactivity was further characterized at the region level. Beta weights were extracted from each structural ROI, averaged across voxels and entered into a 2 x 2 x 2 repeated measures ANOVA with factors 'Laterality' (left *vs.* right), 'Pain' (pain *vs.* no pain) and 'Emotion' (faces *vs.* forms). As expected, analysis revealed a highly significant effect of factor 'Emotion' [$F(1,14)=29.2$, $p<.001$]. Separate t tests (Table 2.3-9) confirmed that both amygdalae are reliably activated in the 'Faces > Forms' contrast. This effect is particularly prominent in the left amygdala [$T(14)=5.08$, $p<.001$, one-tailed]. Specifically, the size of the emotion related response in the left amygdala is by 23.0 percent greater than in the right amygdala. However, a paired samples t-test revealed that this difference is not significant in the sample [$T(14)=-.67$, $p=.26$, one-tailed]. Consistently, the effect of the ANOVA factor 'Laterality' is unreliable: $F(1,14)=1.54$, $p=.701$. However, there is a borderline significant effect of the 'Laterality x Pain' interaction indicating that the magnitude of pain related amygdala activation differs between hemispheres: $F(1,14)=1.40$, $p=.049$. Separate t-tests confirmed that the pain related response in the right amygdala is stronger and more reliable than in the left amygdala (Table 2.3-9). Still, the significance criterion is missed in both amygdalae. Concordantly, the effect of the ANOVA factor 'Pain' is unreliable [$F(1,14)=5.72$, $p=.46$]. The 'Emotion x Pain' interaction and the three way interaction are unreliable, as well [$F(1,14)=1.83$, $p=.20$ and $F(1,14)=1.40$, $p=.26$, respectively].

Table 2.3-9. Amygdala Characterization. ROI Response Behavior in the Matching Task. T-tests.

Contrast	Laterality	Signal change (%)	T value	P value	Active voxels (%)
Faces > Forms					
	L	.32	5.08	<.001	78.64
	R	.26	3.51	.002	87.90
Pain > No Pain					
	L	.01	.14	.45	1.36
	R	.08	1.36	.10	5.24
2 x 2 Interaction					
	L	-.04	-.65	.52	3.64
	R	-.08	-1.98	.07	23.39

For each contrast of interest, response magnitude, T values and uncorrected P values are provided per hemisphere. Response magnitude is expressed as percent signal change relative to the whole brain global mean. The T statistic has 14 degrees of freedom. T tests are two-tailed (interaction contrast) or one-tailed (main effects). The percentage of active voxels that exceed a T threshold of 1.76 and ±2.14 (conforming to a one-tailed and two-tailed P value of .05, respectively) is also listed. L: Left; R: Right.

Amygdala response profiles were created by plotting the extracted beta weights as a function of experimental condition (**Fig. 2-17**, panel *a*). Conditions were arranged along the x-axis in the order of expected signal gain: Forms & No Pain -> Forms & Pain -> Faces & No Pain -> Faces & Pain. The response amplitude is greatest between 'Forms & Pain' and 'Faces & No Pain' conditions, particularly in the left amygdala. In the left amygdala, the response profile displays a sigmoid shape. In the right amygdala, however, activity increases steeply and almost linearly across the first three conditions. Painful stimulation is thus associated with a signal gain that is comparable with the gain produced by emotional stimuli. In the last condition ('Faces & Pain'), where emotional and painful stimuli are combined, amygdala activity saturates (right amygdala) or drops (left amygdala). The interaction plot (panel *b*) summarizes bilateral amygdala responsiveness in the matching paradigm: In the context of neutral visual stimuli (form matching task), amygdala activity is enhanced by painful stimulation. However, exposure to aversive faces (face matching task) reverses this effect: Painful stimulation yields a slightly lower amygdala activity than non painful stimulation (cross interaction). This negative interaction effect is not reliable, but it is present in both amygdalae, more prominently in the right hemisphere [T(14)=-1.98, p=.07, two-tailed, see Table 2.3-9].
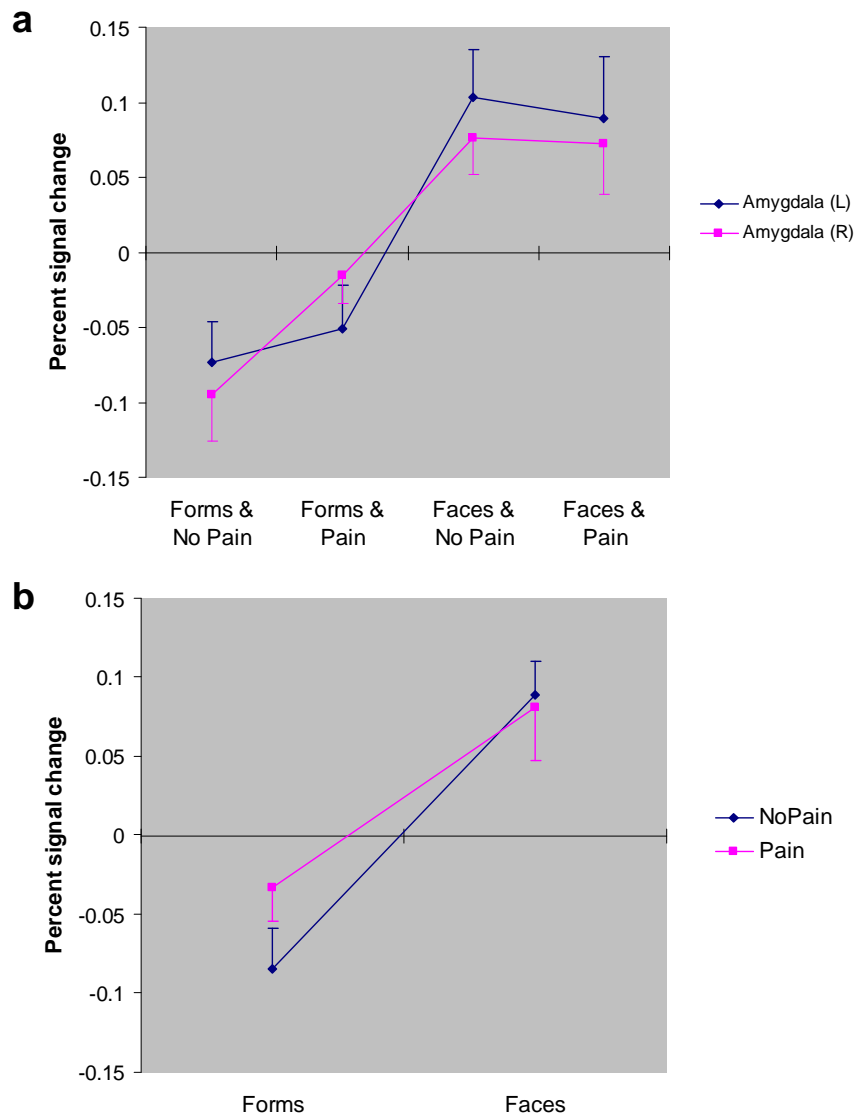
Fig. 2-17. Amygdala activity of as a function of experimental conditions in the Matching Task. *Panel a:*: Activation profiles per hemisphere (right: squares, left: diamonds). *Panel b:* Interaction plot. The mean response (averaged across both ROIs) to painful (squares) and non-painful (diamonds) stimulation in the context of face matching and form matching tasks is provided. Error bars denote the standard error of the mean.

In the following, the amygdala response to the painful stimulation as administered in the Matching Task (pain rating: 5/10) and the Localizer Paradigm (pain rating: 8/10) is investigated. Within the amygdala ROI, SPM analysis did not reveal any significantly active voxels in the 'Pain > No Pain' contrast in both paradigms (p=.001, uncorrected). The analysis was repeated at the region level. The results are given in Table 2.3-10. Bilateral ROIs showed a reliable activation by the highly painful stimulation administered in the Localizer Paradigm (corresponding to a pain rating of 8 out of 10). This response is slightly stronger and more reliable in the left amygdala [T(14)=2.49, p=.01, one tailed] and activates as much as 50.9 percent of the anatomical volume. This pain related activation

survives Bonferroni correction for the number of ROIs (2) entered into the analysis. In the Matching Task, painful stimuli are of medium intensity (corresponding to a pain rating of 5 out of 10) and elicit a clearly weaker response. The significance criterion is missed in both hemispheres. The right amygdala is more sensitive to the medium intense pain in the Matching paradigm [T(14)=1.36, p=.10, one-tailed] that activates 5.2 percent of the anatomical volume. **Fig. 2-18** summarizes amygdala responsiveness to emotional and painful stimuli.
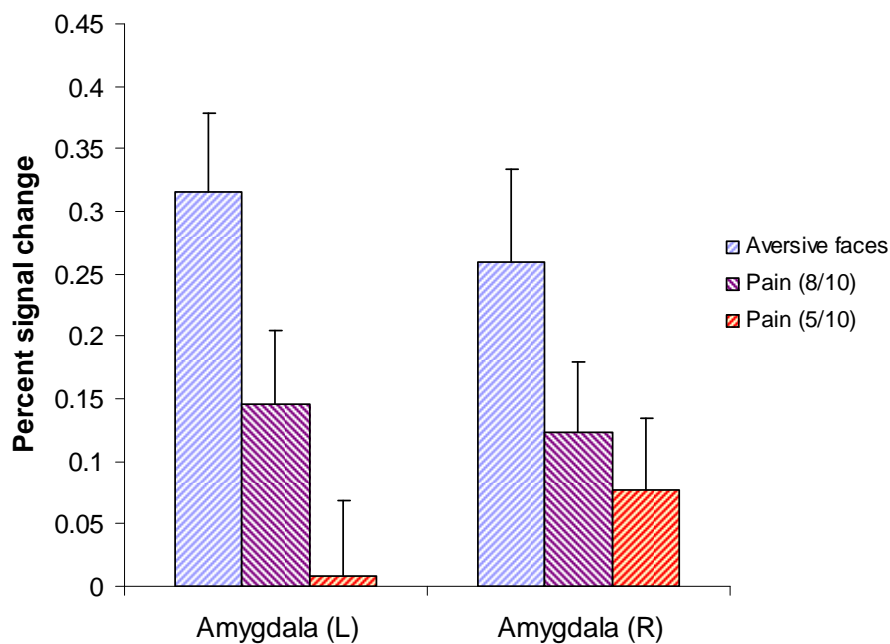
Fig. 2-18. Magnitude of amygdala activation by painful and emotional stimuli. The pain related response refers to a 'Pain > No Pain' contrast performed on data from the Matching Task (medium intense pain, rating: 5/10) and the Localizer Paradigm (high intense pain, rating: 8/10). The response to aversive faces refers to a 'Faces > Forms' contrast. Error bars denote the standard error of the mean.

It was further investigated, whether the amygdala response to painful stimulation can be sharpened by narrowing down the search volume to those subregions that exhibit a reliable response to aversive faces. These regions were defined functionally by a 'Faces > Forms' contrast. The ensuing activation clusters were studied in detail above (**Fig. 2-16** and Table 2.3-8). The analysis was then re-run with these emotion-sensitive ROIs instead of the anatomical ROIs. Table 2.3-10 compares the results of both variants of ROI specification. In emotion sensitive ROIs, the pain specific mean response ('Pain > No Pain') was higher, more reliable, and a greater percentage of voxels was activated compared to the anatomical definition. This holds for both intensity levels (5/10 and 8/10). In particular, the amygdala response to medium intense pain (5/10) benefited from the narrower functional ROI definition, but the significance criterion was still missing here. To

comprehensively assess the amygdala response to pain, a 3 x 2 repeated measures ANOVA was carried out with factors 'Laterality' (left *vs.* right), 'ROI definition' (functional *vs.* anatomical), and 'Intensity' (medium *vs.* high). The analysis revealed a significant effect of factor 'ROI definition' [$F(1,14)=5.77$, p=.031, G.G. corrected]. A paired samples t-test on collapsed data confirmed that the pain related signal in emotion sensitive ROIs was significantly higher (by 16.4 %) than in anatomically defined ROIs: $T(59)=2.74$, p=.008, two-tailed. For factor 'Intensity' and factor 'Laterality' the significance criterion was missed [$F(1,14)=3.04$, p=.10, and $F(1,14)=.77$, p=.40, respectively]. All two-way interactions and the three-way interaction were also non-significant.

Table 2.3-10. Amygdala Characterization. Pain reactivity of anatomical and functional ROIs. T-tests.

Contrast	Amygdala definition	Laterality	Signal change (%)	T value	P value	Active voxels (%)
ROI Localizer Pain > No Pain						
	anatomical					
		L	.15	2.49	.01	50.91
		R	.12	2.25	.02	41.13
	functional					
		L	.16	2.61	.01	79.41
		R	.14	2.31	.02	60.53
Matching Task Pain > No Pain						
	anatomical					
		L	.01	.14	.45	1.36
		R	.08	1.36	.10	5.24
	functional					
		L	.02	.41	.34	2.94
		R	.09	1.40	.09	9.21

Magnitude of pain related response (percent signal change), T and uncorrected P values are provided per hemisphere and type of amygdala ROI definition. amygdala ROIs were defined i) functionally from amygdala clusters exhibiting significant activation in the 'Faces > Forms' contrast, and ii) anatomically according to the AAL Atlas. Heat stimuli in the Matching Task and the Localizer paradigm correspond to medium (rating: 5/10) and intense pain (rating: 8/10), respectively. The T statistic has 14 degrees of freedom. P values refer to one-tailed t-tests. The percentage of active voxels that exceed a T threshold of 1.76 (conforming to a one-tailed P value of .05) is also listed. L: Left; R: Right.

Amygdala activity may be influenced by two sources of inter-subject variability: i) the individual temperatures employed to equalize pain perception in the sample, and ii) the response times related to the incidental task. Covariate effects were assessed in an F-test approach: A full model including the appropriate covariates in addition to the constant term was compared with a reduced model that only consists in the constant term. F-tests were carried out for each contrast of interest. The results are given in Table 2.3-11 for both paradigms. Note that for the 'Face > Forms' contrast (Matching Task) only the response time covariate was studied as the contrast collapses over painful and non-painful conditions. In summary, no significant amount of variance can be explained by covariates.

This holds for both functional and anatomical definitions of the amygdala region of interest. Some effects however, albeit statistically insignificant, are worth mentioning. In the Matching Paradigm, there is a notable covariate effect in the 'Faces > Forms' contrast. 19.1 percent of the left anatomical volume correlated with per subject response times [$F(1,13)=3.32$, $p=.09$]. This number rises to 29.4 percent for the functional ROI definition. The F statistic concordantly indicates are more reliable effect for the functional definition, but the significance criterion was still not met [$F(1,13)=3.83$, $p=.07$]. Separate t-tests (Table 2.3-12) revealed that emotion related activity ('Faces > Forms') increases with growing response time in the left emotion sensitive ROI [$T(13)=1.96$, $p=.07$, two-tailed], and to a lesser extent in the anatomically defined ROI [$T(13)=1.82$, $p=.09$, two-tailed]. Moreover, t-tests revealed that the pain related amygdala response ('Pain > No Pain') and the interaction effect positively correlate with RT, as well. The covariate effect is generally stronger in the left hemisphere and in the functionally defined ROIs. The second-strongest RT effect refers to the pain-related response ('Pain > No Pain') of the functionally defined left amygdala, i.e. the response to pain increases with growing response time: $T(12)=1.69$, $p=.12$, two-tailed. With respect to the Localizer paradigm, there is no substantial covariate effect evident from F-tests (all $p \geq .42$, two-tailed). Separate t-tests referring to the Localizer Paradigm are provided in Table 2.3-13.

Table 2.3-11. Amygdala Characterization. Covariate Assessment. Full model versus reduced model. F-tests.

Paradigm	Contrast	Amygdala definition	Laterality	Extra sum of squares	F value	P value	Percentage of active voxels
ROI Localizer							
	Pain > No Pain						
		anatomical					
			L	.01	.11	.90	.00
			R	.07	.70	.52	4.03
		functional					
			L	.01	.10	.90	.00
			R	.11	.93	.42	11.84
Matching Task							
	Pain > No Pain						
		anatomical					
			L	.15	1.40	.28	3.18
			R	.08	.84	.45	2.02
		functional					
			L	.13	1.43	.28	6.86
			R	.09	.73	.50	1.32
	Faces > Forms						
		anatomical					
			L	.17	3.32	.09	19.09
			R	.00	.00	.98	.00
		functional					
			L	.18	3.83	.07	29.41
			R	.00	.01	.93	.00
	2 x 2 Interaction						
		anatomical					
			L	.07	.74	.50	3.64
			R	.03	.44	.65	.00
		functional					
			L	.05	.49	.62	.98
			R	.02	.16	.85	.00

Models were evaluated at the group level for each contrast of interest in both paradigms. *Faces > Forms:* The full model includes the response time covariate plus the constant term [$F(1,13)$]. *Other contrasts:* The full model includes response time and temperature covariates plus the constant term [$F(2,12)$]. Magnitude of covariate effect (extra sum of squares), F values and uncorrected P values are provided for functional and anatomical ROI definitions. The percentage of active voxels that exceed an uncorrected p-threshold of .05 (equivalent to a voxel-wise $F(1,13)=4.67$ and $F(2,12)=3.89$, respectively) is also listed. L: Left; R: Right.

Table 2.3-12. Amygdala Characterization. Covariate Assessment. Matching Task. Separate t-tests (two-tailed).

Contrast	Covariate	Amygdala definition	Laterality	Covariate effect	T value	P value
Faces > Forms						
	Response Time					
		anatomical				
			L	.28	**1.82**	.09
			R	.00	-.02	.98
		functional				
			L	.29	**1.96**	.07
			R	-.02	-.09	.93
Pain > No Pain						
	Temperature					
		anatomical				
			L	.07	1.03	.32
			R	.05	.78	.45
		functional				
			L	.06	.91	.38
			R	.05	.67	.52
	Response Time					
		anatomical				
			L	.18	**1.65**	.12
			R	.13	1.29	.22
		functional				
			L	.17	**1.69**	.12
			R	.14	1.21	.25
2 x 2 Interaction						
	Temperature					
		anatomical				
			L	.04	.68	.51
			R	-.04	-.85	.41
		functional				
			L	.04	.68	.51
			R	-.02	-.37	.72
	Response Time					
		anatomical				
			L	.13	1.15	.27
			R	.02	.16	.87
		functional				
			L	.11	.88	.40
			R	.04	.32	.75

Covariates were evaluated at the group level. Correlation of response times and temperatures with amygdala activity in each contrast of interest is indicated as covariate effect. Covariate effects (beta weights), T values and uncorrected P values are provided for functional and anatomical ROI definitions. P values refer to two-tailed t-tests. *Faces > Forms:* The t-statistic has thirteen degrees of freedom. *Other contrasts:* The t-statistic has twelve degrees of freedom. L: Left; R: Right.

Table 2.3-13. Amygdala Characterization. Covariate Assessment. ROI Localizer. Separate t-tests (two-tailed).

Covariate	Amygdala definition	Laterality	Covariate effect	T value	P value
Temperature					79
	anatomical				
		L	-.06	-.46	.65
		R	-.08	-.66	.52
	functional				
		L	-.06	-.43	.68
		R	-.15	-1.14	.28
Response Time					
	anatomical				
		L	.03	.19	.85
		R	-.11	-.74	.47
	functional				
		L	.05	.28	.79
		R	-.06	-.37	.72

Covariates were evaluated at the group level. Correlation of response times and temperatures with amygdala activity in the 'Pain > No Pain' contrast is indicated as covariate effect. Covariate effects (beta weights), T values and uncorrected P values are provided for functional and anatomical ROI definitions. P values refer to two-tailed t-tests. The t-statistic has twelve degrees of freedom. L: Left; R: Right.

2.4 Discussion

The aim of the present study was to investigate the interaction between pain and emotion processing in the human brain. Heat stimuli equalized for perceived pain intensity were employed as pain stimuli. Photographs of high valence facial expressions (anger and fear) were employed as socially relevant emotional stimuli. We report four major results: i) pain responsive cortical regions are activated by both factor 'Pain' and factor 'Emotion' in approximately the same relative proportions. ii) The bilateral amygdala responds to high intensity thermal pain. iii) This response is particularly strong in those subregions of the amygdala that exhibit a reliable response to the facial stimuli. iv) Factor 'Pain' and factor 'Emotion' do not interact significantly. There is, however, a consistent trend towards a negative interaction effect. Specifically, neural correlates of thermal pain and emotional stimuli aggregate less than additively (subadditively) in all investigated regions.

Neurobiological studies have identified the amygdala as a key structure in the processing of fear and anxiety (Aggleton, 2000). Concordantly, facial stimuli elicited a strong and reliable bilateral amygdala response in the present study. Given this activation we assume that a negative affective state has been created successfully in the participants. Our paradigm did not provide any rating scheme (e.g., 'unpleasantness' rating) that could confirm the success of emotional induction. On the other hand, asking the participants to rate their feelings would have introduced cognitive effects complicating the interpretation of results (see below). Moreover, employed facial stimuli are well validated (Calder and others, 2000;Calder and others, 1997), and aversive faces have previously been shown to elicit a significant autonomous stress response in the original version of the face matching paradigm (Hariri and others, 2002c). The left amygdala cluster is larger and shows a more reliable emotion related signal than the right hemispheric focus. In most other studies employing the face matching paradigm or its derivatives, the right amygdala is dominant, however. Hariri and colleagues found that aversive faces engage particularly the right amygdala, whereas the left amygdala is more strongly involved in the processing of aversive scenes that are devoid of social elements (Hariri and others, 2002c). It may be argued therefore, that our amygdala activation does not reflect the social signal implied by angry and fearful expressions. This is a point of concern as there is reason to believe that maladaptive processing of social stimuli is a key component of somatoform diseases (Grabe, Spitzer, and Freyberger, 2004). A paradigm that does not reliably probe neural systems related to the social dimension may be useless for validating corresponding

disease models. One must bear in mind, however, that the signal quality in the amygdala region (signal to noise ratio, SNR) is reduced due to susceptibility artifacts cause by the neighboring sinus cavities. LaBar and colleagues point out that the laterality of activation foci in the limbic forebrain is highly variable for this reason and should not be overinterpreted (LaBar and others, 2001). Unsurprisingly, other studies have found a predominantly left sided response to aversive facial stimuli (Heinz and others, 2005). This even holds for (at least) one study employing the face matching paradigm (Hariri and others, 2002a). Hence, our findings do not contradict published results concerning the neural correlates of socially aversive stimuli.

Another point of concern refers to the baseline condition. The emotion related signal was defined as the remainder of the subtraction between the BOLD responses in the face matching and the form matching task. This subtraction principle commonly applied in fMRI studies has been criticized in that experimental conditions are likely to elicit a whole series of changes in the brain (Jezzard, 2001). It follows that the baseline condition must be in every aspect equal to the experimental condition except for the feature of interest, i.e. negative emotionality. In this sense, the 'best' baseline would employ photographs of neutral faces as opposed to abstract geometric forms. In fact, the 'Faces > Forms' contrast in the present study did not only reveal activity in the amygdala but also in the visual cortices and the fusiform 'face' areas. We tried to reduce additional activations by equalizing baseline and experimental conditions in terms of stimulus shape, luminance and position (see method section for details). Meyer-Lindenberg and colleagues defend the usage of simple geometric forms (Meyer-Lindenberg and others, 2008) as it has been shown that a low-level baseline is necessary for a reliable amygdala activation (Lawrie and others, 2002). Moreover, the fMRI environment *per se* can create anxiety and participants may misperceive neutral faces as threatening thus causing amygdala activation in the control condition (Thomas and others, 2001).

We were impressed by the high signal quality in a region that is affected by susceptibility induced signal drop outs. According to our literature research, the amygdala response in our study (peak Z=4.67) was more reliable than in many other neuroimaging studies with similar sample sizes. Our modifications of the original Hariri paradigm have successfully optimized the signal to noise ratio (SNR). It should be stressed that a good signal to noise ratio is crucial for finding an emotion related signal in pain responsive regions, i.e. in brain areas that have been defined according to their response to thermal pain rather than their response to emotional faces. The following key modifications have

been applied to the original face matching paradigm: Firstly, the number of face matching blocks has been increased from two to eight. Note, however, that a significant habituation effect for facial stimuli has been repeatedly found in fMRI studies of the amygdala (Hariri and others, 2002c;Wedig and others, 2005;Wright and others, 2001). Increasing the number of trials by repeating stimuli is probably not enough to improve SNR substantially. Secondly, we reduced the duration of a block from 30 to 20 seconds. This is closer to the theoretical optimum (16 seconds) that applies to the canonical HRF (Henson, 2007). Trial duration was reduced from 5 seconds to 3.3 seconds thus increasing the proportion of time during which the participants are engaged in the matching task. Thirdly, we optimized the covariance structure of the design by inserting 10 second pauses between subsequent blocks. This allows the BOLD signal to settle down improving the estimation efficiency of the statistical model (see Formula 2, p. 50). Fourthly, we employed computer enhanced stimuli that are of higher emotional valence than the original Ekman and Friesen stimuli (Calder and others, 2000). The stimuli were masked at the hairline, i.e. the subjects had to match the photographs according to facial features instead of hairstyle or background details that are devoid of emotional content. The orbital region is most important to determine a person's identity and has been shown to be particularly relevant for producing a BOLD response in the amygdala (Morris, deBonis, and Dolan, 2002).

The percentage of correctly matched images (faces and forms) was close to 100 for all participants indicating a good compliance. Participants matched geometric shapes significantly faster than facial images. This finding may raise concern about the specificity of the reported amygdala activity: It may not exclusively reflect the aversive character of the stimuli but also the higher task difficulty during face matching compared to form matching. However, the slowest response time recorded (1.7 seconds) was still well below the duration of a trial (3.3 seconds). We therefore do not think that task related stress may have contributed to the reported amygdala activation. Covariate assessment nevertheless revealed a borderline significant correlation between response time (RT) and the emotion-related amygdala signal. As illustrated in **Fig. 2-19**, the amygdala response to factor 'Emotion' increases with increasing task specific RT and saturates when RT in the face matching task exceeds the baseline RT (form matching task) by approximately 400 ms. This relationship is well approximated by a logarithmic function (red curve; R^2=.36; $F(1,13)$=7,42, p=.02)
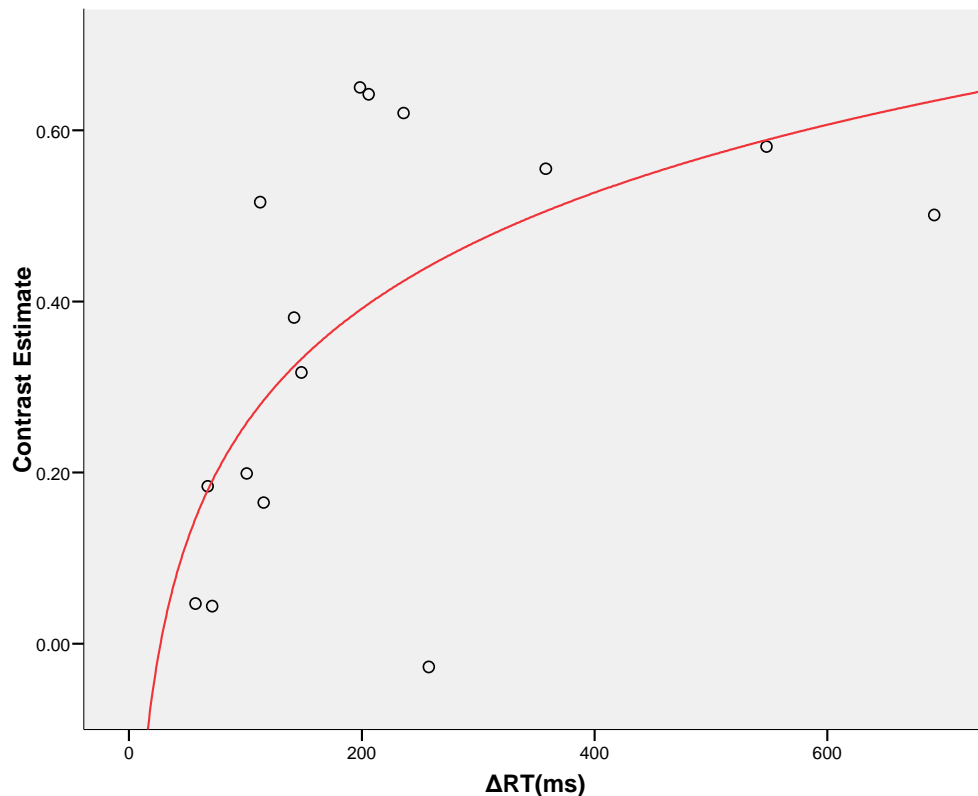
Fig. 2-19. Mean activation in the left emotion sensitive amygdala cluster as a function of response time. The emotion related signal is defined as 'Faces > Forms' contrast. Likewise, ΔRT denotes the (average) RT difference between face matching and form matching trials. Each point in the scatter plot refers to one subject. Data are fitted by a logarithmic function using SPSS (v. 15).

It has been shown that amygdala activity can be modulated by cognitive factors. For instance, activity decreases when facial emotions are explicitly labeled rather than implicitly processed (Hariri, Bookheimer, and Mazziotta, 2000;Critchley and others, 2000). Cognitive top down modulations are worrisome, however, when the cognitive task *per se* is unrelated to the research question. In the present study the employed task is 'incidental', i.e. it shall merely confirm the participants' attention towards the stimuli. Liberzon and colleagues have found that task instructions relating to recognition memory and interoception ('unpleasantness rating') differentially influence amygdala reactivity to aversive stimuli (Liberzon and others, 2000). Taylor and colleagues (Taylor and others, 2003) have suggested that amygdala activity might be preserved best by not combing emotional stimuli with cognitive tasks at all ('passive viewing'). However, this implies that the experimenter must rely on the subjects to attend to the stimuli in an uncontrolled way. As to our knowledge, the influence of RT on amygdala activity in the Matching Task paradigm has never been studied before. Our finding indicates that activity evoked by facial stimuli depends on the amount of time during which participants actively attend towards these stimuli while performing a low level perceptual task. The ceiling effect

shown in **Fig. 2-19** adds credibility to this interpretation. This finding may motivate design optimizations that aim to further improve the signal to noise ratio in the amygdala region of interest. For instance, trial duration could be further reduced in order to increase the period of time the subjects spend in a state of active attention. As an alarm system, the amygdala can respond very rapidly to aversive stimuli, which has been repeatedly shown in fMRI studies (Etkin and others, 2004;Morris, Ohman, and Dolan, 1998). Hence, statistical power might particularly benefit from a reduction of trial duration in favor of a higher number of trials.

We observed that the amygdala was activated by two different modalities, namely by aversive visual stimuli and – to a lesser extent – by physical pain. The response to intense pain (rating: 8/10) accounted for 47% of the response to aversive faces. Moderately painful (rating: 5/10) stimuli elicited a positive but unreliable response. Pain related activity was detected bilaterally in line with a previous fMRI study investigating neural correlates of acute thermal pain (Bornhovd and others, 2002). The amygdala is an alarm system, whose primary role is to signal impending threat and to elicit behavioral and hormonal measures before body harm can be inflicted. In the present study we found amygdala activation during ongoing body injury that causes a first degree skin burn. The amygdala as a nociceptive structure, is well documented in animal research (Neugebauer and others, 2004). In human neuroimaging, however, the role of the amygdala in the processing of pain is less established. Numerous neuroimaging studies failed to report amygdala activity during acute noxious stimulation. Review articles do not mention the amygdala as a core region of the pain processing system (Tracey, 2008;Peyron, Laurent, and Garcia-Larrea, 2000;Neugebauer and others, 2004;Tracey and Mantyh, 2007). Moreover, both activations and deactivations have been reported (Neugebauer and others, 2004). Tracey and colleagues (Tracey, 2008) list the amygdala among those regions that are optionally but not mainly activated by acute pain. These authors suggest a large interindividual variation of the pain related amygdala response depending on context factors. It has been emphasized that the amygdala is a region involved in a variety of different but somewhat related functions. It would therefore be particularly important to select the baseline condition carefully. Different baselines may partly explain the inconsistencies regarding the nociceptive amygdala response, which are, however, "yet to be understood" (Neugebauer and others, 2004). It must be noted in this context that the methodological concerns regarding the form matching baseline discussed above do not apply here. High intensity pain stimuli were administered in a separate paradigm that was

tailored to unambiguously identify pain responsive regions. The two conditions employed there ('pain' *vs.* 'no pain') differ only in the feature of interest, namely high intensity thermal pain corresponding to a subjective rating of 8 out of 10.

Bornhovd and colleagues have identified an important confound regarding the pain related amygdala response (Bornhovd and others, 2002). They presented heat stimuli of various intensities in random order and at random intervals. They found a substantial amygdala response in trials, where the stimulus intensity was actually below the perceptual threshold ('null' trial). During these trials, the participants could not be sure whether a 'null' trial is being presented or a painful trial is about to be initiated. The authors suggest that the amygdala is involved in coding this 'uncertainty'. Concordantly, it has been shown that expectation of pain *per se* can engage anatomical regions implicated in the processing of pain (Ploghaus and others, 1999). In the present study, however, the pain stimulus was announced 10 seconds prior to the trial. There was consequently no uncertainty involved that could have augmented the amygdala response to pain. Moreover, the time intervals (ramping intervals), during which anticipation or preparatory responses might have taken place, were not included in the statistical model, effectively ruling out these confounds.

Psychometric profiling revealed that pain perception of a given stimulus intensity can vary greatly across subjects (**Fig. 1-4**). This observation may partly explain the above-mentioned inconsistencies in the neuroimaging literature regarding the nociceptive amygdala response. In designs that operate with fixed temperatures (i.e. temperatures are identical for all subjects) only a subset of participants may experience a substantial pain sensation. Since amygdala responsiveness largely depends on the subjective perception of pain (Bornhovd and others, 2002;Giesecke and others, 2005;Schneider and others, 2001), fixed temperature designs are less powerful in detecting a pain related signal change. A second reason for the above-mentioned inconsistencies may involve the anatomical location of the amygdala near the sinus cavities. SNR in echo-planar imaging is reduced by macroscopic susceptibility gradients at air-bone interfaces, particularly when higher field strengths are utilized (Deichmann and others, 2003;Krasnow and others, 2003;Merboldt and others, 2001). Research groups investigating pain responsive regions often do not focus on the amygdala. They often employ high field strengths, since 3 Tesla machines become increasingly available and are clearly advantageous in regions that lie remote from air-bone interfaces. However, this general advantage does not apply to the amygdala and the orbitofrontal cortex (Krasnow and others, 2003), which are particularly implicated in psychiatric research. Optimized EPI sequences are available for these elusive regions

(Merboldt and others, 2001;Deichmann and others, 2003), but appear to be underutilized. A third reason for the reported inconsistencies may relate to the task instruction. In the ROI localizer paradigm the task was kept as simple as possible: the subject had to press a button as soon the fixation cross blinks. Many studies employ unpleasantness ratings or pain intensity ratings. Rating of an unpleasant experience represents a cognitive task that produces a feeling of control over that experience. This phenomenon is utilized in a therapeutic setting (Marks, 1985). For our purpose, however, a rating task may reduce the neural response to pain by exerting a top down control over the amygdala. It has already been shown that amygdala activity is attenuated by rating the unpleasantness of aversive visual stimuli compared to passive viewing (Taylor and others, 2003). To avoid interactions between pain processing and cognition, the participants were not required to evaluate their pain experience during fMRI data acquisition. Instead, the pain stimuli were rated in a separate session outside the scanner (see section 1.2.4).

We found that the response to pain was particularly strong in those subregions of the amygdala that exhibited a reliable response to facial stimuli. As shown in **Fig. 2-20**, the pain related activation cluster resides almost entirely within the cluster activated by aversive faces. In a *post hoc* analysis we further investigated the regional specificity of the amygdala response. For this purpose we employed a probabilistic atlas (Eickhoff and others, 2005) that parcellates the human amygdala into three major subdivisions based on differences in cyto, myelo and chemoarchitecture (Amunts and others, 2005): the laterobasal amygdaloid group (LB), the centromedial group (CM), and the superficial (cortical) group (SF). These structures encompass nuclei that have been characterized in animal research: LB comprises the lateral, basolateral, basomedial and paralaminar nuclei, CM the central and the medial nuclei, and SF includes the anterior amygdaloid area, the ventral and posterior cortical nuclei. In humans the functional properties of these subdivisions are largely unexplored. Existing imaging studies rarely assess amygdala response behavior in terms of cytoarchitecture, although some authors report that regional differences in function do indeed exist (Etkin and others, 2004;Whalen and others, 2001). As to our knowledge no imaging study so far investigated correlates of pain in different amygdala subregions.
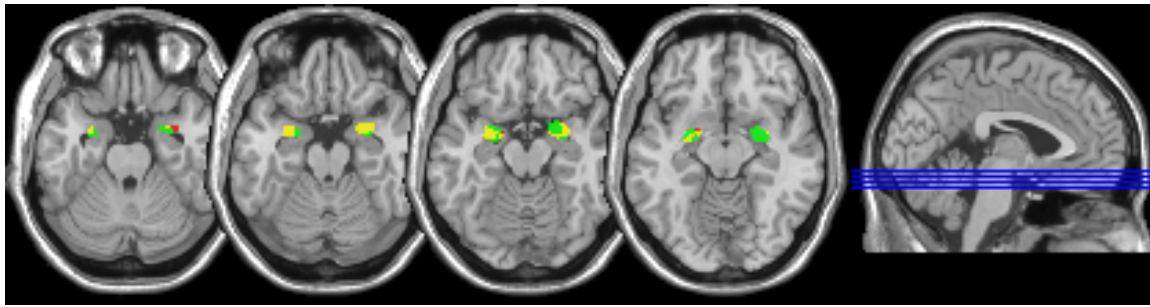
Fig. 2-20. Spatial relationship between emotion and pain related activation clusters in the amygdala. The emotion related signal was defined as 'Faces > Forms' contrast (green). The pain related signal was defined as 'Pain > No Pain' contrast (red) referring to highly painful stimulation (rating: 8/10). The intersection area of both clusters is indicated (yellow).

In mammals, highly processed polymodal information reaches the amygdala from the thalamus and the cerebral cortex through the lateral (LA) and basolateral nucleus (BLA), and is then conveyed to the central nucleus (CeA). The human homolog lies dorsal to the laterobasal part and comprises only 10% of the amygdala volume. This output nucleus has efferences to the hypothalamus, brainstem and forebrain regions, regulating behavioral, emotional and autonomic responses (LeDoux, 2000). The LA–BLA–CeA connection has been described as fear and anxiety related circuitry, which also receives input from pain processing structures such as the insular cortex and the midline nuclei of the thalamus. Single unit recordings in rats revealed a high concentration of nociceptive neurons in the laterocapsular part of the Central nucleus. These neurons typically have a large bilateral receptive field, which is in agreement with our finding of a bilateral nociceptive amygdala response. The neurons receive direct input from the spinal cord (Burstein and Potrebic, 1993) and ascending pain pathways such as the spino-parabrachio-amygdaloid pain pathway (Gauriau and Bernard, 2002). This 'nociceptive' amygdala also has indirect connections with the medial dorsal thalamus, hypothalamus and agranular insular via the substantia innominata dorsalis. These structures are implicated in pain processing, which we were able to confirm in the present study. The amygdala is part of the endogenous pain control system via its efferent projections to midbrain regions such as the periaqueductal grey (LeDoux, 2000). The amygdala activation in the present study may thus reflect both its afferent and its efferent functions, relating to nociception and pain control, respectively.

Given the convergence of polymodal inputs on the same neural circuitry it may be no surprise that aversive faces and thermal pain activated overlapping clusters within the amygdala. The modality specific activation peaks lie only 4.5 mm (left amygdala) and 6.3 mm (right amygdala) apart. Thermal pain and aversive faces engaged all three subdivisions

in almost the same relative proportions **Fig. 2-21**. The SF and LB are prominently activated in line with the recent meta-analysis by Ball and colleagues (Ball and others, 2009). We observed the largest response in the SF subdivision, which is adjacent to the laterobasal group. In rodents this structure is implicated in the acquisition of conditioned fear responses (Gonzalez-Lima and Scheich, 1986).
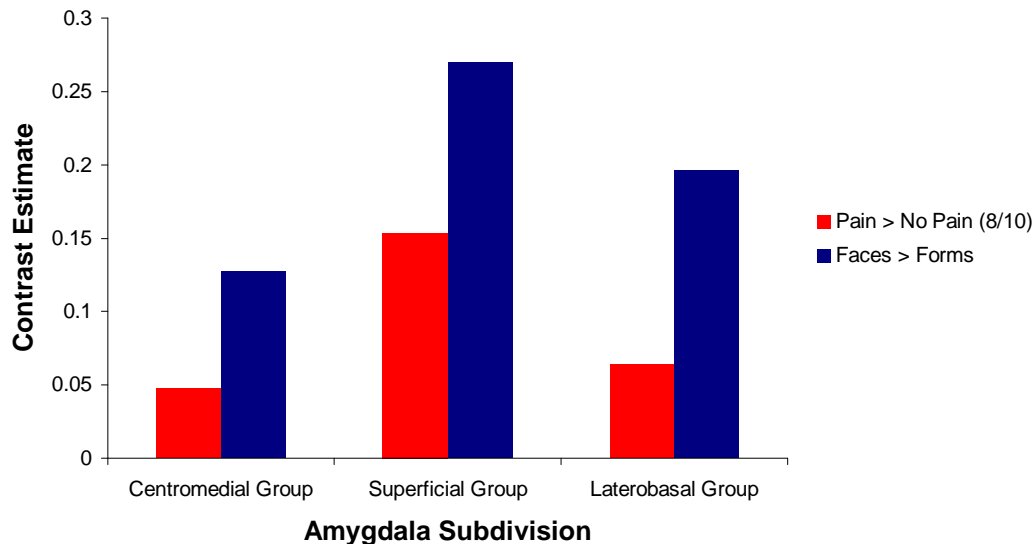
Fig. 2-21. Response of amygdala subdivisions to emotional and painful stimulation. The corresponding SPM contrasts are indicated. Intensity of thermal pain corresponds to a subjective pain rating of 8 out of 10. The amygdala subdivisions are defined according to cytoarchitectonic criteria (Amunts and others, 2005) using the SPM Anatomy toolbox v. 1.5 (Eickhoff and others, 2005).

In summary, facial and pain stimuli share the same neural substrate within the amygdala. Both modalities appear to be processed similarly even at the microscopic level with the only major difference being the higher signal gain observed for facial stimuli compared to thermal pain. Given this concordance and the connection between the amygdala and the descending pain control system, one may speculate that a persistent negative emotional state may affect the PAG and consequently the filtering of sensory information at the dorsal horn. This could be the neural mechanism behind the concept of 'somatic amplification' of sensory stimuli (Barsky and Klerman, 1983), which has been proposed to link states of emotional distress to physical symptoms (McCracken, Faber, and Janeck, 1998).

We cannot determine in the present study, whether noxious information reached the amygdala via spinal pathways or through structures that we identified as pain responsive regions in the localizer experiment. This particularly refers to the midline thalamus and the anterior ('agranular') insular cortex. These structures were shown to be connected to the

amygdala in animal studies (see above) and were strongly activated by the same thermal stimulation that also engaged the amygdala. Visual (aversive faces) and thermal stimulation is processed strikingly similar, which confirms the general notion that the amygdala attaches emotional significance to polymodal sensory inputs. In this sense, the lack of significant amygdala activation in response to moderate pain suggests that the applied thermal intensity was possibly too low to be interpreted as threat. The high relevance of aversive social signals (angry and fearful faces) to social animals like humans (Darwin, 1872;Ekman, Sorenson, and Friesen, 1969) may also explain, why the amygdala responds stronger to these visual cues of threat rather than to body injury caused by noxious heat.

It has been argued that high resolution imaging is more appropriate to differentiate functional aspects of the amygdala nuclei, since their respective centers lie less than 1cm apart (Annemieke M. Apergis-Schoute in response to Ball et al. (2007)). In this way, functional differences within the amygdala could be delineated more accurately. The central nucleus (CeA) as a mediator of the stress response would be particularly interesting for further studies in the context of chronic pain syndromes and affective disorders. Neugebauer and colleagues have focused on the central nucleus of the amygdala in an animal model of chronic pain (Neugebauer and Li, 2003). In this model, monoarthritis in rats was induced in one knee by injection of irritants. Within hours after injection, a subset of neurons within the central nucleus exhibited enhanced responses to mechanical stimuli, not only at the site of injury but also at intact body sites. This indicates a sensitization of neurons by a persistent pain stimulus as well as an enlargement of their receptive fields. This hypersensitivity to pressure stimuli resembles symptoms observed in some chronic pain syndromes, such as fibromyalgia. In the arthritic pain model, whole-cell voltage-clamp recordings on CeA neurons confirmed enhanced synaptic transmission of both spinal and thalamocortical inputs. Moreover, the resting membrane potential of CeA neurons was raised indicating a general hyperexcitability. In the present study, we found an activation of the CeA homolog in humans by both painful and emotional stimuli. In the light of these electrophysiological results, our finding suggests that similar neuroplastic changes may not only be evoked by persistent pain, but also by persistent emotional distress. Emotional distress may cause somatoform complaints by increasing amygdala responsiveness to non noxious stimuli. It would thus be particularly worthwhile to probe the pain and emotion related response behavior of the amygdala in chronic pain patients. Another interesting target of investigation is the connectivity between the CeA and

midbrain regions. The amygdala exerts pain control via its projections to the periaqueductal grey, which is part of the descending inhibitory pain control system. In an fMRI study, Kirsch an colleagues found that Oxytocin, a nonapeptide implicated the formation of social bonds in mammals, modulates functional connectivity between the amygdala and the midbrain region (Kirsch and others, 2005). These authors employed the Hariri matching paradigm. Our factorial design, however, would allow addressing the question, whether modulation of descending pain control systems is specific to visual cues of threat or also applies to physical pain. In this way, the distinguishing functional differences between healthy controls, chronic pain syndromes and affective disorders could be identified at the systems level.

The factorial design in the present study allowed us to assess the interaction between the factor 'Pain' (corresponding to a pain rating of 5 out of 10) and the factor 'Emotion'. We found that neural correlates of thermal pain and aversive faces aggregate less than additively ('subadditively'). This negative interaction effect was consistently present in all regions considered. In the amygdala region, the combination of heat pain with aversive faces did not yield a significantly higher hemodynamic response compared to aversive faces without concomitant thermal pain. This ceiling effect presumably restricts the neural response within a physiological range. It would therefore be particularly interesting to assess whether this physiological response behavior is retained in pathological conditions, e.g. in chronic pain syndromes. Existing neuroimaging studies of clinical pain found that neural correlates of externally applied noxious stimulation are reduced compared to healthy controls (Derbyshire, 1999). To our knowledge, the interaction between non-physical stressors (e.g., emotional faces) and externally applied pain stimuli has not been studied in patients yet. Such studies would be worthwhile, particularly since these syndromes are known to be strongly associated with affective disorders (McCracken, Faber, and Janeck, 1998).

Our findings also provide insights into the phenomenon of stress induced analgesia at the systems level in humans. It is commonly accepted that exposure to aversive contexts results in potent analgesia, so-called stress-induced analgesia (SIA). SIA is of evolutionary significance as it allows an animal in threatening situations to react as if there were no pain, which increases chances of survival (Amit and Galina, 1988). Animal models use physical stressors (e.g., inescapable electric shock) to establish an aversive context. SIA is subsequently assessed using standardized nociceptive tests (e.g., tail flick test). A similar approach has been adopted in humans: Inescapable shock stress increases the threshold of

a nociceptive flexion reflex, an effect reversed by the μ-opioid receptor antagonist naloxone (Willer, Dehen, and Cambier, 1981). Moreover, fear induced by acute uncontrollable shock reduces pain perception in humans (Rhudy, Grimes, and Meagher, 2004). The same holds for phobic anxiety induced by confronting arachnophobes with a spider, i.e. a potent visual cue of threat (Janssen and Arntz, 1997). Neurobiologically, SIA has been linked to opioidergic neurotransmission, but the phenomenon has never been studied with functional imaging techniques before (Ford and Finn, 2008), although behavioral evidence in humans suggest the involvement of supraspinal mechanisms (Rhudy, Grimes, and Meagher, 2004). In the present study we employed aversive social cues. The face matching task has been shown to be associated with a significant increase in the electrodermal response (Hariri and others, 2002c) confirming the effectiveness of this stressor. We found a reduced hemodynamic response to moderately painful heat stimuli during face matching, i.e. in the context of a negative affective state. This observation holds for both the bilateral amygdala and the independently mapped pain responsive regions. Our findings agree with behavioral measures of SIA reported in the studies mentioned above. We suggest that at the supraspinal level, SIA results directly from a physiological ceiling effect evident in those regions that respond to both physical and non physical stressors. Concordantly, the right insular region, which showed the strongest response to aversive faces, also exhibited the most prominent ceiling effect among all pain responsive regions. Moreover, the amygdala response to the emotional stressor could activate the descending pain control systems and therefore attenuate the transmission of nociceptive information at the dorsal horn. This mechanism provides an additional account for the observed negative interaction effect between the factors 'Pain' and 'Emotion'. Placebo analgesia, which depends on expectations and therefore is a function of the cognitive domain, has been found to relate to the functional coupling between the PAG and the rostral ACC (Bingel and others, 2006). On the other hand, stress induced analgesia, which apparently depends on the affective state, may instead relate to the coupling between the PAG and the amygdala. Analyses of connectivity between the amygdala and midbrain regions are therefore warranted.

So far we discussed the modulation of amygdala activity by thermal pain and non painful, but emotionally salient stimuli (aversive faces). Our factorial analysis also includes those brain regions that are involved in the processing of painful heat stimuli. Pain is, however, not processed in a single specialized region but is represented in a distributed network, the so-called pain neuromatrix (Melzack, 1990). We could have identified this

matrix by searching for voxels with a significant main effect of factor 'Pain'. However, this approach is circular, since ROI definition will be biased by ROI characterization, and vice versa, if both objectives are addressed within the same paradigm. We therefore defined the pain neuromatrix separately from the main experiment, i.e. in an independent localizer experiment.

Pain intensity in the matching paradigm was moderate and located in the middle portion of the stimulus response function, where small changes in thermal intensity elicit relatively large changes in subjective pain intensity. By choosing a moderate rather than intense noxious stimulation we wanted to avoid ceiling effects when assessing the modulation of the pain related hemodynamic response by an emotional stressor. As mentioned above, we indeed found a ceiling effect in all pain responsive regions manifesting as a negative interaction effect in the factorial analysis and presumably reflecting saturation of the neural response. This finding confirms our decision to use moderate pain stimuli. More intense physical stimulation would probably have concealed any modulating influence of non-physical stressors (aversive faces) in regions that were actually defined according to their response to physical stressors (thermal pain). In order to define these regions reliably, the localizer experiment was designed to elicit a strong pain related response. For this purpose, 'ceiling' was no matter of concern and a stronger pain stimulus (corresponding to a subjective pain rating of 8 out of 10) could be applied.

The strongest pain related response was observed in the right anterior insula and right Rolandic Operculum, followed by the bilateral medial thalamus and the left Rolandic Operculum. The size of the respective activation clusters descends in the same order. It should be noted that the Rolandic Operculum (Suprasylvian Operculum) is consistent with the secondary somatosensory area (SII) located in the human suprasylvian cortex (Frot and others, 2001). The strongest activation foci were observed contralateral to the stimulation, which is in line with the anatomy of the spinothalamic tract. This pathway conveys nociceptive information from small diameter afferents and crosses at the level of the spinal cord. The activation of the ipsilateral insular/SII cortices in the present study is concordant with the bilaterality of receptive fields in animals (Zhang, Dougherty, and Oppenheimer, 1999). Intracerebral recordings in humans indicated that ipsilateral activation is compatible with transcallosal input (Frot and Mauguiere, 2003). Noteworthy, contralateral insula/SII activation was suggested to reflect the earliest cortical response to heat pain in that study. These regions were also activated by aversive faces in the present study. A negative

affective state may thus be able to modulate processing of somatic pain at the earliest cortical stage.

The bilateral engagement of insula/SII is regularly observed in neuroimaging studies of pain (Peyron, Laurent, and Garcia-Larrea, 2000). This may indicate a role of these cortices that goes beyond the spatial location of an externally applied noxious stimulus. No clear somatotopic organization has been revealed for SII with regard to noxious stimuli (Apkarian and others, 2005). Along with the bilateral amygdala, the insula/SII cortex has been implicated in the coding of perceived pain intensity (Bornhovd and others, 2002). For this reason we equalized subjective pain perception across participants. This approach helps reducing the intersubject variability of the pain related BOLD response thus increasing the statistical power to i) reliably detect neural correlates of pain (localizer experiment) and ii) find an interaction effect between pain and aversive faces (matching task). Differing temperatures needed to be employed in order to equalize individual pain perception. Covariate analysis revealed that this heterogeneity in applied thermal intensity did not introduce a significant amount of variance to any region of interest. This observation confirms that the primary determinant of hemodynamic activity was perceived pain intensity rather than physical stimulus intensity.

On the other hand, the primary somatosensory cortex shows a graded response for non-noxious stimuli but saturates already at moderate pain intensities (Bornhovd and others, 2002). It is therefore less suitable for coding the pain experience. Patients with lesions in the primary somatosensory cortex are unimpaired in evaluating pain intensity (Knecht, Kunesch, and Schnitzler, 1996). Concordantly, reports on pain related SI activation have been "notoriously inconclusive" (Peyron, Laurent, and Garcia-Larrea, 2000). Likewise, neither the 'hand area' of the somatosensory homunculus nor the lateral thalamic relays were reliably activated in the present study. Peyron and colleagues (2000) suggested that the size of stimulated skin area is a crucial factor for SI activation. In the present study we used a thermode with a contact surface of 900 mm^2. This is below the average (estimated) surface in studies showing a SI activity increase (16,300 mm^2). Moreover, we applied an innocuous thermal stimulation during non-painful trials, i.e. we provided an input to SI in the control condition thus reducing the signal gain in the subtraction.

Furthermore, we found a reliable activation cluster in the bilateral thalamus, in line with previous reports. The bilaterality and the location in the medial thalamus suggest that this activation does not reflect a sensory discriminatory response. It is more likely to mirror

a non specific arousal reaction triggered by noxious stimulation (Peyron and others, 1999). In line with this notion, we found a significant reduction of response times during noxious stimulation, i.e. participants detect a target cue earlier, possibly due to the alerting effect of pain. The thalamic cluster extends caudally into the hypothalamus and midbrain regions, perhaps indicating the engagement of autonomous mechanisms that subserve pain control.

In the context of pain processing, midbrain activation is commonly referred to the PAG activation (Peyron, Laurent, and Garcia-Larrea, 2000). The PAG and the rostral ventromedial medulla (RVM) limit transmission of noxious information at the dorsal horn through descending projections. The midbrain activation maximum in the present study is located anteriorly to the PAG. However, given the inaccuracies of stereotactic normalization (Thompson and others, 1996) the focus may be related to the PAG. It should be noted that we applied rigorous statistical thresholds for the definition of pain responsive regions. The signal to noise ratio (SNR) at the brainstem level is, however, compromised by rapid systolic displacements (Poncelet and others, 1992), which reduce the power of BOLD fMRI to detect signal changes in this region. According to a meta-analysis (Apkarian and others, 2005), only 6 from 68 hemodynamic studies on experimental pain in healthy subjects found PAG activation. The SNR problem can be addressed by synchronizing EPI acquisition with the cardiac cycle ('cardiac gating'). Given the role of the PAG and RVM as final output regions of top-down nociceptive control and their implications in the pathogenesis of chronic pain syndromes (Tracey, 2008), application of sophisticated methodology is warranted.

The anterior cingulate (ACC) is commonly linked to the affective dimension of pain. The region is regularly reported in neuroimaging studies but not in the present study. Many paradigms combine noxious stimulation with a rating task that is performed during data acquisition. These designs, however, introduce complex interaction effects between sensory/affective and cognitive domains. Rating is an elaborate cognitive task that involves orienting towards the stimulus, its evaluation in terms of a given category ('intensity' or 'unpleasantness') and the selection of a response from a number of competing options. As a multi-integrative region, the ACC is involved in every single step of this process in a highly context dependent manner (Peyron, Laurent, and Garcia-Larrea, 2000). Rating the unpleasantness of aversive pictures produces ACC activation, but passively viewing them does not (Taylor and others, 2003). Moreover, Peyron and colleagues stress the role of the ACC as mediating attentive and orienting processes (Peyron and others, 1999). In a recent conceptualization of pain perception, affect transaction takes place at the level of the

insular cortex, SII and amygdala, whereas ACC and the prefrontal cortex are responsible for cognitive attention, action planning and response selection (Chen, 2008).

From an evolutionary perspective, the ACC represents a relatively new invention providing a specialized interface between the neocortex and limbic structures (Allman and others, 2001). It is therefore not surprising that this structure is engaged in experiments involving some kind of top-down control of pain, e.g. via hypnosis (Rainville and others, 1999), expectations (Landgrebe and others, 2008) or biofeedback (deCharms and others, 2005). It is very difficult to disentangle the affective components of ACC activation from cognitive/evaluative components as long as the participants are asked to explicitly rate their experience. In the present paradigm we use a simple incidental task that is merely to ensure constant vigilance and does not involve stimulus appraisal. We thus avoid any interplay between the affective/sensory domains and the cognitive domain via the ACC interface. This holds for both matching and localizer paradigms. Emotional induction in the matching task occurs implicitly by attending towards aversive stimuli that are known to elicit an autonomous stress response (Hariri and others, 2002c). Conversely, in a study of pain modulation by affect (Rainville and others, 1997), an affective feeling state was actively induced by the participants following hypnotic suggestions. In the present study, however, participants are passive recipients of painful and emotional stressors rather than active modulators. Our design thus probes the interaction of pain and affect at a rather basal perceptual level, which renders it robust against cognitive confounds.

Early characterizations of the human pain processing system divided it into a lateral and medial component (Bowsher, 1957). The lateral pain system involves somatotopically organized cortices and corresponding relays in the lateral thalamus. It subserves the sensory discriminatory aspects of pain, whereas the medial system processes its affective dimension (Treede and others, 1999). The medial system comprises the medial thalamus and its projections to the limbic system. In the present study, prominent activation of the insula, bilateral medial thalamus including the hypothalamus and the bilateral amygdala highlight the strong engagement of the medial system during painful stimulation. A closely related neurocircuitry has been shown to be engaged in major depressive disorder (Drevets, 1998). In this sense, the medial pathway is conveying the 'suffering' component of both painful and affective experiences.

We observed that the response to a non physical stressor (aversive faces) was positive in all pain responsive regions. This is striking given the fact that these regions were defined according to their response to externally applied pain ('pain neuromatrix').

Both modalities activated the same regions in approximately the same relative proportions. This finding supports the idea that physical and psychical stressors share a common neurosignature. William James regarded somatic feelings from the body as basis for emotions (James, 1890). A close relationship between sensory and affective domains is indeed confirmed in the present study. Aversive faces induce a motivational state ('emotion'), whose neural correlates engage the pain neuromatrix in a way as if somatic pain would be processed ('body feeling'). Conversely, we have shown that intense pain engages the amygdala in those subregions that are also activated by the psychical stressor (faces). We cannot solve the hen and egg problem, whether emotions arise from body states or vice versa. Instead, we suggest that psychic and somatic stress share a common neural network and thus reflect two sides of the same coin.

As mentioned above we found that SII/insula is involved in the processing of facial expressions. The amygdala's importance in recognizing aversive facial emotions has been repeatedly demonstrated (Adolphs and others, 1994; Young and others, 1995; Morris and others, 1996), but the involvement somatosensory cortices may appear counterintuitive. However, an fMRI lesion study on patients revealed that the right somatosensory cortices (SI, SII) and the insula are crucial for identifying facial expressions (Adolphs and others, 2000). These authors also found a correlation between somatosensory deficits and impaired emotion recognition. It has been proposed that the observation of emotion in others automatically activates the neural representation of that emotion in the observer (Preston and de Waal, 2002). This representation includes simulated somatic activity patterns reflecting how the observer would feel when experiencing the depicted emotional state. This account explains the involvement of somatosensory cortices in emotion processing in addition to the amygdala. In the domain of motor processing, the mirror neuron system demonstrates that observation of a motor action automatically evokes neural representations of that action in the observer (Rizzolatti, Fogassi, and Gallese, 2001). The same may indeed apply to the emotional domain. This idea has been further substantiated in a neuroimaging study, where disgusting odorants and facial images of disgust activated the same sites within the anterior insula (Wicker and others, 2003). Our findings indicate that the internal representation of an aversive emotional state – induced by watching angry and fearful faces – evokes correlates of physical pain.

In this context the following animal study is noteworthy (Ferguson and others, 2001). Oxytocin knockout mice show impaired social recognition. Exposure to conspecifics elicits a lower activity in the medial amygdala but a higher activity in the

somatosensory cortex. Since this system, which is specialized in the processing of social signals, is defective, KO mice appear to activate alternative pathways of sensory processing for compensation. As outlined above, Adolphs and colleagues emphasized that both amygdala and the somatosensory cortices are indispensable components in the recognition of emotional stimuli in humans (Adolphs and others, 2000). While our results agree with this notion, the amygdala responded stronger to the social signal than the SII/insula cortices, i.e. the ratio of amygdala activation and somatosensory cortex activation was well above 1. In their animal study Ferguson and colleagues suggest that impaired social recognition translates into an increases activity in somatosensory pathways. According to this logic, the mentioned ratio would change in favor of the somatosensory component of emotion processing in alexithymic human subjects. If this hypothesis proves correct, the shift towards the somatic aspect of emotion may explain a potential association between alexithymia and somatoform disorders (De Gucht and Heiser, 2003).

From all regions constituting the pain neuromatrix, the right insular ROI was most strongly activated during both painful and emotional stimulation. Previous imaging studies confirm the involvement of the right insula in pain processing (Peyron and others, 2002) and emotion processing (Buchel and others, 1998;Phillips and others, 1998). In line with these reports we found that the pain responsive cluster within the insular cortex also responds to aversive faces. What could be the common denominator of these two very different stimulus types (aversive faces and thermal pain)? Craig and colleagues suggest that a phylogenetically distinct pathway supplies the dorsal insula with detailed information about the current physiological state of the body via lamina I spinothalamic neurons (Craig, 2002). The right (non-dominant) anterior insula integrates this information so as to generate a mental image of the bodily self, which subserves maintenance of homeostasis. From a homeostatic point of view, physical pain does not primarily signal a sensation from the external world; it instead signals a disturbance of the internal state of the body, i.e. a threat to homeostasis, which needs to be corrected to ensure survival. Similarly, aversive faces convey a social signal that indicates a disturbance in the social domain. A threat to the integrity of the social sphere may jeopardize survival to the same extent as a threat to body integrity, at least for animals that are dependent on a well functioning social environment. Biological evolution is certainly conservative, i.e. novel functions are piggybacked on established neural systems. From this perspective it makes sense that the same neural mechanisms that ensure body homeostasis are made use of in

order to support 'social homeostasis'. It has been shown that neural systems involved in pain processing are also activated in response to social exclusion (Eisenberger, Lieberman, and Williams, 2003) and when beloved ones are hurt (Singer and others, 2004). We therefore propose that 'threat to homeostasis' could be the common denominator for both stimulus modalities (aversive faces and thermal pain) thus explaining why they engage a common neural network.

Within this network the physical and psychical aspects of stress are predominantly represented in the bilateral insula/SII cortices and the bilateral amygdala, respectively. *Post hoc* correlation analysis revealed that insula/SII activity explains a significant amount of experimental variance in the ipsilateral amygdala (Pearson's r=.49, p < .001). Concordantly, anatomical connections between amygdala and insula are known to exist in the rat (Yasui and others, 1991;Floyd and others, 2000;Ray and Price, 1992) and in primates (Augustine, 1996). It may be speculated that via this connection the amygdala attaches emotional significance to the insular representation of the physiological body state. Conversely, the insula may attach somatic significance to emotionally salient information that is represented in the amygdala. Concordantly, an fMRI lesion study has demonstrated an indispensable role of somatosensory areas including the insula in emotion processing. In this context our findings suggest a dual representation of salient stimuli in terms of their affective/emotional and somatic/physiological significance.
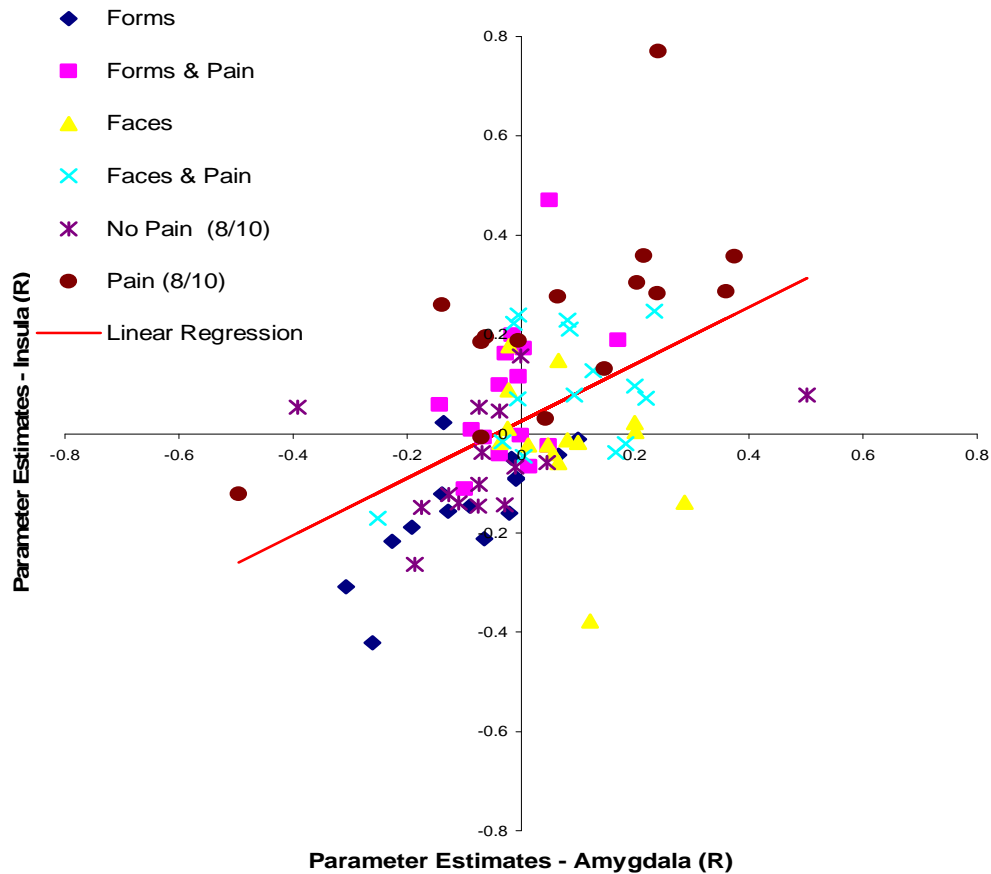
Fig. 2-22. Right insular activity as a function of right amygdala activity. Per subject beta weights for each experimental condition are entered into the scatter plot (see legend).

This conceptualization offers a straightforward explanation for the phenomenon of somatization, which links anxiety and depression symptoms to somatic complaints: a negative affective state would persistently heighten the activity in the pain neuromatrix. Incoming sensory inputs would further augment this increased baseline activity creating a painful percept in response to non-noxious inputs. Chronic pain and depression may thus reflect extremes of an either somatic or psychic amplification of endogenous stress along an insula–amygdala axis. It is therefore of particular interest to determine the aggregation rule by which somatic and non-somatic stressors add up. In the present study on healthy subjects, both stressors appear to attenuate each other thus keeping the neural response within a physiological range. As mentioned above, this saturation behavior is evident throughout the pain neuromatrix and is manifesting statistically in a negative interaction effect between factor 'Pain' and factor' Emotion'. The significance criterion, however, was missed. To uncover brain regions that exhibit a reliable interaction effect, we applied the interaction contrast at the whole brain level. A significant activation cluster was found in the midline thalamus. As part of the medial pain system this structure relays nociceptive

information to limbic areas including amygdala and the insula. It is conceivable, that a thalamic filter function, which prevents the cortical systems from overload, causes the saturation effect in the response to combined emotional and physical stressors. Hence, pathology could already be located at the thalamic level, i.e. at a very early stage of processing. It may be noted in this context that genetic risk factors for affective disorders were shown to be associated with an altered processing in primary sensory cortices in an ERP (Event-Related Potentials) study (Herrmann and others, 2007), i.e. these factors affect an early stage in the processing pipeline indicating an altered encoding of stimuli rather than an altered affective or cognitive appraisal of an otherwise ordinary representation of the environment.
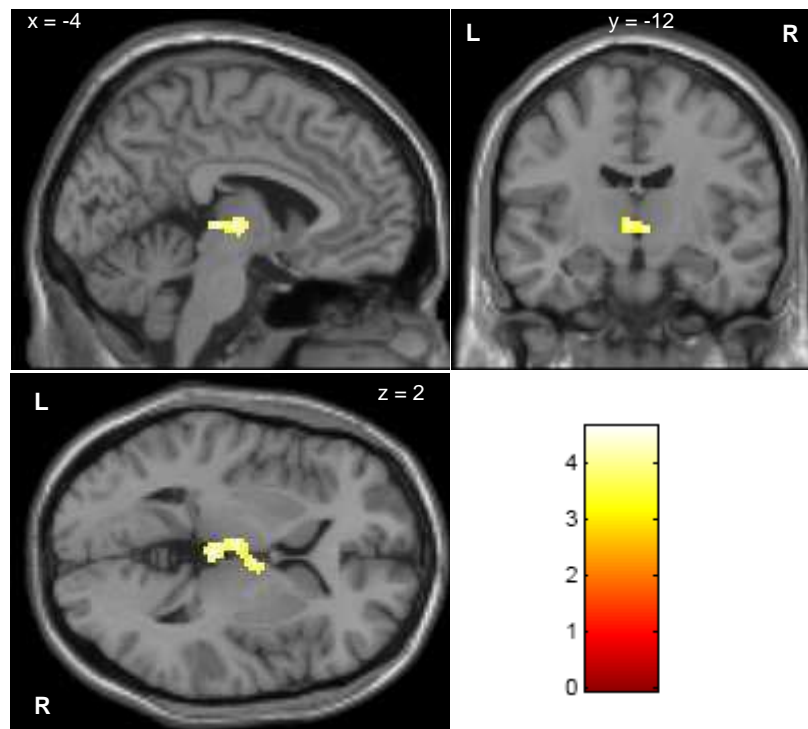
Fig. 2-23. SPM T-maps with clusters exhibiting a negative interaction effect between factor 'Emotion' and factor 'Pain'. The maps were thresholded at T=3.30 (voxel-wise P=.001, uncorrected) and a cluster size of 170 (1360 mm^3) to meet a cluster-wise significance level of P<.05, FWE corrected. The SPM is overlaid on a canonical brain template and is displayed in neurological convention. Slice coordinates (in millimeters) refer to MNI stereotactic space. The colorimeter scale indicates per voxel T values. L: Left; R: Right.

3 Conclusion

In this thesis the author introduced a novel methodology allowing the assessment of psychosocial stress and somatic pain in the human brain employing BOLD fMRI. This multi-step approach involves a) acquisition of psychometric profiles b) functional localization of the pain neuromatrix c) factorial analysis of pain and emotion correlates in predefined regions of interest, i.e. in the pain neuromatrix (as defined in step b) and the bilateral amygdala.

a)

On the behavioral level, psychometric profiles relating subjective pain perception to stimulus intensity were acquired. We devised a computerized rating paradigm that effectively controls for sequence and habituation effects. Fitted stimulus response functions allowed us to determine thermal intensities that equalize pain perception across participants. In this way heterogeneity in the pain related BOLD response was reduced improving the signal to noise ratio. The variability of subjective pain perception was particularly high for medium temperatures and therefore constitutes a serious nuisance variable in designs that rely on fixed temperatures. The acquisition process was completely automatized, i.e. the paradigm can be carried out without the presence of a supervisor. This allows studying the relevance of psychosocial context (e.g. subject-instructor interactions) on pain perception in future experiments. Moreover, the method provides a high resolving power for medium sized samples. Psychometric profiling could be a more powerful tool for defining a pain related phenotype of psychiatric disorders compared to procedures that are based on single thresholds and are more prone to bias and confounds.

b) & c)

We conceived thermal pain (factor 'Pain') and aversive faces (factor 'Emotion') as conveying signals of threat arising in the somatic and social domains, respectively. We found that somatic and social stressors activate a common neural network comprising the bilateral amygdala, insular/SII cortices and the midline thalamus. Specifically, perception of aversive faces activated pain responsive areas, which had been identified by their reactivity to thermal pain in an independent localizer experiment ('pain neuromatrix', step b). Conversely, the amygdala, whose importance in the processing of aversive social

signals is well established, was reliably activated by intense thermal pain. The spatial activity patterns of both sensations within the pain neuromatrix and the amygdala are strikingly similar. These findings indicate that the processing of pain and the processing of psychosocial stressors rely on a common neuromatrix and evoke similar neurosignatures. Within this network, the amygdala particularly responds to aversive faces, whereas the insula/SII cortices are more prominently activated by thermal pain.

Preexisting studies support the idea that perception of threatening bodily signals such as pain and dyspnoe are mapped to common limbic brain areas. We extend this observation from somatic sensations to social signals. According to the action perception model of empathy, the observation of angry and fearful faces evokes the neural representation of these emotions in the observer (Preston and de Waal, 2002). We demonstrated that this representation of an internal emotional state involves a neuromatrix that was independently defined by external noxious stimulation. William James regarded somatic feelings from the body as basis for emotions (James, 1890). We leave open the direction of causality between somatic and emotional sensations. Instead, we stress that negative emotional signals evoke neural correlates of physical pain and vice versa. Our findings indicate that the pain neuromatrix is involved in the generation of somatic representations of anger and fear, whereas the amygdala attaches emotional significance to noxious heat. More recent theories of emotion emphasize the role of the anterior insula in linking somatic sensations to the experience of emotion (Damasio, 1994;Craig, 2002). This idea is supported by the present study as the right anterior insula showed the strongest and most reliable response to both somatic and emotional stressors within in the pain neuromatrix. Given the correlation between amygdala and insula activity in our study and their anatomical interconnection, we suggest a dual representation of emotionally salient stimuli in terms of their affective (amygdala) and somatic (insula) significance.

Social animals like humans are dependent on both physical health and an intact social environment for their survival. In this sense, thermal pain and aversive faces convey signals of threat, which arise in the somatic and social domains, respectively. The striking neural congruency of both stimulus types in the present study may indicate that aversive social and aversive physical signals represent a comparable threat to survival. We suggest that the shared limbic network relates to a common homeostatic control system that processes the threatening character of these otherwise very different stimulus modalities (aversive faces / thermal pain). It follows that the same effector mechanisms that ensure

body homeostasis are also made use of to support adaptive social behavior. Further studies are warranted to substantiate this hypothesis.

The observed common network implies that neural correlates of painful and emotional stimuli need to aggregate when presented simultaneously. The neural response amplitude is limited due to inherent physiological constraints, however. Indeed, we found a saturation of the hemodynamic response when emotional faces were combined with thermal pain. The respective neural correlates aggregate less than additively. This negative interaction effect may reflect physiological constraints preventing the system from overload. It follows that the response to pain is reduced in the presence of the emotional stressor and vice versa. This finding suggests a parsimonious implementation of 'stress induced analgesia' at the systems level, which directly follows from the convergence of physical and affective stressors on a common neural substrate. Alternatively, the amygdala response to aversive faces may engage descending pain inhibitory systems thus limiting the transmission of nociceptive information at the dorsal horn. Additionally, the midline thalamus, where the negative interaction effect is particularly prominent, may act as a filtering element while relaying somatic and affective information between the insula and the amygdala.

The identification of a common neural basis for the processing of physical and emotional stressors may have important implications for clinical research as it offers a unifying perspective on affective disorders and chronic pain syndromes. Our findings designate the insula and the amygdala as target regions for the characterization of chronic pain syndromes and affective disorders at the systems level. In this conceptualization, chronic pain and depression may reflect predominantly somatic and predominantly affective augmentation of stress along an insula–amygdala axis, respectively. Persistent emotional distress may up-regulate the pain neuromatrix thus amplifying non noxious inputs from skin and viscera, which are consequently perceived as pain (allodynia). Conversely, persistent somatic pain may up-regulate the amygdala thus increasing the vulnerability to emotional stressors. This conception would explain the high comorbidity between both syndromes (Bair and others, 2003) and provide a neural rationale for incorporating chronic pain syndromes and depression into unified diagnostic and therapeutic efforts in the context of clinical routine. Neuroplastic changes pertinent to chronic disorders may compromise the observed saturation of the neural response to combined emotional and physical stress thus causing overload in limbic networks. These

assumptions need to be verified in subsequent experiments on patients. If true, new avenues in the diagnosis and therapy of chronic pain syndromes may be opened up.

APPENDIX

A. Materials

Klinik und Poliklinik für Psychiatrie und Psychotherapie
Bezirksklinikum Regensburg
Direktor: Prof. Dr. H.-E. Klein
Universitätsstr. 84, 93053 Regensburg, Tel. 0941-941-1001

Beschreibung für Versuchsteilnehmer

Liebe Versuchsteilnehmerin, lieber Versuchsteilnehmer,

in diesem Experiment geht es um die Untersuchung der Schmerzverarbeitung im Gehirn und deren Beeinflussung durch emotionale Reize. Das Experiment besteht aus 3 Teilversuchen. In allen Teilversuchen werden schmerzhafte Temperaturen über ein kleines Thermoelement zugeführt, das am Handgelenk befestigt wird.

TEILVERSUCH 1: BEWERTUNG VON SCHMERZREIZEN UNTERSCHIEDLICHER STÄRKE

Zunächst wird Ihre persönliche Schmerzschwelle und Ihre persönliche Toleranzschwelle bestimmt. Zur Bestimmung der Schmerzschwelle sind mehrere Wiederholungen nötig. Der Beginn eines jeden Durchgangs wird durch einen Piepton signalisiert.

Zuerst wird Ihre Schmerzschwelle bestimmt.
Ausgehend von einer angenehmen Temperatur (= Baseline) wird das Thermoelement an Ihrem Handgelenk langsam wärmer. Sobald Sie die Leertaste der Tastatur vor Ihnen drücken, kehrt die Temperatur sofort zur Baseline zurück. **Drücken Sie die Leertaste, sobald die Temperatur beginnt, schmerzhaft zu werden.**

Dann wird Ihre Toleranzschwelle bestimmt.
Wie zuvor wird das Thermoelement langsam erwärmt.
Drücken Sie nun die Leertaste, sobald die Temperatur beginnt, unerträglich schmerzhaft zu werden.

Als Drittes wird Ihr persönliches Schmerzprofil aufgezeichnet.
Hierzu werden Ihnen in zufälliger Reihenfolge Temperaturen dargeboten, die zwischen Ihrer persönlichen Schmerz- und Toleranzschwelle liegen. Diese Temperaturen werden durchgehend für 20 Sekunden dargeboten.
Während dieser Zeit sehen Sie auf einem Computerbildschirm eine Schmerzskala angezeigt (siehe Abbildung).

Bitte verschieben Sie den Zeiger entsprechend Ihrer Schmerzempfindung. Der Skalenwert „1" verweist dabei auf Ihre Schmerzschwelle, der Skalenwert „10" auf Ihre Toleranzschwelle (siehe oben). Werte unter 1 verweisen auf schmerzlose Empfindungen. Horchen Sie in sich hinein und versuchen Sie, während der 20 Sekunden einen Skalenwert anzupeilen, der Ihrer Schmerzempfindung am besten entspricht. Durch einen Mausklick geben Sie Ihre Wertung endgültig ab. **Klicken Sie bitte erst nach dem Piepton, der nach 20 Sekunden ertönt.** Ein Zeitdruck besteht nicht. Nach dem Klick kehrt die Temperatur zur Baseline zurück und ein neuer Durchgang beginnt.

Fig. A-1. Written task instructions for study participants. Page 1.
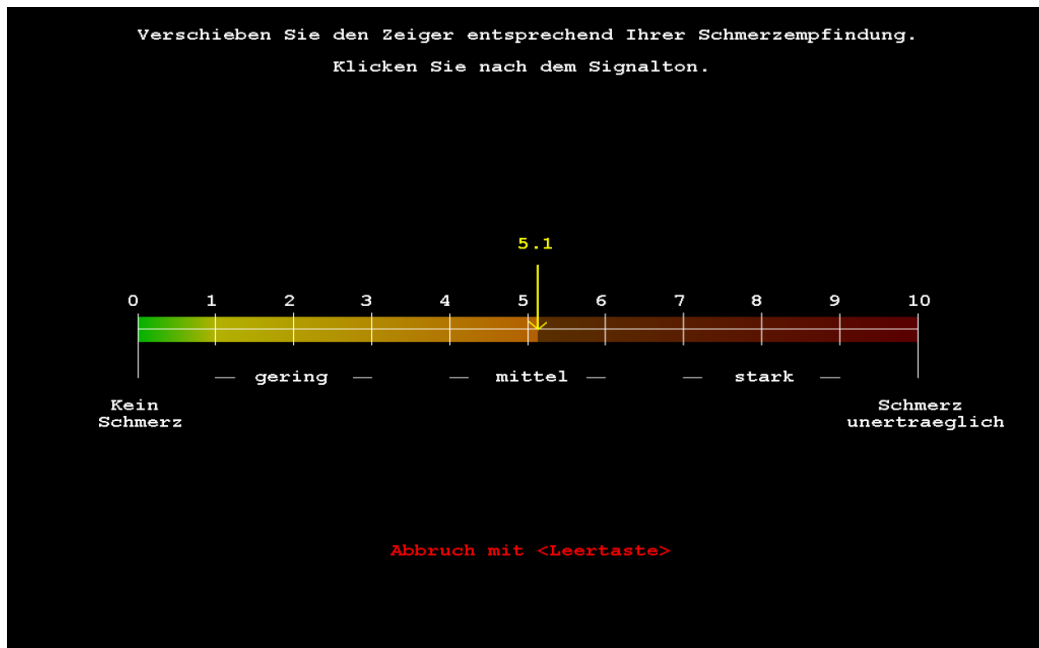
Bitte beachten Sie, dass sie eine Temperatur der Stärke 10 nicht aushalten müssen! Sie können jederzeit durch Druck auf die Leertaste eine sofortige Rückkehr zur Baseline erzwingen. Wenn Sie einen Temperaturreiz auf diese Weise abbrechen müssen, bewerten Sie ihn bitte mit „10".

Fig. A-2. Written task instructions for study participants. Page 2.

Klinik und Poliklinik für Psychiatrie und Psychotherapie
Bezirksklinikum Regensburg
Direktor: Prof. Dr. H.-E. Klein
Universitätsstr. 84, 93053 Regensburg, Tel. 0941-941-1001

Medizinische Einrichtungen
des Bezirks Oberpfalz GmbH

TEILVERSUCH 2: LOKALISIERUNG VON „SCHMERZZENTREN" IM GEHIRN

Dieser Teilversuch findet innerhalb des Kernspintomographen statt. Ihr Kopf befindet sich in einer Röhre. An Ihrem linken Handgelenk befindet sich das bereits bekannte Thermoelement. In der rechten Hand halten Sie eine angepasste Tastatur.

Es ist entscheidend für das Gelingen des Experimentes, dass Sie Ihren Kopf absolut ruhig halten.

In diesem Experiment wird Ihnen eine schmerzhafte Temperatur zugeführt, die einer hohen, aber erträglichen Schmerzbewertung aus dem ersten Teilversuch entspricht. Die Temperatur wird für 20 Sekunden dargeboten und kehrt dann zur Baseline zurück. Es folgt eine Pause. Schmerzhafte Stimulation und schmerzlose Pausen wechseln ab und werden mehrmals wiederholt.

Währenddessen beobachten Sie bitte den Punkt in der Mitte des Bildschirms. Dieser Punkt verschwindet etwa alle 10-15 Sekunden kurz. Wenn Sie dies wahrnehmen, drücken Sie bitte auf die Taste unterhalb Ihres Zeigefingers. Diese Aufgabe dient dazu, eine gleichmäßige Wachsamkeit für die Dauer des Experimentes sicherzustellen.

TEILVERSUCH 3: EINFLUSS EMOTIONALER REIZE AUF DIE SCHMERZVERARBEITUNG IM GEHIRN

Dieser Versuch wird vor oder nach Teilversuch 2 innerhalb des Kernspintomographen durchgeführt.

Es ist entscheidend für das Gelingen des Experimentes, dass Sie Ihren Kopf absolut ruhig halten.

Ihnen werden Fotographien von Gesichtern oder geometrische Formen (Kreise und Ellipsen) gezeigt. Die Gesichter haben dabei einen unangenehmen emotionalen Charakter.

Es werden jeweils drei Bilder gleichzeitig gezeigt: ein Bild oben in der Mitte, zwei Bilder jeweils in der rechten und linken unteren Ecke des Bildschirms. Dabei handelt es sich entweder um drei Gesichter oder um drei Formen (siehe Beispiele unten). Eines der beiden unteren Bilder ist identisch mit dem oberen Bild. Ihre Aufgabe besteht darin, das doppelte Bild zu finden.
> Ist es das linke untere Bild, drücken Sie bitte die Taste unterhalb Ihres Zeigefingers.
> Ist es das rechte untere Bild, drücken Sie bitte die Taste unterhalb Ihres Mittelfingers.

Die Dreierbilder werden stets für 3 Sekunden angeboten, unabhängig von Ihrer Antwort. 6 Dreierbilder einer Kategorie (Gesicht/ Form) werden nacheinander angeboten, also in einem „Block" zu 20 Sekunden. In der Hälfte der Blöcke wird ein moderat schmerzhafter Reiz über das Thermoelement zugeführt. Nach einem schmerzhaften Block folgt immer ein schmerzloser Block.

Fig. A-3. Written task instructions for study participants. Page 3.

Beispiele für eine Reizdarbietung aus Teilversuch 3 aus der Kategorie „Formen" (links) und aus der Kategorie „Gesichter" (rechts). Aufgabe ist es, das jeweils doppelte Teilbild zu finden.

Fig. A-4. Written task instructions for study participants. Page 4.

B. Declaration of consent

Klinik und Poliklinik für Psychiatrie und Psychotherapie
Bezirksklinikum Regensburg
Direktor: Prof. Dr. H.-E. Klein
Universitätsstr. 84, 93053 Regensburg, Tel. 0941-941-1001

Medizinische Einrichtungen
des Bezirks Oberpfalz GmbH

Einverständniserklärung

Teilnahme an der Studie
„Einfluss emotionaler Stimuli auf die Pain Neuromatrix"

Ich habe die Information für Studienteilnehmer mit der Anlage „Aufklärung für die Teilnahme an der Studie" gelesen. Der Ablauf der Experimente und deren Ziele sind mir bekannt. Ich bestätige, dass bei mir keine Gründe vorliegen, die mich von der Studie ausschließen würden. Ich willige ein, dass meine Daten für wissenschaftliche Abhandlungen in anonymer oder pseudonymer Form verwendet werden dürfen. Ich hatte Gelegenheit, offene Fragen mit dem Versuchsleiter zu klären. Mir ist bewusst, dass ich mich bei Fragen auch jederzeit an den Studienleiter wenden kann, dessen Kontaktinformation mir vorliegt. Ich weiß, dass ich jederzeit und ohne Nennung näherer Gründe meine Einwilligung zur Teilnahme an der Studie zurückziehen kann, ohne Nachteile zu erleiden.

Ich _____ (Name des Probanden)

_____ (Straße, Hausnr.)

_____ (PLZ, Wohnort)

willige hiermit ein, an dieser Studie teilzunehmen.

_____   _____
(Ort + Datum)   (Unterschrift des Probanden)

Die Probandeninformation wurde durchgeführt durch: _____

(Name)

_____   _____
(Ort + Datum)   (Unterschrift des Informierenden)

REFERENCES

1. Adler, G. and Gattaz, W. F., 1993, Pain perception threshold in major depression: Biol.Psychiatry, v. 34, p. 687-689.

2. Adolphs, R., Damasio, H., Tranel, D., Cooper, G., and Damasio, A. R., 2000, A role for somatosensory cortices in the visual recognition of emotion as revealed by three-dimensional lesion mapping: J.Neurosci., v. 20, p. 2683-2690.

3. Adolphs, R., Tranel, D., Damasio, H., and Damasio, A., 1994, Impaired recognition of emotion in facial expressions following bilateral damage to the human amygdala: Nature, v. 372, p. 669-672.

4. Aggleton, J. P., 2000, The Amygdala: A Functional Analysis: New York, Oxford University Press.

5. Allman, J. M., Hakeem, A., Erwin, J. M., Nimchinsky, E., and Hof, P., 2001, The anterior cingulate cortex. The evolution of an interface between emotion and cognition: Ann.N.Y.Acad.Sci., v. 935, p. 107-117.

6. Amit, Z. and Galina, Z. H., 1988, Stress induced analgesia plays an adaptive role in the organization of behavioral responding: Brain Res.Bull., v. 21, p. 955-958.

7. Amunts, K., Kedo, O., Kindler, M., Pieperhoff, P., Mohlberg, H., Shah, N. J., Habel, U., Schneider, F., and Zilles, K., 2005, Cytoarchitectonic mapping of the human amygdala, hippocampal region and entorhinal cortex: intersubject variability and probability maps: Anat.Embryol.(Berl), v. 210, p. 343-352.

8. Apkarian, A. V., Bushnell, M. C., Treede, R. D., and Zubieta, J. K., 2005, Human brain mechanisms of pain perception and regulation in health and disease: Eur.J.Pain, v. 9, p. 463-484.

9. Ashburner, J. and Friston, K. J., 1997, The role of registration and spatial normalization in detecting activations in functional imaging: Clinical MRI/Developments in MR, v. 7, p. 26-28.

10. Ashburner, J. and Friston, K. J., 1999, Nonlinear spatial normalization using basis functions: Hum.Brain Mapp., v. 7, p. 254-266.

11. Ashburner, J., Neelin, P., Collins, D. L., Evans, A., and Friston, K., 1997, Incorporating prior knowledge into image registration: Neuroimage., v. 6, p. 344-352.

12. Augustine, J. R., 1996, Circuitry and functional aspects of the insular lobe in primates including humans: Brain Res.Brain Res.Rev., v. 22, p. 229-244.

13. Bair, M. J., Robinson, R. L., Katon, W., and Kroenke, K., 2003, Depression and pain comorbidity: a literature review: Arch.Intern.Med., v. 163, p. 2433-2445.

14. Baliki, M. N., Chialvo, D. R., Geha, P. Y., Levy, R. M., Harden, R. N., Parrish, T. B., and Apkarian, A. V., 2006, Chronic pain and the emotional brain: specific brain activity associated with spontaneous fluctuations of intensity of chronic back pain: J.Neurosci., v. 26, p. 12165-12173.

15. Ball, T., Derix, J., Wentlandt, J., Wieckhorst, B., Speck, O., Schulze-Bonhage, A., and Mutschler, I., 2009, Anatomical specificity of functional amygdala imaging of responses to stimuli with positive and negative emotional valence: J.Neurosci.Methods, v. 180, p. 57-70.

16. Bär, K. J., Brehm, S., Boettger, M. K., Boettger, S., Wagner, G., and Sauer, H., 2005, Pain perception in major depression depends on pain modality: Pain, v. 117, p. 97-103.

17. Bär, K. J., Brehm, S., Boettger, M. K., Wagner, G., Boettger, S., and Sauer, H., 2006, Decreased sensitivity to experimental pain in adjustment disorder: Eur.J.Pain, v. 10, p. 467-471.

18. Barsky, A. J. and Klerman, G. L., 1983, Overview: hypochondriasis, bodily complaints, and somatic styles: Am.J.Psychiatry, v. 140, p. 273-283.

19. BAXTER, D. W. and OLSZEWSKI, J., 1960, Congenital universal insensitivity to pain: Brain, v. 83, p. 381-393.

20. Berthier, M., Starkstein, S., and Leiguarda, R., 1988, Asymbolia for pain: a sensory-limbic disconnection syndrome: Ann.Neurol., v. 24, p. 41-49.

21. Bingel, U., Lorenz, J., Schoell, E., Weiller, C., and Buchel, C., 2006, Mechanisms of placebo analgesia: rACC recruitment of a subcortical antinociceptive network: Pain, v. 120, p. 8-15.

22. Blackburn-Munro, G. and Blackburn-Munro, R. E., 2001, Chronic pain, chronic stress and depression: coincidence or consequence?: J.Neuroendocrinol., v. 13, p. 1009-1023.

23. Bond, M. R. and Pilowsky, I., 1966, Subjective assessment of pain and its relationship to the administration of analgesics in patients with advanced cancer: J.Psychosom.Res., v. 10, p. 203-208.

24. Bornhovd, K., Quante, M., Glauche, V., Bromm, B., Weiller, C., and Buchel, C., 2002, Painful stimuli evoke different stimulus-response functions in the amygdala, prefrontal, insula and somatosensory cortex: a single-trial fMRI study: Brain, v. 125, p. 1326-1336.

25. BOWSHER, D., 1957, Termination of the central pain pathway in man: the conscious appreciation of pain: Brain, v. 80, p. 606-622.

26. Breivik, E. K., Bjornsson, G. A., and Skovlund, E., 2000, A comparison of pain rating scales by sampling from clinical trial data: Clin.J.Pain, v. 16, p. 22-28.

27. Brett, M., Anton, J.-L, Valabregue, R., and Poline, J.-B. Region of interest analysis using an SPM toolbox. 8th International Conference on Functional Mapping of the Human Brain. 6-2-2002. 6-2-0002.
Ref Type: Conference Proceeding

28. Brett, M., Johnsrude, I. S., and Owen, A. M., 2002, The problem of functional localization in the human brain: Nat.Rev.Neurosci., v. 3, p. 243-249.

29. Buchel, C., Morris, J., Dolan, R. J., and Friston, K. J., 1998, Brain systems mediating aversive conditioning: an event-related fMRI study: Neuron, v. 20, p. 947-957.

30. Bulmer, M. G., 1979, The X^2, t And F Distributions Principles of statistics: New York, Dover.

31. Burstein, R. and Potrebic, S., 1993, Retrograde labeling of neurons in the spinal cord that project directly to the amygdala or the orbital cortex in the rat: J.Comp Neurol., v. 335, p. 469-485.

32. Calder, A. J., Rowland, D., Young, A. W., Nimmo-Smith, I., Keane, J., and Perrett, D. I., 2000, Caricaturing facial expressions: Cognition, v. 76, p. 105-146.

33. Calder, A. J., Young, A. W., Rowland, D., and Perrett, D. I., 1997, Computer-enhanced emotion in facial expressions: Proc.Biol.Sci., v. 264, p. 919-925.

34. Caraceni, A., Cherny, N., Fainsinger, R., Kaasa, S., Poulain, P., Radbruch, L., and De, C. F., 2002, Pain measurement tools and methods in clinical research in palliative care: recommendations of an Expert Working Group of the European Association of Palliative Care: J.Pain Symptom.Manage., v. 23, p. 239-255.

35. Chen, A. C., 2008, Pain perception and its genesis in the human brain: Sheng Li Xue.Bao., v. 60, p. 677-685.

36. CLARK, J. W. and BINDRA, D., 1956, Individual differences in pain thresholds: Can.J.Psychol., v. 10, p. 69-76.

37. Cleeland, C. S. and Ryan, K. M., 1994, Pain assessment: global use of the Brief Pain Inventory: Ann.Acad.Med.Singapore, v. 23, p. 129-138.

38. Coghill, R. C., Sang, C. N., Maisog, J. M., and Iadarola, M. J., 1999, Pain intensity processing within the human brain: a bilateral, distributed mechanism: J.Neurophysiol., v. 82, p. 1934-1943.

39. Collins, D. L., Neelin, P., Peters, T. M., and Evans, A. C., 1994, Automatic 3D intersubject registration of MR volumetric data in standardized Talairach space: J.Comput.Assist.Tomogr., v. 18, p. 192-205.

40. Craig, A. D., 2003, A new view of pain as a homeostatic emotion: Trends Neurosci., v. 26, p. 303-307.

41. Craig, A. D., 2002, How do you feel? Interoception: the sense of the physiological condition of the body: Nat.Rev.Neurosci., v. 3, p. 655-666.

42. Craig, A. D. and Blomqvist, A., 2002, Is there a specific lamina I spinothalamocortical pathway for pain and temperature sensations in primates?: J.Pain, v. 3, p. 95-101.

43. Critchley, H., Daly, E., Phillips, M., Brammer, M., Bullmore, E., Williams, S., Van, A. T., Robertson, D., David, A., and Murphy, D., 2000, Explicit and implicit neural mechanisms for processing of social information from facial expressions: a functional magnetic resonance imaging study: Hum.Brain Mapp., v. 9, p. 93-105.

44. Croft, P. R., Papageorgiou, A. C., Ferry, S., Thomas, E., Jayson, M. I., and Silman, A. J., 1995, Psychologic distress and low back pain. Evidence from a prospective study in the general population: Spine (Phila Pa 1976.), v. 20, p. 2731-2737.

45. Damasio, A. R., 1994, Descartes' Error: Emotion, Reason, and the Human Brain: New York, Putnam Publishing.

46. Darwin, C. R., 1872, Expression of the Emotions in Man and Animals: London, Albemarle.

47. De Gucht, V. and Heiser, W., 2003, Alexithymia and somatisation: quantitative review of the literature: J.Psychosom.Res., v. 54, p. 425-434.

48. deCharms, R. C., Maeda, F., Glover, G. H., Ludlow, D., Pauly, J. M., Soneji, D., Gabrieli, J. D., and Mackey, S. C., 2005, Control over brain activation and pain learned by using real-time functional MRI: Proc.Natl.Acad.Sci.U.S.A, v. 102, p. 18626-18631.

49. Deichmann, R., Gottfried, J. A., Hutton, C., and Turner, R., 2003, Optimized EPI for fMRI studies of the orbitofrontal cortex: Neuroimage., v. 19, p. 430-441.

50. Derbyshire, S. W., 1999, Meta-Analysis of Thirty-Four Independent Samples Studied Using PET Reveals a Significantly Attenuated Central Response to Noxious Stimulation in Clinical Pain Patients: Curr.Rev.Pain, v. 3, p. 265-280.

51. Drevets, W. C., 1998, Functional neuroimaging studies of depression: the anatomy of melancholia: Annu.Rev.Med., v. 49, p. 341-361.

52. Eickhoff, S. B., Stephan, K. E., Mohlberg, H., Grefkes, C., Fink, G. R., Amunts, K., and Zilles, K., 2005, A new SPM toolbox for combining probabilistic cytoarchitectonic maps and functional imaging data: Neuroimage., v. 25, p. 1325-1335.

53. Eisenberger, N. I., Lieberman, M. D., and Williams, K. D., 2003, Does rejection hurt? An FMRI study of social exclusion: Science, v. 302, p. 290-292.

54. Ekman, P. and Friesen, W., 1978, Pictures of Facial Affect: Palo Alto, CA, Consulting Psychologists Press.

55. Ekman, P., Sorenson, E. R., and Friesen, W. V., 1969, Pan-cultural elements in facial displays of emotion: Science, v. 164, p. 86-88.

56. Enck, P. and Klosterhalfen, S., 2009, The story of O--is oxytocin the mediator of the placebo response?: Neurogastroenterol.Motil., v. 21, p. 347-350.

57. Etkin, A., Klemenhagen, K. C., Dudman, J. T., Rogan, M. T., Hen, R., Kandel, E. R., and Hirsch, J., 2004, Individual differences in trait anxiety predict the response of the basolateral amygdala to unconsciously processed fearful faces: Neuron, v. 44, p. 1043-1055.

58. Etkin, A. and Wager, T. D., 2007, Functional neuroimaging of anxiety: a meta-analysis of emotional processing in PTSD, social anxiety disorder, and specific phobia: Am.J.Psychiatry, v. 164, p. 1476-1488.

59. Ferguson, J. N., Aldag, J. M., Insel, T. R., and Young, L. J., 2001, Oxytocin in the medial amygdala is essential for social recognition in the mouse: J.Neurosci., v. 21, p. 8278-8285.

60. Floyd, N. S., Price, J. L., Ferry, A. T., Keay, K. A., and Bandler, R., 2000, Orbitomedial prefrontal cortical projections to distinct longitudinal columns of the periaqueductal gray in the rat: J.Comp Neurol., v. 422, p. 556-578.

61. Foltz, E. L. and White, L. E., 1968, The role of rostral cingulumotomy in "pain" relief: Int.J.Neurol., v. 6, p. 353-373.

62. Ford, G. K. and Finn, D. P., 2008, Clinical correlates of stress-induced analgesia: evidence from pharmacological studies: Pain, v. 140, p. 3-7.

63. Forman, S. D., Cohen, J. D., Fitzgerald, M., Eddy, W. F., Mintun, M. A., and Noll, D. C., 1995, Improved assessment of significant activation in functional magnetic resonance imaging (fMRI): use of a cluster-size threshold: Magn Reson.Med., v. 33, p. 636-647.

64. Friston, K. J., Frith, C. D., Frackowiak, R. S., and Turner, R., 1995, Characterizing dynamic brain responses with fMRI: a multivariate approach: Neuroimage., v. 2, p. 166-172.

65. Frot, M., Garcia-Larrea, L., Guenot, M., and Mauguiere, F., 2001, Responses of the supra-sylvian (SII) cortex in humans to painful and innocuous stimuli. A study using intra-cerebral recordings: Pain, v. 94, p. 65-73.

66. Frot, M. and Mauguiere, F., 2003, Dual representation of pain in the operculo-insular cortex in humans: Brain, v. 126, p. 438-450.

67. Gauriau, C. and Bernard, J. F., 2002, Pain pathways and parabrachial circuits in the rat: Exp.Physiol, v. 87, p. 251-258.

68. Giesecke, T., Gracely, R. H., Williams, D. A., Geisser, M. E., Petzke, F. W., and Clauw, D. J., 2005, The relationship between depression, clinical pain, and experimental pain in a chronic pain cohort: Arthritis Rheum., v. 52, p. 1577-1584.

69. Gonzalez-Lima, F. and Scheich, H., 1986, Classical conditioning of tone-signaled bradycardia modifies 2-deoxyglucose uptake patterns in cortex, thalamus, habenula, caudate-putamen and hippocampal formation: Brain Res., v. 363, p. 239-256.

70. Grabe, H. J., Spitzer, C., and Freyberger, H. J., 2004, Alexithymia and personality in relation to dimensions of psychopathology: Am.J.Psychiatry, v. 161, p. 1299-1301.

71. Gracely, R. H., Petzke, F., Wolf, J. M., and Clauw, D. J., 2002, Functional magnetic resonance imaging evidence of augmented pain processing in fibromyalgia: Arthritis Rheum., v. 46, p. 1333-1343.

72. Greenwood-Van, M. B., Gibson, M., Gunter, W., Shepard, J., Foreman, R., and Myers, D., 2001, Stereotaxic delivery of corticosterone to the amygdala modulates colonic sensitivity in rats: Brain Res., v. 893, p. 135-142.

73. Hariri, A. R., Bookheimer, S. Y., and Mazziotta, J. C., 2000, Modulating emotional responses: effects of a neocortical network on the limbic system: Neuroreport, v. 11, p. 43-48.

74. Hariri, A. R., Mattay, V. S., Tessitore, A., Fera, F., Smith, W. G., and Weinberger, D. R., 2002a, Dextroamphetamine modulates the response of the human amygdala: Neuropsychopharmacology, v. 27, p. 1036-1040.

75. Hariri, A. R., Mattay, V. S., Tessitore, A., Kolachana, B., Fera, F., Goldman, D., Egan, M. F., and Weinberger, D. R., 2002b, Serotonin transporter genetic variation and the response of the human amygdala: Science, v. 297, p. 400-403.

76. Hariri, A. R., Tessitore, A., Mattay, V. S., Fera, F., and Weinberger, D. R., 2002c, The amygdala response to emotional stimuli: a comparison of faces and scenes: Neuroimage., v. 17, p. 317-323.

77. Heinz, A., Braus, D. F., Smolka, M. N., Wrase, J., Puls, I., Hermann, D., Klein, S., Grusser, S. M., Flor, H., Schumann, G., Mann, K., and Buchel, C., 2005, Amygdala-prefrontal coupling depends on a genetic variation of the serotonin transporter: Nat.Neurosci., v. 8, p. 20-21.

78. Helmstetter, F. J., Bellgowan, P. S., and Tershner, S. A., 1993, Inhibition of the tail flick reflex following microinjection of morphine into the amygdala: Neuroreport, v. 4, p. 471-474.

79. Henson, R., 2007, Efficient Experimental Design for fMRI, *in* Friston, K. J. and others, editors, Statistical Parametric Mapping: The Analysis of Functional Brain Images: Academic Press, p. 193-210.

80. Herrmann, M. J., Huter, T., Muller, F., Muhlberger, A., Pauli, P., Reif, A., Renner, T., Canli, T., Fallgatter, A. J., and Lesch, K. P., 2007, Additive effects of serotonin transporter and tryptophan hydroxylase-2 gene variation on emotional processing: Cereb.Cortex, v. 17, p. 1160-1163.

81. Holmes, A. P. and Friston, K. J., 1998, Generalisability, Random Effects and Population Inference: NeuroImage, v. 7, p. 754.

82. Hopfinger, J. B., Buchel, C., Holmes, A. P., and Friston, K. J., 2000, A study of analysis parameters that influence the sensitivity of event-related fMRI analyses: Neuroimage., v. 11, p. 326-333.

83. James, W. The Principles of Psychology. http://psychclassics.yorku.ca/James/Principles/index.htm . 1890.
Ref Type: Electronic Citation

84. Janssen, S. A. and Arntz, A., 1997, No evidence for opioid-mediated analgesia induced by phobic fear: Behav.Res.Ther., v. 35, p. 823-830.

85. Jezzard, P., 2001, Functional MRI and Introduction to Methods: Oxford, Oxford University Press.

86. Ji, G., Fu, Y., Ruppert, K. A., and Neugebauer, V., 2007, Pain-related anxiety-like behavior requires CRF1 receptors in the amygdala: Mol.Pain, v. 3, p. 13.

87. KEELE, K. D., 1948, The pain chart: Lancet, v. 2, p. 6-8.

88. Kirsch, P., Esslinger, C., Chen, Q., Mier, D., Lis, S., Siddhanti, S., Gruppe, H., Mattay, V. S., Gallhofer, B., and Meyer-Lindenberg, A., 2005, Oxytocin modulates neural circuitry for social cognition and fear in humans: J.Neurosci., v. 25, p. 11489-11493.

89. Knecht, S., Kunesch, E., and Schnitzler, A., 1996, Parallel and serial processing of haptic information in man: effects of parietal lesions on sensorimotor hand function: Neuropsychologia, v. 34, p. 669-687.

90. Knorring, L., 1975, The exerience of pain in depressed patients. A clinical and experimental study: Neuropsychobiology, v. 1, p. 155-165.

91. Korzeniewska-Rybicka, I. and Plaznik, A., 1998, Analgesic effect of antidepressant drugs: Pharmacol.Biochem.Behav., v. 59, p. 331-338.

92. Kosturek, A., Gregory, R. J., Sousou, A. J., and Trief, P., 1998, Alexithymia and somatic amplification in chronic pain: Psychosomatics, v. 39, p. 399-404.

93. Krasnow, B., Tamm, L., Greicius, M. D., Yang, T. T., Glover, G. H., Reiss, A. L., and Menon, V., 2003, Comparison of fMRI activation at 3 and 1.5 T during perceptual, cognitive, and affective processing: Neuroimage., v. 18, p. 813-826.

94. Kudoh, A., Ishihara, H., and Matsuki, A., 2000, Inhibition of the cortisol response to surgical stress in chronically depressed patients: J.Clin.Anesth., v. 12, p. 383-387.

95. Kudoh, A., Katagai, H., and Takazawa, T., 2002, Increased postoperative pain scores in chronic depression patients who take antidepressants: J.Clin.Anesth., v. 14, p. 421-425.

96. Kundermann, B., Hemmeter-Spernal, J., Huber, M. T., Krieg, J. C., and Lautenbacher, S., 2008, Effects of total sleep deprivation in major depression: overnight improvement of mood is accompanied by increased pain sensitivity and augmented pain complaints: Psychosom.Med., v. 70, p. 92-101.

97. LaBar, K. S., Gitelman, D. R., Mesulam, M. M., and Parrish, T. B., 2001, Impact of signal-to-noise on functional MRI of the human amygdala: Neuroreport, v. 12, p. 3461-3464.

98. Landgrebe, M., Barta, W., Rosengarth, K., Frick, U., Hauser, S., Langguth, B., Rutschmann, R., Greenlee, M. W., Hajak, G., and Eichhammer, P., 2008, Neuronal correlates of symptom formation in functional somatic syndromes: a fMRI study: Neuroimage., v. 41, p. 1336-1344.

99. Lautenbacher, S. and Krieg, J. C., 1994, Pain perception in psychiatric disorders: a review of the literature: J.Psychiatr.Res., v. 28, p. 109-122.

100. Lautenbacher, S., Roscher, S., Strian, D., Fassbender, K., Krumrey, K., and Krieg, J. C., 1994, Pain perception in depression: relationships to symptomatology and naloxone-sensitive mechanisms: Psychosom.Med., v. 56, p. 345-352.

101. Lawrie, S. M., Buechel, C., Whalley, H. C., Frith, C. D., Friston, K. J., and Johnstone, E. C., 2002, Reduced frontotemporal functional connectivity in schizophrenia associated with auditory hallucinations: Biol.Psychiatry, v. 51, p. 1008-1011.

102. LeDoux, J. E., 2000, Emotion circuits in the brain: Annu.Rev.Neurosci., v. 23, p. 155-184.

103. Leino, P. and Magni, G., 1993, Depressive and distress symptoms as predictors of low back pain, neck-shoulder pain, and other musculoskeletal morbidity: a 10-year follow-up of metal industry employees: Pain, v. 53, p. 89-94.

104. Liberzon, I., Taylor, S. F., Fig, L. M., Decker, L. R., Koeppe, R. A., and Minoshima, S., 2000, Limbic activation and psychophysiologic responses to aversive visual stimuli. Interaction with cognitive task: Neuropsychopharmacology, v. 23, p. 508-516.

105. Lussier, D., Huskey, A. G., and Portenoy, R. K., 2004, Adjuvant analgesics in cancer pain management: Oncologist., v. 9, p. 571-591.

106. Madrazo, I., Franco-Bourland, R. E., Leon-Meza, V. M., and Mena, I., 1987, Intraventricular somatostatin-14, arginine vasopressin, and oxytocin: analgesic effect in a patient with intractable cancer pain: Appl.Neurophysiol., v. 50, p. 427-431.

107. Maes, F., Collignon, A., Vandermeulen, D., Marchal, G., and Suetens, P., 1997, Multimodality image registration by maximization of mutual information: IEEE Trans.Med.Imaging, v. 16, p. 187-198.

108. Magni, G., Marchetti, M., Moreschi, C., Merskey, H., and Luchini, S. R., 1993, Chronic musculoskeletal pain and depressive symptoms in the National Health and Nutrition Examination. I. Epidemiologic follow-up study: Pain, v. 53, p. 163-168.

109. Maldjian, J. A., Laurienti, P. J., Kraft, R. A., and Burdette, J. H., 2003, An automated method for neuroanatomic and cytoarchitectonic atlas-based interrogation of fMRI data sets: NeuroImage, v. 19, p. 1233-1239.

110. Marazziti, D., Castrogiovanni, P., Rossi, A., Rosa, C., Ghione, S., Di, M. A., Panattoni, E., and Cassano, G. B., 1998, Pain threshold is reduced in depression: Int.J.Neuropsychopharmacol., v. 1, p. 45-48.

111. Marks, I., 1985, Behavioral psychotherapy for anxiety disorders: Psychiatr.Clin.North Am., v. 8, p. 25-35.

112. May, A., 2007, Neuroimaging: visualising the brain in pain: Neurol.Sci., v. 28 Suppl 2, p. S101-S107.

113. McCracken, L. M., Faber, S. D., and Janeck, A. S., 1998, Pain-related anxiety predicts non-specific physical complaints in persons with chronic pain: Behav.Res.Ther., v. 36, p. 621-630.

114. Melzack, R., 2001, Pain and the neuromatrix in the brain: J.Dent.Educ., v. 65, p. 1378-1382.

115. Melzack, R., 1975, The McGill Pain Questionnaire: major properties and scoring methods: Pain, v. 1, p. 277-299.

116. Melzack, R., 1990, Phantom limbs and the concept of a neuromatrix: Trends Neurosci., v. 13, p. 88-92.

117. Melzack, R., 1999, Pain--an overview: Acta Anaesthesiol.Scand., v. 43, p. 880-884.

118. Melzack, R. and Loeser, J. D., 1978, Phantom body pain in paraplegics: evidence for a central "pattern generating mechanism" for pain: Pain, v. 4, p. 195-210.

119. Merboldt, K. D., Fransson, P., Bruhn, H., and Frahm, J., 2001, Functional MRI of the human amygdala?: Neuroimage., v. 14, p. 253-257.

120. Meyer-Lindenberg, A., Kolachana, B., Gold, B., Olsh, A., Nicodemus, K. K., Mattay, V., Dean, M., and Weinberger, D. R., 2008, Genetic variants in AVPR1A linked to autism predict amygdala activation and personality traits in healthy humans: Mol.Psychiatry.

121. Mogil, J. S., 1999, The genetic mediation of individual differences in sensitivity to pain and its inhibition: Proc.Natl.Acad.Sci.U.S.A, v. 96, p. 7744-7751.

122. Moldin, S. O., Scheftner, W. A., Rice, J. P., Nelson, E., Knesevich, M. A., and Akiskal, H., 1993, Association between major depressive disorder and physical illness: Psychol.Med., v. 23, p. 755-761.

123. Morgan, B. J. T., 2000, Basic Likelihood Tools Applied stochastic modelling: London, Arnold.

124. Moroz, B. T., Nuller, I., Ustimova, I. N., and Andreev, B. V., 1990, [Study of pain sensitivity based on the indicators of electro- odontometry in patients with depersonalization and depressive disorders]: Zh.Nevropatol.Psikhiatr.Im S.S.Korsakova, v. 90, p. 81-82.

125. Morris, J. S., deBonis, M., and Dolan, R. J., 2002, Human amygdala responses to fearful eyes: Neuroimage., v. 17, p. 214-222.

126. Morris, J. S., Frith, C. D., Perrett, D. I., Rowland, D., Young, A. W., Calder, A. J., and Dolan, R. J., 1996, A differential neural response in the human amygdala to fearful and happy facial expressions: Nature, v. 383, p. 812-815.

127. Morris, J. S., Ohman, A., and Dolan, R. J., 1998, Conscious and unconscious emotional learning in the human amygdala: Nature, v. 393, p. 467-470.

128. Narita, M., Kaneko, C., Miyoshi, K., Nagumo, Y., Kuzumaki, N., Nakajima, M., Nanjo, K., Matsuzawa, K., Yamazaki, M., and Suzuki, T., 2006, Chronic pain induces anxiety with concomitant changes in opioidergic function in the amygdala: Neuropsychopharmacology, v. 31, p. 739-750.

129. Nestler, E. J., Barrot, M., DiLeone, R. J., Eisch, A. J., Gold, S. J., and Monteggia, L. M., 2002, Neurobiology of depression: Neuron, v. 34, p. 13-25.

130. Neugebauer, V. and Li, W., 2003, Differential sensitization of amygdala neurons to afferent inputs in a model of arthritic pain: J.Neurophysiol., v. 89, p. 716-727.

131. Neugebauer, V., Li, W., Bird, G. C., and Han, J. S., 2004, The amygdala and persistent pain: Neuroscientist., v. 10, p. 221-234.

132. Noble, B., Clark, D., Meldrum, M., ten, H. H., Seymour, J., Winslow, M., and Paz, S., 2005, The measurement of pain, 1945-2000: J.Pain Symptom.Manage., v. 29, p. 14-21.

133. Ochsner, K. N., Ludlow, D. H., Knierim, K., Hanelin, J., Ramachandran, T., Glover, G. C., and Mackey, S. C., 2006, Neural correlates of individual differences in pain-related fear and anxiety: Pain, v. 120, p. 69-77.

134. Oertel, B. G., Preibisch, C., Wallenhorst, T., Hummel, T., Geisslinger, G., Lanfermann, H., and Lotsch, J., 2008, Differential opioid action on sensory and affective cerebral pain processing: Clin.Pharmacol.Ther., v. 83, p. 577-588.

135. Onghena, P. and Van, H. B., 1992, Antidepressant-induced analgesia in chronic non-malignant pain: a meta-analysis of 39 placebo-controlled studies: Pain, v. 49, p. 205-219.

136. Otto, M. W., Dougher, M. J., and Yeo, R. A., 1989, Depression, pain, and hemispheric activation: J.Nerv.Ment.Dis., v. 177, p. 210-218.

137. Penny, W. "% Signal Change" (SPM Mailing List Contribution). Vanni, S. 10-18-2004. Ref Type: Internet Communication

138. Petersson, M., Alster, P., Lundeberg, T., and Uvnas-Moberg, K., 1996, Oxytocin increases nociceptive thresholds in a long-term perspective in female and male rats: Neurosci.Lett., v. 212, p. 87-90.

139. Peyron, R., Frot, M., Schneider, F., Garcia-Larrea, L., Mertens, P., Barral, F. G., Sindou, M., Laurent, B., and Mauguiere, F., 2002, Role of operculoinsular cortices in human pain processing: converging evidence from PET, fMRI, dipole modeling, and intracerebral recordings of evoked potentials: Neuroimage., v. 17, p. 1336-1346.

140. Peyron, R., Garcia-Larrea, L., Gregoire, M. C., Costes, N., Convers, P., Lavenne, F., Mauguiere, F., Michel, D., and Laurent, B., 1999, Haemodynamic brain responses to acute pain in humans: sensory and attentional networks: Brain, v. 122 (Pt 9), p. 1765-1780.

141. Peyron, R., Laurent, B., and Garcia-Larrea, L., 2000, Functional imaging of brain responses to pain. A review and meta-analysis (2000): Neurophysiol.Clin., v. 30, p. 263-288.

142. Pezawas, L., Meyer-Lindenberg, A., Drabant, E. M., Verchinski, B. A., Munoz, K. E., Kolachana, B. S., Egan, M. F., Mattay, V. S., Hariri, A. R., and Weinberger, D. R., 2005, 5-HTTLPR polymorphism impacts human cingulate-amygdala interactions: a genetic susceptibility mechanism for depression: Nat.Neurosci., v. 8, p. 828-834.

143. Phillips, M. L., Drevets, W. C., Rauch, S. L., and Lane, R., 2003, Neurobiology of emotion perception I: The neural basis of normal emotion perception: Biol.Psychiatry, v. 54, p. 504-514.

144. Phillips, M. L., Young, A. W., Scott, S. K., Calder, A. J., Andrew, C., Giampietro, V., Williams, S. C., Bullmore, E. T., Brammer, M., and Gray, J. A., 1998, Neural responses to facial and vocal expressions of fear and disgust: Proc.Biol.Sci., v. 265, p. 1809-1817.

145. Ploghaus, A., Tracey, I., Gati, J. S., Clare, S., Menon, R. S., Matthews, P. M., and Rawlins, J. N., 1999, Dissociating pain from its anticipation in the human brain: Science, v. 284, p. 1979-1981.

146. Poncelet, B. P., Wedeen, V. J., Weisskoff, R. M., and Cohen, M. S., 1992, Brain parenchyma motion: measurement with cine echo-planar MR imaging: Radiology, v. 185, p. 645-651.

147. Preston, S. D. and de Waal, F. B., 2002, Empathy: Its ultimate and proximate bases: Behav.Brain Sci., v. 25, p. 1-20.

148. Rainville, P., Carrier, B., Hofbauer, R. K., Bushnell, M. C., and Duncan, G. H., 1999, Dissociation of sensory and affective dimensions of pain using hypnotic modulation: Pain, v. 82, p. 159-171.

149. Rainville, P., Duncan, G. H., Price, D. D., Carrier, B., and Bushnell, M. C., 1997, Pain affect encoded in human anterior cingulate but not somatosensory cortex: Science, v. 277, p. 968-971.

150. Ray, J. P. and Price, J. L., 1992, The organization of the thalamocortical connections of the mediodorsal thalamic nucleus in the rat, related to the ventral forebrain-prefrontal cortex topography: J.Comp Neurol., v. 323, p. 167-197.

151. Rhudy, J. L., Grimes, J. S., and Meagher, M. W., 2004, Fear-induced hypoalgesia in humans: effects on low intensity thermal stimulation and finger temperature: J.Pain, v. 5, p. 458-468.

152. Rizzolatti, G., Fogassi, L., and Gallese, V., 2001, Neurophysiological mechanisms underlying the understanding and imitation of action: Nat.Rev.Neurosci., v. 2, p. 661-670.

153. Robert, I., 2007, Part II: Methods of Clinical Neurobiological Research, *in* Charney, D. S. and Nestler, E. J., editors, Neurobiology of Mental Illness: New York, Oxford University Press.

154. Schneider, F., Habel, U., Holthusen, H., Kessler, C., Posse, S., Muller-Gartner, H. W., and Arndt, J. O., 2001, Subjective ratings of pain correlate with subcortical-limbic blood flow: an fMRI study: Neuropsychobiology, v. 43, p. 175-185.

155. Schoenberg, B. S., 1983, Calculating Confidence Intervals for Rates and Ratios: Neuroepidemiology, v. 2, p. 257-265.

156. Shepard, J. D., Barron, K. W., and Myers, D. A., 2000, Corticosterone delivery to the amygdala increases corticotropin-releasing factor mRNA in the central amygdaloid nucleus and anxiety-like behavior: Brain Res., v. 861, p. 288-295.

157. Singer, T., Seymour, B., O'Doherty, J., Kaube, H., Dolan, R. J., and Frith, C. D., 2004, Empathy for pain involves the affective but not sensory components of pain: Science, v. 303, p. 1157-1162.

158. Stahl, S. M., 2002, Does depression hurt?: J.Clin.Psychiatry, v. 63, p. 273-274.

159. Talairach, J. and Tournoux, P., 1988, Co-planar Stereotaxic Atlas of the Human Brain 3-Dimensional Proportional System: An Approach to Cerebral Imaging: Stuttgart, New York.

160. Taylor, S. F., Phan, K. L., Decker, L. R., and Liberzon, I., 2003, Subjective rating of emotionally salient stimuli modulates neural activity: Neuroimage., v. 18, p. 650-659.

161. Thomas, K. M., Drevets, W. C., Whalen, P. J., Eccard, C. H., Dahl, R. E., Ryan, N. D., and Casey, B. J., 2001, Amygdala response to facial expressions in children and adults: Biol.Psychiatry, v. 49, p. 309-316.

162. Thompson, P. M., Schwartz, C., Lin, R. T., Khan, A. A., and Toga, A. W., 1996, Three-dimensional statistical analysis of sulcal variability in the human brain: J.Neurosci., v. 16, p. 4261-4274.

163. Tottenham, N., Tanaka, J. W., Leon, A. C., McCarry, T., Nurse, M., Hare, T. A., Marcus, D. J., Westerlund, A., Casey, B., and Nelson, C., 2009, The NimStim set of facial expressions: Judgments from untrained research participants: Psychiatry Res..

164. Tracey, I., 2008, Imaging pain: Br.J.Anaesth., v. 101, p. 32-39.

165. Tracey, I. and Mantyh, P. W., 2007, The cerebral signature for pain perception and its modulation: Neuron, v. 55, p. 377-391.

166. Treede, R. D., Kenshalo, D. R., Gracely, R. H., and Jones, A. K., 1999, The cortical representation of pain: Pain, v. 79, p. 105-111.

167. Tzourio-Mazoyer, N., Landeau, B., Papathanassiou, D., Crivello, F., Etard, O., Delcroix, N., Mazoyer, B., and Joliot, M., 2002, Automated anatomical labeling of activations in SPM using a macroscopic anatomical parcellation of the MNI MRI single-subject brain: Neuroimage., v. 15, p. 273-289.

168. von Leupoldt, A., Sommer, T., Kegat, S., Baumann, H. J., Klose, H., Dahme, B., and Buchel, C., 2009, Dyspnea and pain share emotion-related brain network: Neuroimage., v. 48, p. 200-206.

169. Von, K. M., Dworkin, S. F., Le, R. L., and Kruger, A., 1988, An epidemiologic comparison of pain complaints: Pain, v. 32, p. 173-183.

170. Ward, N. G., Bloom, V. L., Dworkin, S., Fawcett, J., Narasimhachari, N., and Friedel, R. O., 1982, Psychobiological markers in coexisting pain and depression: toward a unified theory: J.Clin.Psychiatry, v. 43, p. 32-41.

171. Ward, N. G., Bloom, V. L., and Friedel, R. O., 1979, The effectiveness of tricyclic antidepressants in the treatment of coexisting pain and depression: Pain, v. 7, p. 331-341.

172. Wedig, M. M., Rauch, S. L., Albert, M. S., and Wright, C. I., 2005, Differential amygdala habituation to neutral faces in young and elderly adults: Neurosci.Lett., v. 385, p. 114-119.

173. Whalen, P. J., Shin, L. M., McInerney, S. C., Fischer, H., Wright, C. I., and Rauch, S. L., 2001, A functional MRI study of human amygdala responses to facial expressions of fear versus anger: Emotion., v. 1, p. 70-83.

174. White, T., O'Leary, D., Magnotta, V., Arndt, S., Flaum, M., and Andreasen, N. C., 2001, Anatomic and functional variability: the effects of filter size in group fMRI data analysis: Neuroimage., v. 13, p. 577-588.

175. Wicker, B., Keysers, C., Plailly, J., Royet, J. P., Gallese, V., and Rizzolatti, G., 2003, Both of us disgusted in My insula: the common neural basis of seeing and feeling disgust: Neuron, v. 40, p. 655-664.

176. Willer, J. C., 1977, Comparative study of perceived pain and nociceptive flexion reflex in man: Pain, v. 3, p. 69-80.

177. Willer, J. C., Dehen, H., and Cambier, J., 1981, Stress-induced analgesia in humans: endogenous opioids and naloxone-reversible depression of pain reflexes: Science, v. 212, p. 689-691.

178. Worsley, K. J., Marrett, S., Neelin, P., Vandal, A. C., Friston, K. J., and Evans, A. C., 1996, A unified statistical approach for determining significant signals in images of cerebral activation: Human Brain Mapping, v. 4, p. 58-73.

179. Wright, C. I., Fischer, H., Whalen, P. J., McInerney, S. C., Shin, L. M., and Rauch, S. L., 2001, Differential prefrontal cortex and amygdala habituation to repeatedly presented emotional stimuli: Neuroreport, v. 12, p. 379-383.

180. Yasui, Y., Breder, C. D., Saper, C. B., and Cechetto, D. F., 1991, Autonomic responses and efferent pathways from the insular cortex in the rat: J.Comp Neurol., v. 303, p. 355-374.

181. Young, A. W., Aggleton, J. P., Hellawell, D. J., Johnson, M., Broks, P., and Hanley, J. R., 1995, Face processing impairments after amygdalotomy: Brain, v. 118 (Pt 1), p. 15-24.

182. Young, A. W., Perrett, D. I., Calder, A. J., Sprengelmeyer, R., and Ekman, P. Facial expressions of emotion: Stimuli and tests (FEEST). 2002. Bury St. Edmunds, U.K., Thames Valley Test Company. Ref Type: Computer Program

183. Zhang, Z. H., Dougherty, P. M., and Oppenheimer, S. M., 1999, Monkey insular cortex neurons respond to baroreceptive and somatosensory convergent inputs: Neuroscience, v. 94, p. 351-360.

CURRICULUM VITAE

Persönliche Angaben

Name:	Andreas Harald Heckel
Anschrift:	Finkenweg 4, 93059 Regensburg
E-Mail:	heckelandreas@googlemail.com
Geburtsdatum/-ort:	06.02.1978 in Regensburg

Schule

1984 – 1988	Volksschule Regensburg-Reinhausen
1988 – 1997	Werner-von-Siemens Gymnasium Regensburg

Zivildienst

1997 – 1998	Krankenhaus Barmherzige Brüder in Regensburg

Universität Regensburg

1998	Beginn Studium Human-Medizin
2000	Ärztliche Vorprüfung
2001	1. Abschnitt der ärztlichen Prüfung
2003	Fortgeschrittenenausbildung in EDV
2004	2. Abschnitt der ärztlichen Prüfung
2006	Ende des Praktischen Jahres im Bezirksklinikum Regensburg (Neurologie) und im Lehrkrankenhaus Weiden (Kardiologie, Gastroenterologie, Onkologie)
	3. Abschnitt der ärztlichen Prüfung. Approbation.
Ende 2007	Abschluss des Masterstudiengangs „Experimental and Clinical Neurosciences" im „Elitenetzwerk Bayern"
Frühjahr 2008	Dissertationsprojekt an der Universitätsklinik für Psychiatrie und Psychotherapie in Regensburg
März 2010	Rigorosum